THE UTILITY OF A FACS BASED MICRONUCLEUS ASSAY FOR ASSESSMENT OF DNA DAMAGE

Thesis submitted in accordance with the requirements

of the University of Liverpool for the degree of

Doctor in Philosophy

By

Jehad Farouq Alhmoud

September, 2019

Dedication

To my beloved father '**Dr Farouq Abdullah Alhmoud**', who never hesitate to put all of his effort to support me throughout my life emotionally as well as financially.

Abstract

The cytokinesis-block micronucleus (CBMN) assay is one of many well-established techniques used for assessing DNA damage within cells. However, due to limitations of this and other techniques, there is a need to develop more reliable and high-throughput methods for a more objective evaluation of DNA damage after genotoxic exposures. A major goal of this project was to establish a sensitive, high throughput, and robust fluorescence activated cell sorting (FACS) based assay to enumerate micronuclei for clinical application in the context of haematological cancers. Having established and optimised a MN-FACS assay using cell lines and primary CLL patient samples, and compared the performance of the technique with traditional techniques such as the Comet, CBMN assays. By performing correlation analyses, we have found that the results obtained within the MN-FACS assay are comparable. Significantly, the Comet assay was more suitable to assess early DNA damage whereas MN enumeration was better at assessing long-term effects. The studies outlined also provided important insights in to the effects of cell cycle and proliferation status on the MN-FACS assay and MN frequencies. To recapitulate clinical practice, we investigated the impact of sequential treatments with Fludarabine and Bendamustine combined with irradiation in various B cell lines on MN frequencies. The sequencing of the drugs and the incorporation of irradiation was found to be critical and influenced MN frequencies and has potential significance for the order of treatments in low-grade lymphoid malignancies such as CLL and MCL. As primary and fresh CLL cells have low proliferative capacity, we used a CD40, IL4 and IL21 dependent system to stimulate cell division *in vitro* and assessed MN frequencies. Finally, using the MN-FACS assay, we show that there is a wide variation in MN frequencies within fresh primary CLL patient cells likely based on clinical characteristics and treatment history. In summary, this thesis summarises our efforts to establish and optimise a FACS based MN enumeration assay. The assay has allowed us to make novel observations pertinent to assessment of DNA damage. With further modifications, the

technique should allow serial assessment of patients to assess genomic instability inherent of cancer cells and the effects of treatment modalities to assess long-term safety.

Declaration

I, Jehad Alhmoud declare that the entire data presented in this thesis is a result of my own work and effort and was generated from the experiments that I have performed during my work in this project. This was carried out in the laboratory of Dr Nagesh Kalakonda, Department of Molecular and Clinical Cancer Medicine, Institute of Translational Medicine, University of Liverpool, Liverpool, UK.

Jehad Alhmoud

2019

Acknowledgements

First, I would like to express my sincere gratitude to my primary supervisor Dr Nagesh Kalakonda, who gave me this opportunity to join his lab. Also, for his support, encouragement and guiding me throughout my study. I extend my acknowledge to my secondary supervisor Dr Joseph Slupsky for his supervision and help.

Also, I would like to thank my other supervisor's Dr Mark Glenn and Dr Alix Bee for guiding me in the practical aspects. A special appreciation to Dr Kathleen Till, Dr Vanessa Marensi, Dr Umair Khan, Dr Indrani Karpha, Dr Tony Carter, Dr Sandra Pereira Cachinho, Dr Christopher Law, Dr Andrew Duckworth, Dr Jemma Blocksidge, Dr Jason Parsons, Dr David Mason, Dr Ke Lin for their support and valuable suggestions.

I wish to thank my colleagues in both departments 'Molecular and Clinical Cancer Medicine' and 'Molecular and Clinical Pharmacology' for their friendship throughout my PhD study. I also would like to thank all CLL patients who have donated their precious blood for research purpose.

I take this opportunity to give my deepest honour to my beloved parents for their endless support, sacrifices and encouragement. I also thanks my cute daughter 'Rama', you are the pride and happiness of my life and I appreciate your patience during my absence. Lastly, special thanks to my soul mate, my lovely wife 'Mira Abu-Radini' for her kind heart, bottomless love, and being infinite tolerant and sacrifice throughout my doctoral journey 'without you I could not achieve this'.

Table of Contents

List of Figures

List of Tables

Abbreviations

ALL	Acute Lymphocytic leukaemia
ATCC	American type culture collection
ATM	Ataxia telangiectasia mutated
ATR	RAD3-related
B-ALL	B-precursor acute lymphoblastic leukaemia
BER	Base excision repair
BM	Bone marrow
BN	Bi-nucleated
BR	Bendamustine and Rituximab
BTK	Bruton's tyrosine kinase
CBMN	Cytokinesis-block micronucleus cytome assay
CHOP	Cyclophosphamide, doxorubicin, vincristine, and prednisone
CIN	Enhance chromosomal instability
CLL	Chronic Lymphocytic Leukaemia
CNAs	Copy number alterations
CO_2	Carbon dioxide
CR	Complete response
CRC	Colorectal cancer
DAPI	4, 6-diaminodino-2-phenylindole
DBD	DNA breakage detection
DDR	DNA damage response
DDRP	DNA damage repair pathway
DLBCL	Diffuse large B-cell Lymphoma
DMEM	Dulbecco's Modified Eagle Medium

DMSO	Dimethyl Sulfoxide
DSBs	Double strand breaks
DSMZ	Leibniz Institute DSMZ
EDTA	Ethylenediaminetetraacetic acid
EMA	Ethidium monoazide
FBS	Fetal bovine serum
FCR	Fludarabine, Cyclophosphamide and Rituximab
FISH	Fluorescence in situ hybridization
FL	Follicular lymphoma
GII	Genomic instability index
HL	Hodgkin’s lymphoma
HPLC	High performance liquid chromatography
HR	Homologous recombination
HRS	Hodgkin and Reed-Sternberg
IMDM	Iscove's Modified Dulbecco's Medium
MCL	Mantle cell lymphoma
mL	Millilitre
MM	Multiple myeloma
MMC	Mitomycin C
MMR	Mismatch repair
MN	Micronuclei
MoAbs	Monoclonal antibodies
MS	Mass spectrometry
MSCs	Mesenchymal stem/stromal cells
NBUDs	Nuclear buds
NER	Nucleotide excision repair
NF-κB	Nuclear factor-kB

NHEJ	Non-homologous end joining
NHL	Non-Hodgkin's lymphoma
NPBs	Nucleoplasmic bridges
OC	Ovarian carcinoma
^{o}C	Centigrade
ORR	Overall response rates
PBL	Peripheral blood lymphocytes
PBS	Phosphate buffer solution
PCD	Programmed cell death
PI	Propidium Iodide
PI3K	Phosphatidylinositol-3-phosphate
rhIL-4/ 21	Recombinant human interleukin-4/ 21
ROS	Reactive oxygen species
RPMI	Roswell Park Memorial Institute medium
SCGE	Single cell gel electrophoresis
SCLC	Small cell lung cancer
SCNA	Somatic copy number alterations
SKY	Spectral karyotyping
SOP	Standard operating procedures
SSBs	Single strand breaks
Syk	Spleen tyrosine kinase
T-ALL	T-cell acute lymphoblastic leukaemia
t-MDS/ AML	Therapy-related myelodysplasia and/or acute myeloid
TORC1	Target of rapamycin complex 1
UK	United Kingdom
UT	Untreated
UV	Ultraviolet

WT	Wild type
ZAP-70	Zeta-chain-associated protein kinase-70
γH2AX	H2AX phosphorylation
μg	Microgram
μl	Microlitre
μM	Micromolar

Chapter 1: General Introduction

1.1 DNA damage

1.1.1 DNA damage overview

DNA damage can alter nucleotide sequences and lead to expression of dysfunctional proteins impact normal cellular physiology. Sources of DNA damage can be endogenous or exogenous and include reactive oxygen species (ROS) or radiation respectively [1]. DNA damaging agents can broadly be classified into two different categories; Clastogens that cause chromosomal breaks and induce micronuclei (MN) due to generation of acentric chromosomal fragments. In contrast, aneugens lead to incorporation of whole chromosomes in MN by generation of aneuploidy that affects cell proliferation and mitotic spindle apparatus [2].

Genotoxic agents cause structural changes in DNA by disrupting covalent bonds between nucleotides preventing accurate replication of the genome [3, 4]. Significant numbers of cells in the human body are subjected to DNA damage on a continuous basis and lead to alterations in genome replication and transcription. Although the DNA repair machinery can correct some of these lesions, unrepaired or misrepaired DNA can lead to genome aberrations and mutations that affect cellular function [5]. Genetic defects, especially those occurring in oncogenes, tumour-suppressor genes, genes that control the cell cycle etc. can impact cell survival or proliferation [6]. Such DNA damage can be carcinogenic [7]. DNA repair proteins trigger

checkpoints to recognize sites of damage and either activate corrective pathways or induce apoptosis [8].

Endogenous agents induce replication stress or generate free radicals derived from oxidative metabolism, whereas exogenous agents, such as ionizing or ultraviolet (UV) radiation and chemotherapy induce structural changes such as single strand (SSB) or double strand breaks (DSB) in DNA via base modifications, helix-distorting bulky lesions, or cross-links of DNA strands and are repaired by biochemically distinct DNA repair pathways [9]. DSBs are the most severe form of DNA damage in eukaryotic cells, because they lead to an inefficient repair and cause mutations or induce cell death.

1.1.2 Genomic instability in Cancer

Genomic instability can result in human cancers due to alterations of the cell cycle, transcription, induction of metabolic stress, ROS formation or activation of oncogenes. Mutations or deletion of genes responsible for regulating cell division or tumour suppressors can also lead to genomic instability and cancer [10]. Genetic alterations that lead to cancer are more likely to occur in actively proliferating tissues. Cells with high rates of proliferation are more susceptible to DNA damage and tumorigenesis [11].

1.1.3 DNA damage and cell survival

Apoptosis or programmed cell death (PCD), plays a vital role in maintaining tissue homeostasis by removing diseased or injured cells. Mitochondrial fragmentation within such cells leads to caspase activation and cell death when cells pass through critical checkpoints [12, 13]. Conversely, survival

pathways, such as target of rapamycin complex 1 (TORC1), are activated in response to genotoxic stress in order to maintain deoxynucleoside triphosphate pools.

1.2 Sources of DNA damage

1.2.1 Ionizing radiation

Ionizing irradiation causes direct or indirect DNA damage leading to changes in the structure of DNA that affects nuclear stability through additional mechanisms [14]. Ionizing radiation can be of various types; alpha particles, beta particles or gamma radiation. All types of radiation release energy when passing through cellular material and may cause cell death [15]. Irradiation can cause DSB at the phosphodiester backbone [16]. The level and complexity of DNA damage is influenced by the dose of radiation. Radiation dose can also impact the cellular microenvironment and the type of DNA damage [17].

1.3 DNA repair and damage response

DNA repair pathways are encoded by a class of proteins that detect DNA double stand breaks, chromosomal fragmentation, translocation and deletions and can correct some alterations [18]. Cells suffer constant and regular insults by genotoxic agents. The DNA damage response (DDR) pathway responds to cellular damage by using signal sensors, transducers and effectors [19]. Such mechanisms help the genome to tolerate or correct damage on an ongoing basis. Endogenous cellular processes produce free radicals, which affect human cells around 10,000 times/day and cause

oxidative DNA damage [20]. The presence of DNA damage or DNA replication stress leads to abnormalities in DNA structure which subsequently stimulate the DDR pathway [21].

DDR mechanisms include multiple DNA repair pathways, damage tolerance processes, and cell-cycle checkpoints [22]. DNA replication stress activates DDR, and causes DNA double-strand breaks (DSBs) and genomic instability [23]. DDR can regulate genomic stability by repairing damaged DNA or removing defective cells by programmed cell death [24]. Conversely, genomic instability and deregulation of DNA damage repair (DDR) pathways can be associated with cancer progression [25].

The tumour suppressor protein Tp53 identifies the presence of DSB and activates signalling pathways that regulate tumour progression and promote apoptosis. Mutations in the p53 gene affect DNA damage repair and promote cancers [26]. A functional DDR is essential for human health, and dysfunction can lead to several diseases such as immune deficiency, neurodegeneration, premature aging, and cancer [27].

The PIKK kinase family members, Ataxia telangiectasia mutated (ATM) and RAD3-related (ATR), are major regulators of DDR. They are sensor proteins and often work together in response to DNA damage signals [28]. ATM and ATR recognize changes in the DNA structure and, as a consequence, mediate downstream protein phosphorylation events and facilitate DDR [29]. Well studied DNA repair pathways include; base excision repair (BER) for SSBs, nucleotide excision repair (NER) for bulky adducts, non-homologous end joining (NHEJ) and homologous recombination (HR) for DSBs, and DNA

mismatch repair (MMR) for correction of replication errors such as base-pair mismatches and loops/bubbles arising from a series of mismatches [30].

1.3.1 Cell cycle as a checkpoint in DNA damage

Cell cycle checkpoints are control mechanisms that regulate the order, integrity, and fidelity of the cell cycle. These include monitoring of cell size, ensuring correct replication of chromosomes, and their accurate segregation at mitosis [31]. Chromosomal segregation and cell division occur in the G2/M phases of the cell cycle [32]. Protein phosphorylation of signal transducers, mediators, and effectors (e.g. p53) induce cell cycle arrest at the G1/S, intra-S, or G2/M checkpoints until DNA repair is complete.

The cell cycle has various checkpoints that can be activated in the presence of DNA damage. These checkpoints decide cell fate, and if the damage is not repairable, cell death is triggered via permanent cell cycle arrest or apoptosis. Successfully repaired cells, however, progress to further stages of the cell cycle [33].

1.4 DNA damage and therapy response

Cancer chemotherapy and radiotherapy are designed to cause apoptosis in cancer cells by inducing catastrophic DNA damage such as DSBs. Traditional therapeutic strategies have been developed based on DNA damage response properties of cancer cells that often have specific abnormalities in the pathway [34]. The abnormal expression of a particular DDR protein can be used as a biomarker of therapy resistance, especially when the damage is recognized and misrepaired by intrinsic DNA repair pathways [35].

1.5 Types of Lymphoid malignancies

Lymphoid tissues are made up of B- and T-lymphocytes that have passed through complex processes of genetic modification required to generate immune responses [36]. They are divided into two types: 1) the central or primary tissues (bone marrow and thymus) where lymphoid precursor cells mature to a stage at which they can express antigen receptors, and 2) peripheral or secondary lymphoid tissues (lymph nodes and spleen), where antigen-specific responses are generated [37].

Lymphoid malignancies include lymphomas (HL and NHL), acute or chronic lymphocytic leukemias (ALL, and CLL), and myeloma (**Tables 1.1**).

Table 1. 1: WHO classification of mature lymphoid neoplasms [38].

Lymphoid malignancy	Disease
Precursor B-cell and T-cell neoplasms	• Precursor B-lymphoblastic leukemia/lymphoblastic lymphoma • Precursor T-lymphoblastic leukemia/lymphoblastic lymphoma
Mature B-cell neoplasms	• Chronic lymphocytic leukemia/Small lymphocytic lymphoma • B-cell prolymphocytic leukemia • Lymphoplasmacytic lymphoma • Splenic marginal zone lymphoma • Hairy cell leukemia • Plasma cell myeloma • Extranodal marginal zone B-cell lymphoma of mucosa-associated lymphoid tissue (MALT-lymphoma) • Nodal marginal zone B-cell lymphoma • Follicular lymphoma • Mantle cell lymphoma • Diffuse large B-cell lymphoma • Mediastinal (thymic) large B-cell lymphoma • Intravascular large B-cell lymphoma • Primary effusion lymphoma • Burkitt lymphoma/leukemia
Leukemic	• T-cell prolymphocytic leukemia • T-cell large granular lymphocytic leukemia • Aggressive NK-cell leukemia • Adult T-cell leukemia/lymphoma

Hodgkin lymphoma	• Nodular lymphocyte predominant Hodgkin's lymphoma • Classical Hodgkin's lymphoma

1.5.1 Acute Lymphoblastic leukaemia (ALL)

ALL is a malignant transformation and proliferation of lymphoid progenitor cells in the bone marrow, blood, and extramedullary sites. ALL is predominantly seen in children, and seems to be more aggressive when it occurs in adults [39]. T-cell acute lymphoblastic leukemias (T-ALLs) harbour genetic mutations in NOTCH, deletions of the CDKN2A locus in chromosome 9p21, and translocations that upregulate specific oncogenes [40]. The most common B-precursor acute lymphoblastic leukaemia (B-ALL) is associated with the t(12;21) translocation that encodes a fusion ETV6-RUNX1 transcript [41].

1.5.2 Hodgkin's lymphoma (HL)

HL derives from mature B-cells, and is considered to be one of the most common type of lymphomas. The tumour cells are rare within involved tissues and are called Hodgkin and Reed-Sternberg (HRS) cells. Although HRS cells are derived from mature B-cells, they exhibit very uncommon co-expression of markers of various hematopoietic cell types [42]. The NF-κB and JAK/STAT pathways are commonly associated with stimulation of tumour cell proliferation and cell survival in HL [43].

1.5.3 Non- Hodgkin's lymphoma (NHL)

The most common sub-types of non-Hodgkin lymphoma are:

A. Low grade NHL such as; 1) Follicular lymphoma (FL) is the second most frequent NHL. FL is usually characterized by asymptomatic peripheral adenopathy in cervical, axillary, inguinal and femoral regions. FL cells survive by escaping the normal germinal centre apoptotic programs [44, 45].

2) Mantle cell lymphoma (MCL) is a rare sub-type of non-Hodgkin lymphoma with unique clinical, biologic, and molecular characteristics [46] and will be discussed further in a later section.

B. High grade NHL such as; 1) Diffuse large B-cell Lymphoma (DLBCL), which represents about 30% of all cases. DLBCL is considered an aggressive NHL and is inclined to spread from the lymph nodes to other areas of the body including the skin, gut, central nervous system and bone marrow [47]. 2) Burkitt's lymphoma is an uncommon and very aggressive sub-type of lymphoma. Burkitt's lymphoma invariably results from abnormalities of the MYC gene on chromosome 8q and requires intensive chemotherapy [48].

1.5.4 Multiple myeloma (MM)

MM is a malignant disorder of plasma cells that typically affects multiple sites within the bone marrow and is associated with secretion of a monoclonal antibody [49]. MM patients can present with lytic lesions of the bone, cytopenias, hypercalcaemia, and renal insufficiency [50].

1.5.5 Chronic Lymphoid Leukaemia (CLL)

1.5.5.1 CLL Overview

CLL is a haematological malignancy characterised by accumulation of clonal mature B-lymphocytes in the peripheral blood, bone marrow, and lymphoid tissues. CLL cells are identified by the expression of the surface membrane proteins CD5 and CD23 [51]. The most common symptoms of CLL are: fatigue, weight loss, night sweats, and increased likelihood of infections. Some patients can present with autoimmune cytopenias, enlarged lymph nodes, hepatomegaly and splenomegaly [52]. Several genetic aberrations can contribute to CLL pathogenesis and/or disease progression and include; 13q14 del (most common), 11q-, 17p- and Trisomy 12. These karyotypic abnormalities can be detected by conventional cytogenetics, FISH analysis or next generation sequencing. In addition, cells within the microenvironment cells, such as stromal cells, T-cells and nurse-like cells in the lymph nodes are essential for supporting cell growth and survival of CLL cells [53, 54].

The clinical behaviour of the disease can vary considerably among CLL patients. Whereas some patients require immediate treatment, others can have indolent disease for long periods after diagnosis that does not require treatment. Factors to consider before deciding on treatment in order to achieve an optimal response include patient characteristics, disease stage, genetic factors etc. Treatment consists of chemotherapy or chemoimmunotherapy, inhibitors of B cell receptor signalling or anti-apoptotic inhibitors such as BCL2 [55, 56].

1.5.5.2 Diagnosis

The diagnosis of CLL is usually through blood counts, differential counts, immunophenotyping, lymph node or bone marrow biopsies, and imaging. The number of circulating clonal B lymphocytes in the peripheral blood should be more than 5000 cells/ µL for three months and the phenotype of the malignant cells needs to be confirmed by flow cytometry. CLL cells are small, mature lymphocytes with a thin cytoplasmic membrane, a dense nucleus, absent visible nucleoli and partially aggregated chromatin [57].

CLL cells express the cell surface markers CD5 (a T-cell antigen), CD19, CD20, and CD23 (B-cell antigens) [58]. The levels of surface immunoglobulin CD20, and CD79b are lower in CLL compared with other normal B-cells. Prevalent cytogenetic aberrations, such as, 13 del (13q14.1), 11 del (11q), 6 del (6q), 17 del (17p) or Trisomy 12 are found in 80% of all CLL cases and can be confirmed by Interphase FISH [59].

Prognostic markers in B-CLL include the mutation status of Ig VH gene and the expression of CD38. Generally, patients with unmutated V_H experience more aggressive disease and inferior survival rates compared with patients with somatic mutations of IgVH [60, 61]. Other prognostic markers include ZAP70 expression, specific karyotypic abnormalities, disease stage (Rai and Binet classification) etc. [62].

1.5.6 Mantle cell lymphoma (MCL)

MCL is an intermediate grade mature B-cell neoplasm and accounts for 6% of all non-Hodgkin lymphomas (NHLs) [63]. The pathognomonic lesion in MCL is the chromosomal translocation t(11;14) resulting in abnormal expression of cyclin D1, which is not typically expressed in normal lymphocytes. Cyclin D1 causes cell-cycle progression and leads to pronounced genetic instability. MCL pathogenesis is mediated by several signalling pathways responsible for cell growth and survival, including the PI3K/ AKT/ mTOR pathway [64]. MCL can be difficult to treat and relapses are common with short median survival of 5-7 years [65].

1.6 Treatment of Lymphoid malignancies

The various classes of agents that are used in cancer therapeutics are depicted in **Figure 1.1**. They target either cell cycle specific events or function to disrupt DNA, RNA or protein function or processing within cancer cells. The chemotherapeutic agents that are employed either as single agents or in combination for treating lymphoid malignancies are based on the type and stage of the lymphoid malignancy [66]. Standard agents used in lymphoid cancers include cyclophosphamide (or ifosfamide), vinca alkaloids (such as vincristine and vinblastine), anthracyclines (doxorubicin), bleomycin, bendamustine, gemcitabine, platinum analogues, topoisomerase inhibitors (e.g. etoposide) etc. [67]. Steroids such as prednisolone or dexamethasone are lympholytic and routinely combined with chemotherapy [68].

The standard cytotoxic treatment for CLL patients is chemo-immunotherapy with FCR (Fludarabine, cyclophosphamide and rituximab) and can induce

long-term remissions. The combination of rituximab and bendamustine has also gained wide acceptance in low-grade lymphomas [69].

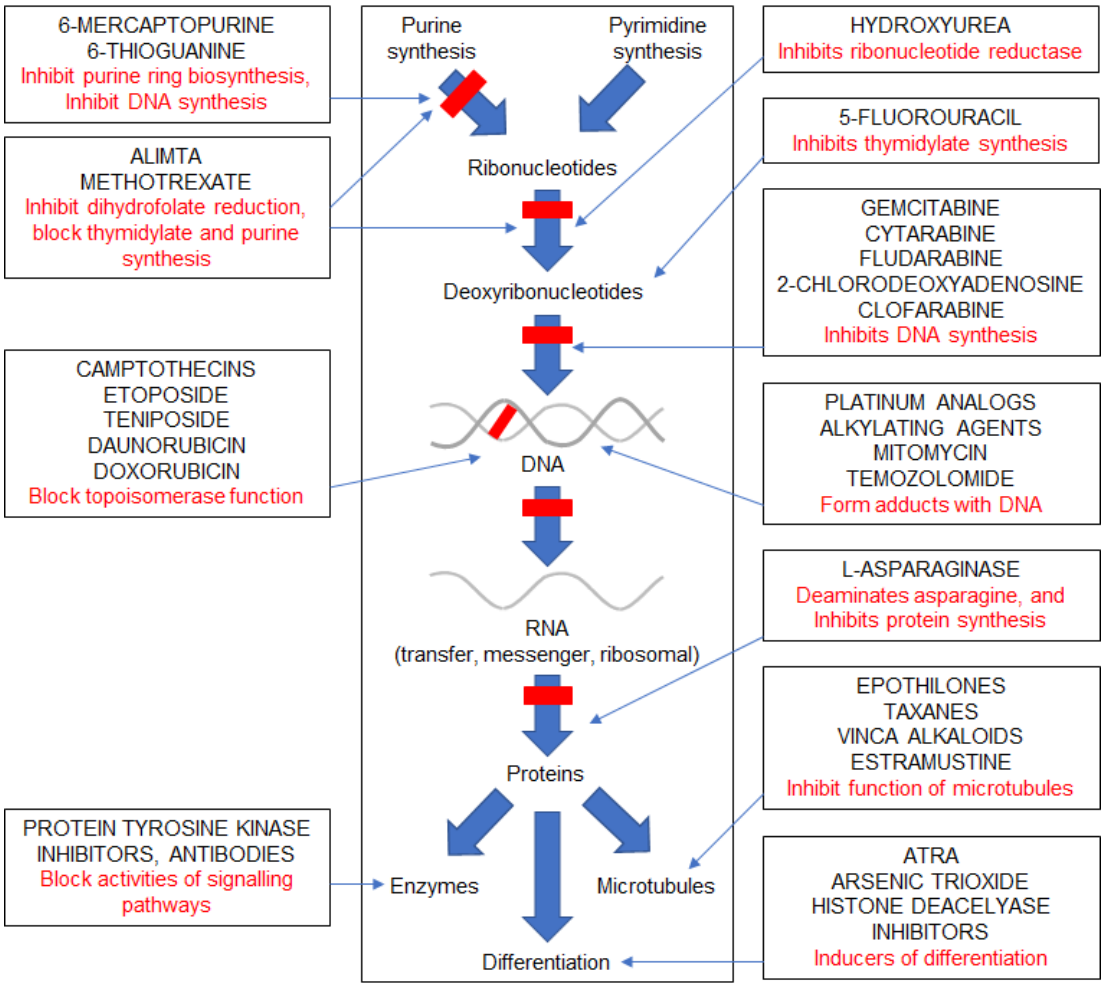

Figure 1. 1: Various classes of agents that are used in cancer therapeutics [70].

The incorporation of monoclonal antibodies into therapeutic regimens that target lymphocyte-specific antigens such as CD20 has significantly improved outcomes in B-lymphoid malignancies such as NHL. Other CD20 targeting monoclonal antibodies include ofatumumab and obinutuzumab [71].

More recently, small molecule inhibitors of the BCR signalling intermediates such as Bruton's tyrosine kinase (BTK) and phosphatidylinositol 3-kinase (PI3K) have emerged as major therapeutic agents in both CLL and MCL patients and induce peripheral lymphocytosis [72]. Similarly, venetoclax a small molecule inhibitor of the anti-apoptotic protein BCL2 is also emerging as a useful treatment especially in CLL.

Radiation can play an important role in the treatment of lymphomas as adjunct to chemoimmunotherapy. Lymphocytes respond to γ-irradiation during interphase. Radiotherapy causes apoptotic death of lymphocytes in interphase and pre-mitotic phases [73].

1.6.1 CLL treatments

1.6.1.1 Traditional chemotherapeutic agents

For many years, the mainstay of CLL treatment was monotherapy with alkylating agents. Chlorambucil was the gold standard for treatment but is associated with low complete response (CR) rates and propensity for side-effects after prolonged use such as; long-lasting cytopenias, myelodysplasia and secondary acute leukaemia [74, 75]. The combination of anti-CD20 monoclonal antibodies (MoAbs) with chlorambucil improves responses and the combination is now mainly used for elderly patients [76]. In more recent years, purine analogs such as Fludarabine have been used for CLL therapy mainly in combination with Cyclophosphamide and Rituximab (FCR) for fit and younger patients.

Fludarabine (FAMP) is a potent and extensively studied purine analog in indolent B-cell malignancies and recommended for frontline treatment of B-

CLL [77]. The presence of 9-β-d-Arabinofuranosyl-2-fluoroadenine 5′-triphosphate (F-ara-ATP) is essential for Fludarabine to aggregate intracellularly and inhibit DNA synthesis [78]. Fludarabine treatment can cause toxicities such as myelosuppression, immunosuppression and opportunistic infections especially in elderly and unfit patients. Fludarabine chemotherapy is associated with a poor outcome in patients with 17q- and p53 mutations [79].

Bendamustine is a novel agent that combines the alkylating properties of mechlorethamine and the purine antimetabolite properties of benzimidazole. Bendamustine inactivates DNA repair, affects the cell cycle through suppression of mitotic checkpoints, and promotes p53-dependent DNA-damage stress response to cause cell death. In clinical trials, Bendamustine has shown comparable or higher overall response rates (ORR) compared with chlorambucil [80].

1.6.1.2 Combination therapy and Chemo-immunotherapy

The combination of chemotherapeutic agents and monoclonal antibodies has improved the outcomes in CLL. The most beneficial combination includes fludarabine, cyclophosphamide and rituximab (FCR). Chemo-immunotherapy can prolong survival and is used as standard treatment for previously untreated CLL patients [81]. In clinical trials, the overall response rate with FCR was 95% with 72% achieving complete remission [82].

Recent studies investigating the efficiency of Bendamustine and Rituximab (BR) in recurrent CLL have shown an overall response rate of 59% with

activity in patients previously treated with Fludarabine [83]. A study conducted on 651 patients that compared BR and FCR in the frontline setting showed that the median progression free-survival was higher in the FCR than BR but was associated with more neutropenia and infections [84].

1.6.1.3 Monoclonal antibodies

Chemotherapeutic approaches during the last decade have failed to improve the overall survival in the CLL patients. In an effort to improve outcomes, several monoclonal antibodies are now routinely used in B-cell lymphomas.

Rituximab is a well-known chimeric (human-mouse) monoclonal antibody that targets the CD20 antigen on B-cells. Rituximab induces antibody dependent cytoxicity of B-cells and causes their apoptosis [85].

Ofatumumab is a humanized monoclonal antibody that recognises and targets a different epitope of the extracellular domain of CD20 compared to rituximab. It has shown activity in CLL [86].

Obinutuzumab is a fully humanized anti-CD20 monoclonal antibody that is approved in combination with chlorambucil for the treatment of patients with previously untreated CLL; it is also used in combination with bendamustine, for the treatment of patients with follicular lymphoma [87].

1.6.1.4 BCR signalling inhibitors

B-cell receptor (BCR) signalling is essential for survival and proliferation of CLL cells. In CLL, several tyrosine kinases mediate BCR signalling and include Bruton tyrosine kinase (BTK), Spleen tyrosine kinase (Syk), ZAP70,

Src family kinases (Lyn), and Phosphatidylinositol-3-phosphate (PI3K). Targeting BCR receptor signalling has emerged as a potential strategy for CLL therapy. Inhibitors of BCR signalling do seem to improve the prognosis of the disease [88].

BTK is a key mediator of BCR signalling in CLL cells that impacts downstream cell survival pathways and several inhibitors are now emerging as potential treatments. These include ibrutinib, acalibrutinib etc.

Ibrutinib is a potent BTK inhibitor that is now approved for the treatment of CLL due to promising results in recent clinical trials [89]. Ibrutinib is effective in both low- and high-risk CLL patients, and leads to lasting remissions with continuous therapy in the majority of patients. Ibrutinib lacks myelotoxicity and is well tolerated by older and unfit patients.

Other BCR signalling inhibitors with activity in low-grade lymphomas include those that target PI3K signalling.

Idelalisib is a small-molecule inhibitor of PI3K selective for the δ isoform that promotes apoptosis of CLL cells in patients with relapsed or refractory disease [90]. **Duvelisib (IPI-145)** is a PI3k inhibitor that inhibits both δ and γ isoforms [91].

Venetoclax (ABT-199) is a highly selective inhibitor of BCL2 that induces apoptosis of CLL cells [92]. It is used for relapsed/ refractory CLL patients, including those with high-risk genomic features such as; chromosome 17p deletion, mutated p53, or progressive disease following B-cell receptor pathway inhibitor treatment failure [93, 94].

1.6.2 MCL treatment

The mainstay of treatment for MCL is combination chemo-immunotherapy with a good initial response. For patients younger than 65 years a more aggressive approach has been advocated. This includes either Ritoximab-cyclophosphamide, doxorubicin, vincristine, and prednisone (R-CHOP) chemotherapy or more intensive regimes (NORDIC protocol) that incorporate cytarabine followed by transplantation. The combination of Rituximab and Bendamustine can be used for older patients or as sequential therapy in recurrent MCL. Agents such as; Ibrutinib, lenalidomide, temsirolimus, and bortezomib, are reserved for patients with relapsed disease or those who fail frontline treatments [95].

1.7 Effects of chemotherapy or radiation treatments on CLL and low-grade NHL

Chemotherapeutic agents induce DNA damage and cancer cell death via immunogenic cell death, apoptosis and other forms of non-apoptotic death, including senescence, mitotic catastrophe and autophagy [96]. Radiotherapy is generally an immune-stimulatory process that causes immunogenic cell death, inflammatory reactions and recruitment of T cells to the tumour microenvironment. Radiotherapy causes lysis of cancer cells. Release of tumour-associated antigens attract T-cells and dendritic cells and elicit an anti-tumour response [97].

Exposure to chemotherapy can cause several early and late long-term toxicities, including ovarian failure (with resultant infertility and sexual dysfunction), bone loss, weight gain, neurotoxicity, neurocognitive changes,

cardiac toxicity and secondary malignancy. Such effects have the potential to reduce the life quality and overall health status. Understanding such chemotherapy-related toxicities is of utmost importance [98].

Whilst the effects of cytotoxic chemotherapy on normal bystander cells is widely studied, the specific effects of treatments on cancer genomes is also of importance. Persistence of DNA abnormalities introduced into cancer cells (mutations and chromosomal aberrations etc.) can result in further genomic instability. A similar outcome is also envisaged for radiotherapy. Hence, understanding the long-term effect of radiotherapy and chemotherapy is of interest and important [99, 100].

DNA damage and misrepair can persist within normal bystander cells as well as cancer cells and lead to clonal evolution with more aggressive features. Such abnormalities include the formation of abnormal nuclear bodies called micronuclei [101].

1.8 Micronuclei

1.8.1 Micronuclei formation

Micronuclei (MN) are small extranuclear bodies formed during cell division when the chromosome or a part of the chromosome fails to join the mitotic spindle, during M phase [102]. MN are formed spontaneously or induced by chromosomal breaks that form an acentric/ whole chromosome fragment. These chromosome fragments are not incorporated into the main nucleus during the restructure of nuclear envelope around two daughter cells at

telophase. Thus, they encapsulate and break up into small nuclear fragments called micronuclei (**Figure 1.2**) [103, 104].

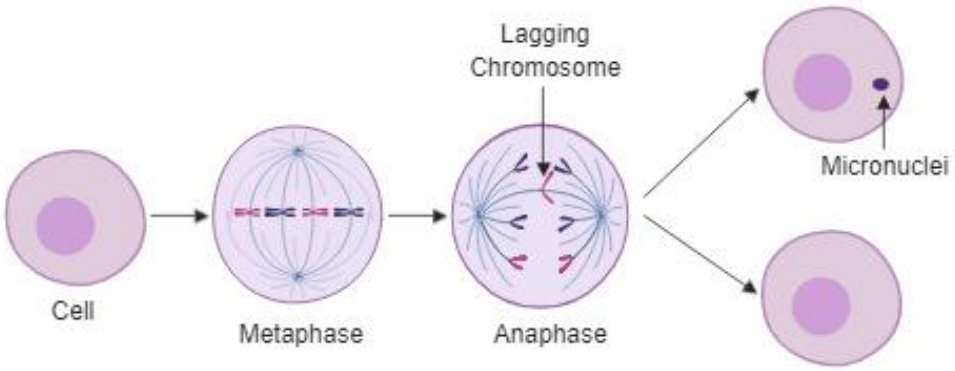

Figure 1. 2: Micronucleus formation in the cell [105].

Several studies have described the effects of the exposure to genotoxic agents that result in chromosomal aberrations and genomic instability of cancer cells leading to clonal evolution and progression [106]. Genotoxic agents can induce formation of MN [107]. Identifying MN is an effective method for determining genotoxic effects of chemo-radiotherapy [108].

In cancer cells, mutated p53 alleles lead to reduce apoptosis. A published study showed that the cells with mutated p53 formed more MN after treated with chemotherapy or irradiation compared with the cancerous cells with wild-type p53 gene as the p53 protein expression is essential for the balance between cell cycle arrest, DNA repair and apoptosis induction [109].

A published study on patients with breast cancer specified that significant increases in MN frequencies in both groups of patients; at the diagnosis stage (baseline damage) and after RT. The study also investigated the

relation between control group and baseline damage. The results showed that the patients after RT have higher MN count. This indicates that, after RT, the patients were more genetically unstable, probably due to the effects of aneugenic and/or clastogenic [110].

Defects of DNA repair mechanisms of chromosome breaks leads to the formation of di-centric chromosomes, which are the chromosomes with two centromeres. This process can impair genomic stability predisposing cells to carcinogenesis [111]. In addition, a defect in the spindle or centromere-kinetochore complex can also prevent aberrant chromosomes to attach to the mitotic spindle. These structural changes in chromosomes can lead to the formation of MN [112].

The genotoxicity of anti-cancer drugs has previously been assessed using MN enumeration. For e.g. Adriamycin can cause significant MN formation in cells that survive its cytotoxic effects [113]. MN may also be induced by exposure to gamma-rays [114].

Cells that harbour abnormal mitotic events exhibit MN formation [115]. Multipolar mitosis is a defect in mitosis, where the chromosomal material is pulled to more than two poles. This phenomena can generate lagging chromatids or chromatin bridges, which are stimulated by low concentrations of anti-cancer chemotherapy drug such as hydroxyurea [116]. Generally, it is thought that micronuclei are formed from whole chromosomes or fragments [117]. Several published studies suggest that epigenetic regulators play an important role in MN formation [118]. Kinetochore orientation and the attachment to the mitotic spindle are affected by the presence of DNA

hypomethylation in the centromeric region leading to defects in chromosome segregation and subsequent formation of MN [119]. However, the genotoxicity of arsenic categorized by the production of free radicals, alter the DNA methylation, reduce of DNA repair and formation of MN. In a published study showed that the treatment with S-adenosyl-methionine (SAM) reduced arsenic and leads to the formation of MN that containing fragments of chromosomes. This finding indicated that SAM may prevent chromosome loss and aneuploidy, but not able to reduce chromosomal breaks and clastogenicity [120].

A previous study used lymphocyte cultures to prove that 5-azacytidine is significantly stimulated the heterochromatic regions of chromosomes 1, 9, 15, 16, and Y which associated with the induction of MN frequency [121].

Another study investigated the relation between MN count and folate as an essential B group vitamin which engage in homocysteine cycle and plays a crucial role as a methyl donor in the folate-methionine pathway [122]. A published study on human lymphocyte has shown a relation between folate deficiency and DNA damage, MN formation and other nuclear anomalies [123]. The study outcome showed that DNA damage and MN formation are obviously reduced after Folate supplementation [124].

1.9 Potential biomarkers of chromosomal abnormalities

Nuclear anomalies are initiated by structural errors in a chromosome or due to abnormal number of chromosomes. Such anomalies include nucleoplasmic bridges (NPB) and nuclear buds (NBUD) and are biomarkers

of genotoxic events and manifestations of chromosomal instability that often indicate cancer risk. Genetic damage events such as MN, NPB and NBUD provide valid measures of mis-repaired DNA breaks [125]. MN, NPB and NBUD formation could be due to the multiple molecular mechanisms. Several studies have reported the association between MN, NPB and NBUD. Increased frequencies of MN, NPB and NBUD in lymphocytes are associated with higher levels of DNA damage [126].

1.10 Clonal evolution in cancer

Clonal evolution can contribute to disease progression in human cancers and is a characteristic of cells that survive anti-cancer treatments [127]. Chemotherapy can stimulate clonal evolution, metastasis and relapse of tumours in about 20% of cases (**Figure 1.3**) [128].

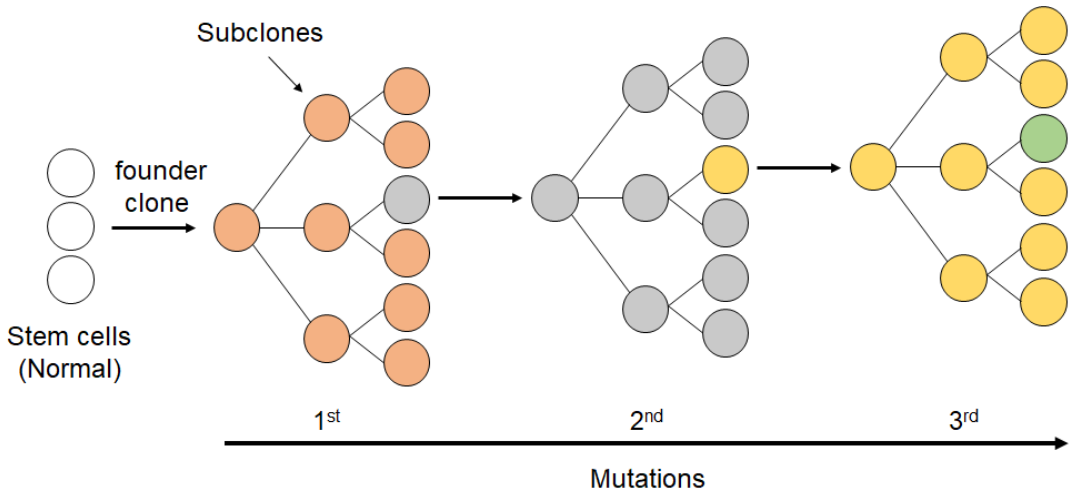

Figure 1. 3: Clonal evolution of cancer [129].

Toxicity associated with chemotherapy is a major therapeutic challenge and is caused by chemotherapy-induced DNA damage and inflammation.

Chemotherapy causes selective pressure that creates tumour heterogeneity and subsequent clonal evolution [130]. Target therapies are improving the outcomes of many cancers with less side effects. Whether such specific treatments can also cause DNA damage, genomic instability and chromosome aberrations is less clear.

The clonal evolution that causes genomic instability could be responsible for more aggressive behaviour of cancer cells [131]. This may manifest as higher frequencies of MN due to genomic instability in parallel with the accumulation of mutations. Serial measurements of MN could be useful to monitor levels of DNA damage with various treatments and provide clues to clonal evolution.

1.11 Assessment of DNA damage

There are different strategies include several assays available to investigate DNA damage. Most of these techniques are not automated or semi-automated, which increase the necessity to improve an automated technique.

1.11.1 Techniques for the analysis of DNA damage

DNA breaks and lesions can be detected by PCR or using agarose gel electrophoresis [132]. Detection of γH2AX protein phosphorylated at Serine-139 is useful for detecting and quantifying DNA DSBs, as the number of Serine-139-γH2AX molecules is associated with the levels and sites of DNA damage [133]. γH2AX activates within seconds after DNA damage in order to recruit and maintain DNA repair and signalling factors to regulate DSBs [134]. The advantages of this technique that allow evaluating treatment

efficiency, quick technique, and high sensitivity assay. The disadvantage of this assay that the detection of γH2AX affected by the level of background which differ between various tumour cells [135].

1.11.2 Fluorescence-based assays

The Comet assay is simple and considered to be one of the gold standard methods for measuring single and double DNA strand breaks in eukaryotic cells, UV-induced pyrimidine dimers, oxidized bases and alkylation damage following the introduction of lesion-specific endonucleases [136].

DNA breakage detection (DBD) - fluorescence in situ hybridization (FISH), is used to visualize nucleic acids. The resolution, speed and safety of this technique is much improved compared with older methods that use isotopic detection. FISH allows detection and quantification of SSBs and DSBs in the genome or in a specific DNA sequence within single cells [137].

Another technique called FCM-Annexin V, is a labelling stain used for differentiating between necrosis, and apoptosis after DNA breakage. FCM was developed to detect apoptosis; this method allows for the measurement of a large number of cells, and also used to detect DNA strand fragmentation and chromosomal aberrations [138].

1.11.3 Chemiluminescence based assays

Chemiluminescence depends on the emission of light during a chemical reaction. Immunological assay is one of the main techniques for measuring the presence of oxidative DNA via the immuno-blot system, and uses chemiluminescent detection and secondary antibodies that are conjugated to

alkaline phosphatase enzymes and radioactive iodine [139]. The advantages of this assay are dynamic range, stronger signal intensity, high specificity, stability of reagents and their conjugates, and short incubation time. While the disadvantages are; limited Ag detection, expensive, limited tests panel, and low background level of emission in the lack of analyte [140].

1.11.4 Analytical strategies

High performance liquid chromatography (HPLC) and electrospray tandem mass spectrometry (MS) were improved with an electrospray ionization mode. These techniques seem to be a sensitive and accurate method to detect modified bases due to the oxidative-damaged DNA and UV-induced dimeric pyrimidine [141, 142]. The disadvantages of this assay that are expensive and complicated in troubleshoot problems or to develop new methods.

1.11.5 Methods to assess Micronuclei

The significance of MN was evaluated in the mid-twentieth century. Dawson and Bury (1961) found MN in red cells within the bone marrow during different pathological states. The formation of Howell–Jolly bodies was also observed with folic acid and vitamin B deficiency. Later, MN were described in lymphocytes following irradiation *in vitro* with the demonstration that there is a linear relationship between the dose and micronucleus induction [143, 144].

The Cytokinesis-block micronucleus (CBMN) is the gold standard technique used to enumerate MN within cells. This is a widely used method for

genotoxic studies, especially in the context of environmental mutagens and to assess safety of potential agents for agricultural and pharmaceutical use [145].

Recent studies have focused on the use of automated techniques for MN enumeration: e.g. Flow cytometry and MN counting by image analysis. Both of these techniques have their advantages and disadvantages. The disadvantages of flow cytometry is that the results cannot be rechecked after measurement and data on MN frequencies in individual cells cannot be inferred [146]. The drawback with image analysis is that sometimes the background signals might affect the results of the MN count [147]. The main advantages of the automated systems are the fast acquisition of results, which allows the analysis of large numbers of slides or cell populations and the exclusion of subjective judgement and individual scoring skills and can be less time consuming [148].

1.12 Summary

Micronuclei can serve as important biomarkers to predict and investigate DNA damage in several cancers [149]. MN form in the cells due to exposure to cytotoxic agents. Two main factors that affect the frequency of MN are the levels of DNA damage and the efficiency of DNA repair mechanisms [150].

Cancers such as CLL and other low-grade lymphomas frequently require serial and recurrent chemotherapeutic approaches as well as radiotherapy in some cases. Such treatments could increase the levels of DNA damage and genomic instability and may be reflected in MN counts within cells.

1.13 Hypothesis

Robust and reproducible methods for enumeration of MN frequency can be used to assess cumulative DNA damage following cancer treatments.

1.14 Aims and objectives

The aims of this thesis are:

1- To establish and optimise an objective flow cytometry based technique to enumerate MN in cell populations.
2- Compare the optimized flow cytometry technique to existing methods to assess DNA damage.
3- Understanding the effects of sequential chemotherapeutic treatments and accumulation of genomic instability on the formation of MN.
4- Investigate MN frequencies in CLL cells from treated and untreated patients.

These aims discussed in more details in the introduction section for each chapter.

The following chapter (**Chapter 2**) describes the general materials and methods used in this thesis. Four experimental chapters followed by the summary and conclusions, general discussion and suggestions for future work.

Chapter 2: Materials and Methods

This chapter describes the general materials and methods employed during the course of the project. Techniques and methods of importance to specific chapters are described in relevant sections and chapters. Buffer recipes, lists of antibodies, and details of primary CLL cases are included in Appendix B.

2.1 Tissue culture

2.1.1 Cell lines

The details of cell lines used in this thesis including; origin, growth pattern and doubling time are summarised in **Table 2.1**. Suspension cell lines were purchased from Leibniz Institute (DSMZ) German collection of Microorganism and cell culture, Germany. HeLa cells were a gift from Dr Jason Parsons, North West Cancer Research Centre, University of Liverpool, UK and CD154 expressing fibroblasts were purchased from the American type culture collection (ATCC), USA.

Cell lines were cultured and maintained in vented culture flasks under aseptic techniques within a secondary tissue culture cabinet. MEC-1 cells were grown in complete Iscove's Modified Dulbecco's Medium (IMDM) (Sigma Aldrich, UK), whereas the other suspension cells were cultured in Roswell Park Memorial Institute medium (RPMI) (Sigma Aldrich, UK). All media were supplemented with L-glutamine (4mM), penicillin (1000 units/ml),

streptomycin (1 mg/ml) (Sigma Aldrich, USA) and Fetal bovine serum (FBS) (10% v/v) (Life Technologies, USA).

The HeLa cell line and CD154 expressing fibroblasts were cultured in Dulbecco's Modified Eagle Medium (DMEM) with added glucose (4500 mg/L) (Sigma Aldrich, UK) and 4mM L-glutamine, penicillin (1000 units/ml), streptomycin (1 mg/ml) (Sigma Aldrich, USA) and Fetal bovine serum (FBS) (10% v/v) (Life Technologies, USA).

2.1.2 Maintenance of Suspension cell lines

Suspension cultures were maintained in Roswell Park Memorial Institute (RPMI) media for EHEB, HG3, MAVER-1 and JeKo-1 cells and Iscove's Modified Dulbecco's Media (IMDM) media for MEC1 cells. Cells were passaged every 2-3 days to maintain optimal growth and nutrients. Cells were split by re-suspending the cells 1:3 with fresh IMDM medium. Cell lines were cultured and maintained in a humidified incubator at 37˚C with 5% carbon dioxide (CO_2) for downstream experiments and discarded after ten sub-passages [151].

2.1.3 Maintenance of Adherent cell lines

Adherent cell lines were passaged (1:4) every 3-5 days to maintain optimal growth. Cells were detached by adding 2 ml of Trypsin/ Ethyene-diamine-tetra-acetic acid (EDTA) (Sigma Aldrich, USA) and incubating at 37˚C for 5 mins. Flasks were gently tapped and detached cells were re-suspended with DMEM medium to stop the trypsin/EDTA activity. Harvested cells were

centrifuged at 500 g for 5 mins, and re-suspended with 15 ml fresh complete DMEM medium and transferred to a new flask. Cells were incubated in a humidified incubator at 37˚C with 5% carbon dioxide (CO_2) until use and discarded after 10 passages.

Table 2. 1: Features of cell lines used in this study [152-157].

Cell line	Cell type	Patient age/ sex	Doubling time (h)	Karyotype
HeLa	Adenocarcinoma	31/ Female	23	der(1) t(1;3)(q11;q11.2) and der(1;9)(p10;q10)
EHEB	Chronic B cell leukaemia	69/ Female	50-70	Normal or +11
MEC-1	Chronic B cell leukaemia	61/ Male	40	12-, 17p-
HG3	Chronic B cell leukaemia	70/ Male	50-70	13q- ×2
MAVER-1	Mantle Cell Lymphoma	77/ Male	24	t(11;14)
JeKo-1	Mantle Cell Lymphoma	78/ Female	24-72	t(10;11;14)

2.1.4 Cell viability and counts

Cell counts and viability were checked for both primary CLL cells and B-cell lines using plastic counting chambers (VWR International Hunter Boulevard, UK) using a trypan blue exclusion assay. This dye penetrates dead cells through ruptured cell membranes and is not able to stain the live cells with intact membranes. Cells were diluted 1:1 with trypan-blue, mixed and 20 µl loaded onto counting chamber. Both cell counts and viability (%) were measured using Nexcelom apparatus (Nexcelom Biosciences, UK) and Cellometer Auto T4 software.

2.1.5 Irradiation of cell lines and CD154 expressing fibroblasts

Harvested cells were irradiated using Gammacell® 3000 Elan. Cell lines were irradiated with 3Gy or 5Gy by exposure for 60 sec and 84 sec respectively. CD154 expressing fibroblasts were irradiated with 72Gy for 20 mins based on the following equation to calculate length of exposure to irradiation: Time (mins) = Gy / 3.59268 (Central dose rate x decay factor). After irradiation, fibroblast cells were counted and plated at a density of 4×10^5 cells/ml. Cells were incubated overnight at 37˚C to allow fibroblast cells to promote adherence before co-culture experiments.

2.1.6 Cryopreservation of cell lines

Cells were grown to a density of 4×10^7 cells/ml to prepare at least 10 vials for storage. Cells were centrifuged at 500g for 5 mins and re-suspended with ice cold DMEM/ RPMI/ IMDM medium containing 10% FBS depending on the cell type. Then complete medium containing 20% Dimethyl Sulfoxide

(DMSO) (Fisher scientific, UK) was added to the cell suspension over 30 mins using a drop wise technique to a final ratio of 1:1. The resulting cell suspension was transferred to cryopreservation vials in 1 ml aliquots containing 4×10^6 cells and stored at -80°C before transfer to a -150°C freezer for long-term storage [158].

2.1.7 Revival of cryopreserved cells

Cryopreserved cells were quickly thawed at 37°C in a water bath and transferred to 20 ml universal tubes before complete medium was added drop-wise while the cells were on ice. Cells were centrifuged at 500 g for 5 mins and re-suspended with fresh medium before culture.

2.1.8 Preparing growth arrest cell lines

Some experiments required the use of growth-arrested cells in G_0/G_1 phases of the cell cycle. Cells were cultured at a density at 1×10^6 cells/ml, washed with phosphate buffer saline PBS and re-suspended in serum low medium (1% FBS) for 24hrs prior to the experiment. The following day cells were spun at 500 g for 5 mins and re-suspended in fresh medium before irradiation [159].

2.1.9 Mycoplasma detection

Every six weeks our lab required quality control testing for Mycoplasma infection using a e-Myco^{TM} Mycoplasma PCR Detection Kit (ver. 2.0) (Lilif Diagnostics, iNtRON Biotechnology, Korea) following manfacturer's protocol guidelines.

2.2 Techniques to assess DNA damage

2.2.1 Cytokinesis Block Micronucleus Cytome (CBMN) assay

DNA damage was induced by gamma irradiation at 3Gy or 5Gy with a 0Gy control. Cultured HeLa cells were harvested and re-suspended at density of 3×10^5 cells/ml in 6mls complete DMEM containing 4.51 µg/ml Cytochalasin B (Sigma Aldrich). Cells were then seeded in 6-well plates for each irradiation exposure and also for time points 0, 24 and 48 hrs. At each time point cells were harvested by trypsinisation and washed. Cytopsins (800 rpm/ 6 mins) for each concentration and time point were performed, and slides were then dried for 30 mins.

Slides were fixed with methanol for 10 mins and then stained with May Grunwald's solution (diluted 1:1 with phosphate buffer solution (PBS)) for 10 mins, followed by Giemsa staining (diluted 1:10 with PBS) for 20 mins. Slides were rinsed with PBS to remove excess stain and then dried. Slides were observed using a light microscope and scored for micronuclei and nucleoplasmic bridges in bi-nucleated cells [160].

2.2.2 Comet Assay

HeLa cells (3×10^5 cells/ml) were irradiated in a Gammacell® 3000 Elan to induce DNA damage. Concentrations of gamma irradiation used were 3Gy (50 Sec) or 5Gy (84 Sec). Cells were then centrifuged at 500 g for 5 mins and re-suspended in complete DMEM media and incubated at 37°C for 0, 10 mins, or 1, 24 and 48 hrs in 6-well plates. HeLa cells were then mixed with 1% low melting point agarose gel (Sigma Aldrich, UK), and immediately transferred to slides pre-coated with normal melting agarose slide (1%) and protected with a coverslip (22mm × 50mm). Slides were placed on ice for 2 - 3 mins to ensure that the agarose had completely set. Coverslips were then removed and slides placed in the cold cell lysis buffer (10 mM Tris (pH 10.5), 2.5 M NaCl, 100 mM Ethylenediaminetetraacetic acid (EDTA), 1% DMSO and 1% Triton-X-100) and incubated overnight at 4 °C to prevent DNA repair.

Slides were then placed in electrophoresis buffer (300 mM NaoH, 1mM EDTA, and 1% DMSO) in a darkened electrophoresis tank to allow the DNA to unwind for 30 mins and then electrophoresed at 25V (300 mA) for 25 mins.

Slides were then washed three times (5 minutes each) with neutralization buffer (500 mM Tris-HCL, pH 8.0) and then dried overnight in the dark. Slides were rehydrated after 24 hrs with distilled water (pH 8.0) for 30 mins and stained with SYBR gold (Life Technologies, USA) diluted 1:10000. Slides were dried, images captured using a fluorescent microscope (Olympus) and FRAP-AI (MAG Biosystems Software), and analysed using Image J 1.48 (Open Comet Software) [161].

2.2.3 Detection of H2AX phosphorylation by Flow cytometry

Cells were harvested at a density 1.5×10^6 cells/ml. Cells were exposed to irradiation (3Gy) and incubated in a CO_2 incubator at 37˚C. Cells were collected at 0, 0.5, 1, 2, 6, or 24 hours. For each time point, cells were centrifuged at 450 g for 5 mins and washed with 5 ml PBS and centrifuged again (450g/ 20 mins). Cell pellets were re-suspended with 400 μl PBS and cells fixed by adding 400 μl of cell suspension dropwise to 1ml ice cold 70% ethanol before transferring to -20˚C for 1 hr. The cells were then transferred to 1.5 ml Eppendorf tubes and centrifuged at 1400 g for 7 mins at 4˚C. After removal of supernatant cells were re-suspended in 1 ml PBS and centrifuged at 1400 g for 7 mins at 4˚C. Finally, after discarding the supernatant cells were re-suspended in 1.4 ml (PBS + 0.25% Triton X-100) and incubated on ice for 25 min. Cells were used to study protein expression and an isotype control included. Cells were centrifuged at 1400 g for 7 mins and re-suspended in 100 μl PBS-BA (PBS containing 1% bovine serum albumin and 0.02% sodium azide) + 0.75 μg rabbit polyclonal anti-phospho Histone H2AX (Ser139) antibody (Cell signalling technology, UK). The tubes were incubated at room temperature for 2-3 hours with inversion every 15 mins. In parallel a cell pellet was re-suspended in 100 μl PBSBA + 0.75 μg rabbit IgG Isotype control (Invitrogen, UK). Cells were centrifuged at 1400 g for 7 mins and supernatant discarded. The pellet was the re-suspended in 1.3 ml of PBS-BA. After further centrifugation (1400 g for 7 mins), the cell pellet was re-suspended in 100 μl PBS-BA containing Alexa - labelled donkey anti-rabbit secondary antibody (Invitrogen, UK) and incubated for 30 mins at room temperature in the dark with gentle mixing. Add 1.3 ml PBSBA and invert to

mix, then centrifuge at 1400 g for 7 mins. After a final centrifugation step, the samples were analysed by FACS [162].

2.2.4 Micronuclei enumeration using a Flow cytometry based assay (MN-FACS assay)

Suspension or trypsinised adherent cells were re-suspended at a density of 3×10^5 cells/ml in complete DMEM or RPMI media and irradiated with 3Gy or 5Gy. A non-irradiated sample was included as a negative control for each experiment. Cells were incubated for 0, 24 or 48hrs. Cells were washed with 2% PBS and re-suspended in 300 μl of EMA solution (0.125 mg/ml in PBS with 2% of FBS). Place the tubes on ice and allow to photo-activation for 25 mins. The tubes should be protected from light during the remaining steps. The samples were washed twice with ice cold PBS containing 2% FBS and then centrifuged at 500 g for 5 mins before a two-step lysis. Initially the cells were incubated in the dark for 90 mins in 500 µl lysis buffer containing 1 µg/ml DAPI (Sigma-Aldrich), 0.584 mg/ml NaCl (Melford), 1mg/ml Sodium Citrate (Sigma-Aldrich), 0.3 µg/ml IGEPAL-630 (Sigma-Aldrich), and 250 µg/ml RNase A (Invitrogen). Then 500 µl of lysis buffer 2 (1 µg/ml DAPI, 85.6 mg/ml Sucrose (Sigma-Aldrich), 15 mg/ml Citric Acid (VWR), pH 9.7 with NaOH (Sigma-Aldrich)) was added. Cells were then vortexed and incubated in the dark for another 30 mins. The cells were spun at 10000 g for 10 mins and the supernatant gently discard and re-suspended in 500 µl FACS flow buffer (BD Biosciences) and passed through a 0.22 µm filter (Millex Gp, Ireland) to remove any micro particles before FACS analysis. Ten thousand DAPI positive events were analysed per sample [163].

2.3 Flow cytometry techniques

2.3.1 Measuring cell apoptosis

Cell apoptosis was measured by flow cytometry using Annexin V/ PI staining. 3×10^5 cells were re-suspended in 100 μl Annexin V binding buffer (10mM HEPES, 140 mM NACL, and 2.5 mM $CaCl_2$). Then, 2 μl of Annexin V-FITC (BD Biosciences, UK) was added and incubated for 8 mins. Following this step 5 μl of PI stain (Sigma/ UK) (1.0 mg/ml in water) diluted (1:20) in dH_2O was added to each sample and incubated in the dark at RT for 5 mins. Finally, 200 μl of Annexin V binding buffer was added prior to FACS analysis [164].

2.3.2 Cell cycle analysis

0.5×10^6 cells/ml were washed with PBS, and 70% ethanol added dropwise to ensure fixation and minimize clumping. The fixed cells were placed on ice for 30 mins, and centrifuged at 550 g for 5 min. The cells were washed twice with 500 μl PBS. The cells were then treated with RNase (50 μl of 100 μl/ml stock was added) and incubated at 37˚C for 30 mins. Finally, 20 μL of PI stain (1 mg/ml stock) was added for 5 mins before FACS analysis [165].

2.3.3 CFSE staining to assess cell division rates

This stain was used to gauge the number of mitotic events. During cell division the CFSE fluorescence intensity reduces by half in the daughter cells as monitored by flow cytometry at different time points (1 to 9 days). Briefly, cells were harvested at a density of 3×10^6 cells/ml, spun at 500 g for 5 mins,

and re-suspended in PBS. Then, CFSE stain CellTrace™ Cell Proliferation Kits (C34554) (Thermo Fisher Scientific, UK) was added to the cells to an effective 1:1000 dilution (stock concentration: 0.5 mM), and cells incubated for 30 mins in a 37˚C water bath. All the samples should be protected from light with constant shaking every 5 mins. Then, the cells were centrifuged at 500 g for 5 mins and re-suspended in fresh RPMI medium and incubated for 15 mins at 37˚C in a CO_2 incubator. Lastly, cells were subjected to centrifugation at 500 g for 5 mins and re-suspended with the fresh RPMI to a cell density of 5×10^6 cells/ml for primary cells before FACS analysis.

2.4 Isolation of primary CLL cells

Ethical approval for blood collection, processing and biobanking for the project is in place and is part of a wider approval granted to the University of Liverpool Leukaemia Biobank. Standard operating procedures (SOP) for collection, handling and processing are in place within the department. Peripheral blood samples were obtained from consented CLL or MCL patients and collected in BD Vacutainer® CPT™ Heparinised tubes.

Whole blood was slowly layered over Lymphoprep™ (Alis-Shield PoC AS, Oslo, Norway) in a ratio of 2:1 in 50 ml falcon tubes (e.g. 50 ml of whole blood to 25 ml of Lymphoprep). The tubes were centrifuged at 800 g for 30 mins with slow deceleration. Peripheral blood mononuclear cells at the interface of plasma and Lymphoprep™ were collected and diluted in 50 ml of RPMI-1640 medium (Sigma Aldrich, Gillingham, UK) for washing and then centrifuged at 550 g for 10 mins. The supernatant was discarded and cell pellet re-suspended with cold FCS before cell counting using a

haemocytometer. The number of desired lymphocyte cells needed for MN-FACS assay were collected at this stage [166]. The purity of CLL cells has been check by flow cytometry using CD5, CD19, and CD20 antibody markers.

2.5 Induction of CLL cell proliferation by CD154-expressing fibroblasts + IL21 + IL-4

To induce CLL-cell proliferation by CD40 + IL-4 + IL-21 stimulation CLL cells were collected at a density 5×10^6 cells/ml and re-suspended in fresh RPMI medium supplemented with 10 ng/ml recombinant human IL-4 and 15 ng/ml recombinant Human IL-21, (Invitrogen, USA) before layering on CD154 fibroblasts. The multi-well plates included a negative control (no IL-21 + IL-4) with only CD154-expressing fibroblasts and CLL cells. Some cells were plated after exposure to irradiation and treated with IL-21 and IL-4 as a positive control. At day 4 and 7 the culture medium was partially replaced with fresh complete RPMI medium supplemented with the fresh IL-4 and IL-21. Then, at the selected time points CLL cells were harvested and analysed using flow cytometry [167].

2.6 Statistical analysis

The data in this thesis were analysed by using GraphPad Prism 6 and ImageJ (Open Comet) software. Details of analyses are indicated in the relevant results section.

Chapter 3: Establishment and optimization of a Flow cytometry based micronucleus enumeration assay

3.1 Introduction

All organisms and their constituent cells are constantly exposed to endogenous or exogenous insults that can induce varying degrees of DNA damage. DNA damage can be transient or permanent with multiple consequences as shown in (**Figure 3.1**) and cumulative changes may affect the organism or impact future generations [168].

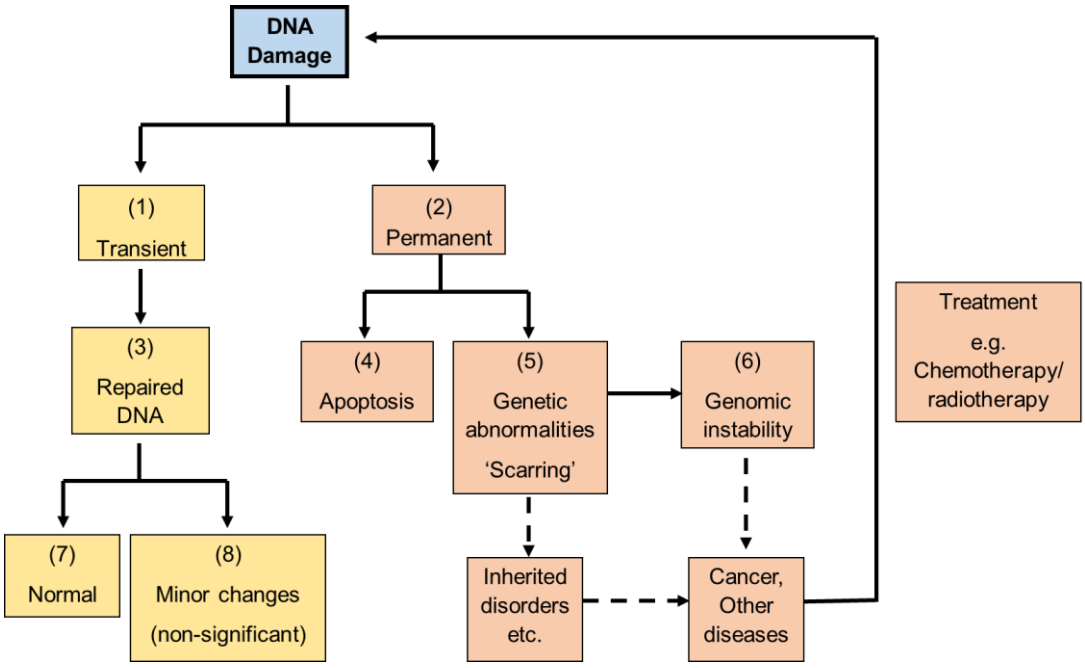

Figure 3. 1: Consequences of DNA damage. This schematic figure summarizes the potential consequences of transient or permanent DNA damage.

Such genotoxic exposures may result in genomic instability and cause various disease states, including cancer [169]. Paradoxically, cancer treatments, such as chemotherapy and radiotherapy, may also induce DNA damage that may have long-term consequences.

Qualitative and Quantitative assessment of cumulative DNA damage within cells may help us to understand its relevance for cellular behaviour. Moreover, assessing the types and levels of DNA damage within cells may be useful to understand the thresholds for survival, long-term effects, apoptosis and disruption of cellular homeostasis [170].

Over the years, many assays have been developed to study and assess DNA damage and subsequent repair pathways. These have found wide applications including the pharmaceutical sector for assessing drug safety and toxicities, and to improve drug design.

Understanding the levels of DNA damage within cells can help in predicting the risks of particular diseases especially in the context of aging, impact of drugs, toxins and therapies [171, 172].

Techniques traditionally employed to assess DNA damage are summarised in **Table 3.1**.

Table 3. 1: Traditional techniques to assess DNA damage (adapted from references [173, 174]). The table provides a summary of each technique with a focus on advantages and disadvantages. The numbers in Column 3 (Purpose) are cross-referenced to the specific defects mentioned in Figure 3.1: i.e. 1) Transient; 2) Permanent; 3) DNA repair; 4) Apoptosis; 5) Genetic abnormalities (Scarring); 6) Genetic instability; 7) Normal; 8) Minor changes (non-significant).

Assays to assess DNA damage	Year established	Type of DNA damage assessed	Advantages	Disadvantages
Halo assay	1965	4	• Able to measure the DNA damage of a single cell. • No labelling of DNA with radioactive precursors required.	Not sensitive.
DNA breakage detection (DBD) - FISH	1970	1, 2, 5, 6	• High resolution through visualization of nucleic acids. • Fast and safe compared to other methods that use radio-isotopic detection.	Less reproducibility and irregularity of the signals, and background auto-fluorescence.
Comet assay	1984	1, 2, 3	• Low cost, low number of cells required. • Detection of DNA strand damage in individual cells and in	• Time consuming, and has multiple steps • May not detect small fragments of DNA.

			cell populations. • Widely accepted method	• Cell Type Dependent (and not applicable to all cell types).
Cytokinesis-block micronucleus cytome assay	1990	1, 2, 6, 7, 8	Cheap, easy and quick protocol.	• Variable micronucleu-s (MN) background frequency. • Labour intensive • Subjective
Polymerase chain reaction (PCR)	1990	2, 6	Simple and reliable method in which particular segments of DNA are specifically replicated and visualized using agarose gels	• Only detects damage that disrupts progression of the polymerase. • Inability to resolve which specific type of lesion is detected. • Requires high quality DNA.
Terminal deoxynucleotidyl transferase (TdT) dUTP nick-end labeling (TUNEL) assay	1992	1, 2, 4	• Able to detect DNA fragments with fluorescence or radioactivity, microscopy techniques and FCM. • Samples can be stored for months before analyses.	• Limited in sensitivity and specificity • Cannot differentiate apoptosis from necrosis • Fixation and handling of tissue can significantly alter the results

			• Allows correlation of the phase of the cell cycle with apoptosis.	
Phosphorylated histone 2AX (γH2AX)	1998	1, 2, 3	Highly sensitive (enables detection of small changes in genomic integrity at single cell resolution).	The intensity of γ-H2AX antibody binding per cell is dependent on the number of DSBs.

The Comet assay, a widely used technique to assess DNA damage relies on embedding cells in an agarose gel followed by electrophoresis. The damaged DNA appears as a tail, and the length of the 'comet' tail reflects the extent of DNA damage. A second widely used method, and the current gold standard, is the Cytokinesis-block micronucleus cytome assay (CBMN). CBMN involves spreading cells on a slide using cytospin followed by DNA staining and examination of 'micronuclei' (described in detail later in this chapter) frequency by light microscopy. The main drawbacks of this technique are the need for cell culture steps, preparing slides, and the laborious process of subjective scoring of cells for micronuclei. In addition, counting > 1000/cells is in most cases unrealistic.

From **Figure 3.1** and **Table 3.1** it is clear that the majority of currently used DNA damage assessment assays can only detect 1 – 4 types of defects; The CBMN does allow assessment of five distinct defects. Assays such as the comet assay, CBMN, Halo assay and the DBD-FISH assay are all very subjective and hence may be prone to variability of results obtained. In

addition, techniques such as the Halo and comet assays do not lend themselves to easy automation. In contrast, assays such as TUNEL, γH2A-X, PCR etc. do incorporate automated steps. The main drawback with these latter techniques is that they are limited in their ability to measure a wider spectrum of DNA damage lesions.

As indicated previously, the most widely used methods to assess genotoxicity are the CBMN and Comet assays. **Figs 3.2 A and B** highlight the essential steps in the two assays.

The main principle of the CBMN assay is to block cytokinesis in the mitotic phase of the cell cycle resulting in bi-nucleated (BN) cells, a stage when micronuclei are most likely to form. In addition, binucleation indicates that cells are alive and this allows differentiation from necrotic and apoptotic cells under light microscopy. MN appears as a small and detached nuclear body in the cytoplasm of the cells undergoing division (Figure 3.3A and B) [175].

The essential principle of the comet assay, first established by Ostling and Johanson in 1984, is to observe the length of the ‘tail’ on gel electrophoresis that is a measure of short segments of damaged DNA released from cells. Subjectivity, stringency of the protocol steps, level of cytokinesis block achieved in different cell types etc. can compromise the results of both assays and influence interpretation and inference.

A

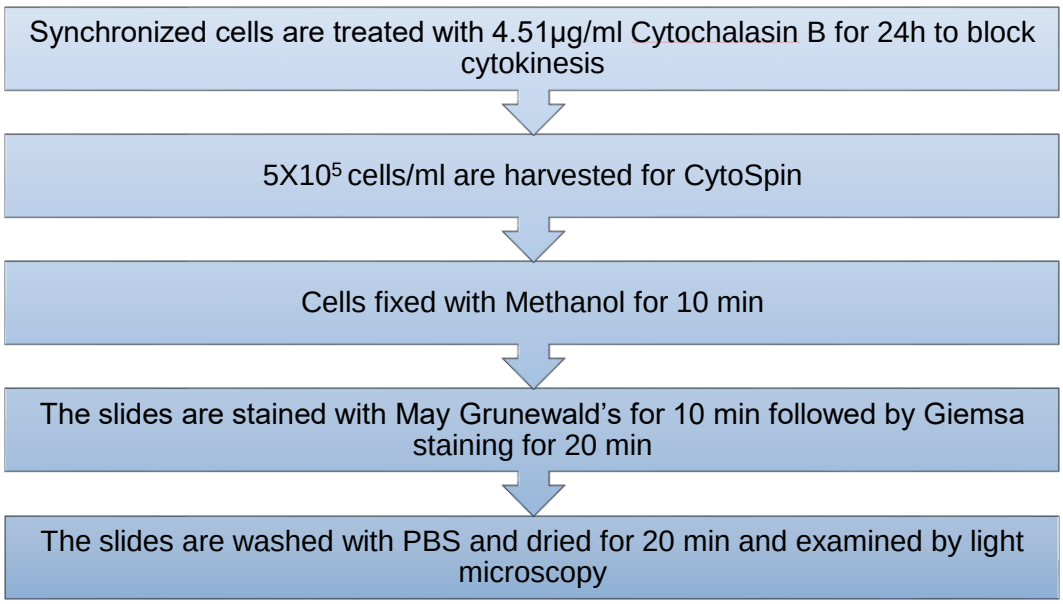

B

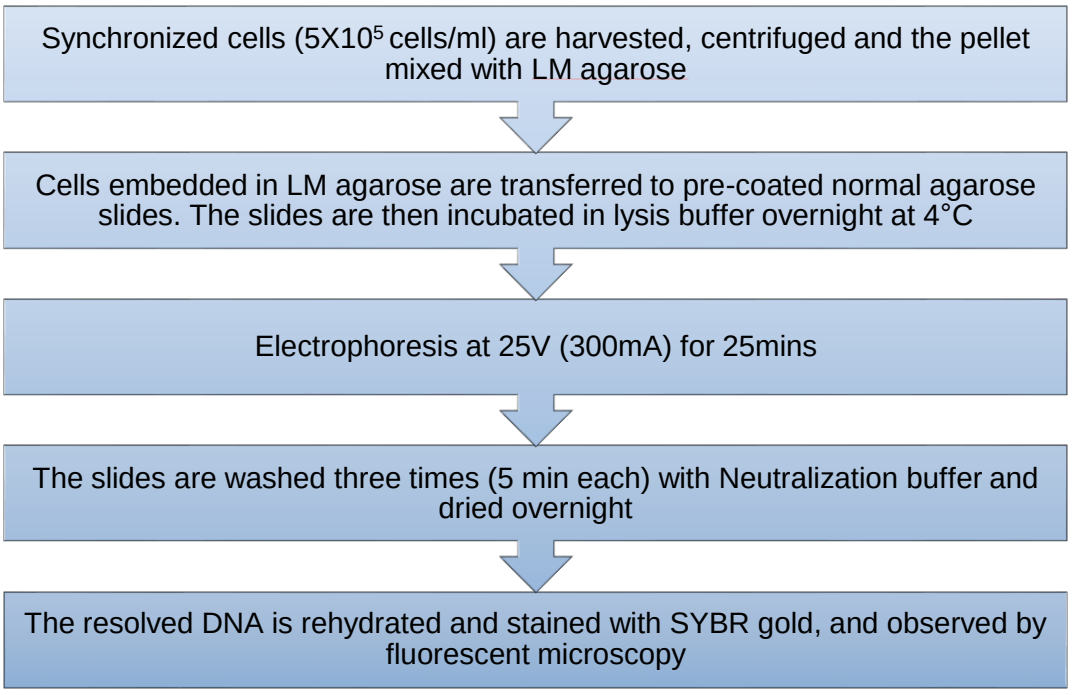

Figure 3. 2: Segmented flow charts for A) CBMN assay; **B)** COMET assay**.** Critical technical process steps for both Comet and CBMN assays are shown.

There is, hence, a need for more objective and high-throughput techniques that provide information on a larger number of cells and for a wider spectrum of DNA damage lesions (illustrated in **Fig 3.1)**. Such techniques will minimise the subjective bias in interpretation of results to lessen variability and ensure reproducibility.

As discussed above, the comet assay (**Fig 3.3 D, E**) does not readily lend itself to incorporation of steps that would help increase automation and objectivity. The CBMN assay (**Fig 3.3 A, B, C**), however, may be more suitable to explore methods to eliminate subjective bias, increase the number of cells analysed and ensure high throughput. We hypothesised that, as the CBMN assay does include steps that could be performed by FACS this may help us to improve the assay. Importantly, of all the previously described methods in **Table 3.1,** the CBMN assay detects a larger spectrum of DNA damaging lesions and hence is the better option to explore automation.

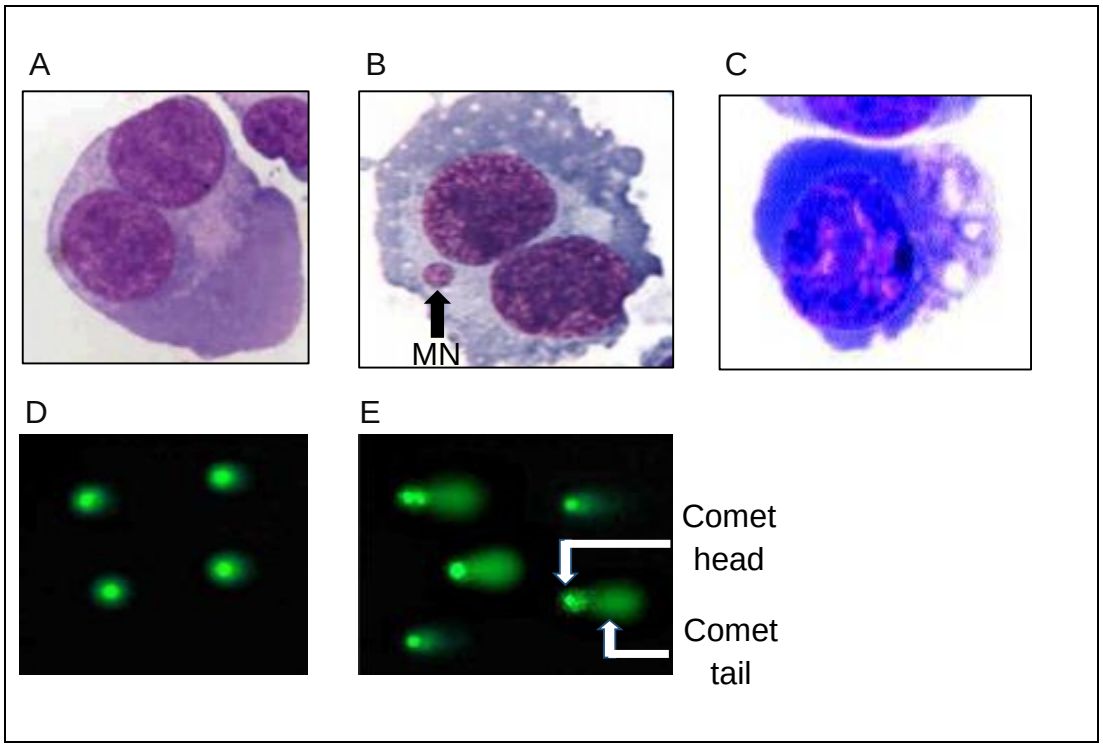

Figure 3. 3: Images generated in the CBMN assay: A) Normal bi-nucleated cells (BN); **B)** Typical bi-nucleated cell with a micronucleus (MN); **C)** An apoptotic cell showing condensed nuclear chromatin and dark cytoplasmic staining; Comet assay: **D)** Normal cells with no DNA damage and hence no 'tails' **E)** Cells with DNA damage showing a 'comet-like' appearance with a head (of intact DNA) and a tail (short fragments of damaged DNA) [176, 177].

We hypothesised that a flow cytometry based assay would provide an automated scoring system of MN frequency. The advantages of this technique are that it would be less time consuming, more high-throughput as many samples can be treated and analysed together and should be suitable for both primary and secondary cells. In addition, the technique would be more robust, inexpensive, highly reproducible, and not subjective.

Previous attempts at automation of CBMN have used cell image analysis or FACS analyses [163, 178-180]. Nüsse and Kramer established a modified MN assay by using a detergent solution containing Nonidet P40 and citric acid-sucrose solution to separate the nuclei from MN [181]. A technique employing genotoxicants, SYTOX Green and ethidium monoazide (EMA) stains followed by flow cytometric evaluation of treated and untreated cells has been described [175, 178, 182]. Another study of human lymphocytes has reported that EMA and 4, 6-diaminodino-2-phenylindole (DAPI) staining improve the sensitivity of flow cytometry. DAPI is a nuclear and chromosome counterstain that binds strongly to adenine–thymine rich regions in DNA and is a better discriminator of live and apoptotic cells [163]. An independent study has focused on generating automated MN counts using image software called ‘cell profiler’ to help reduce the time for analysis and to improve consistency of the micronucleus assay [179].

The main challenge of using a FACS based assay is the ability to differentiate MN from cellular debris and apoptotic bodies, and ensuring that the protocol steps do not affect MN counts. It is unclear whether previous attempts have fully addressed these two main issues. Furthermore, the problem with the imaging analysis is that the literature does not provide the details of the software.

A further drawback of the previous FACS based techniques is that EMA needs photo-activation followed by multiple washing steps, which may result in cell loss. Although EMA is good for identifying dead cells, the long incubation (25 minutes) can result in false positive staining of live cells. In

addition, the requirement of high-speed centrifugation in the final steps in previous attempts may lead to loss of MN.

To address some of the perceived problems with previous attempts at flow cytometry, we have focused on some specific changes to improve the protocol. We first considered using Propidium Iodide (PI) as an alternative to EMA. This step is essential to identify and separate MN from chromatin originating from dead cells [183]. PI molecules only integrate with the DNA double helix of dead cells that have lost their membrane integrity [184]. PI permeates the cell and stains the intracellular components in a shorter time period (5 mins vs 25 min for EMA) and hence may prevent the stain from penetrating live or intact cells. Furthermore, in order to minimise MN loss, the final centrifugation step was omitted from the established MN-FACS assay protocol. Thus, the cells are run directly through the machine after incubation in the second lysis buffer. The sequential gating strategy of previous published methods was further revised to improve results and prevent auto-fluorescence [185].

We investigated various stains to evaluate DNA staining efficiency within live cells and in order to quantify MN using flow cytometry. These included DAPI, 7-AAD and SYTOX red. 7-AAD staining was found to be suboptimal as it was not good at differentiating cell size, and did not always separate live from dead cells. The main disadvantages for using SYTOX Red are that it is not well known, rarely used, and very expensive. Our experiments suggested that the DAPI stain gives the most reliable and accurate results.

In summary, the **aims** of this aspect of the study and chapter are as follows:

1- To improve, optimise and establish a more robust and reliable Flow cytometry based MN enumeration assay.
2- To evaluate the optimised flow cytometry based technique to enumerate MN in primary cells from CLL patients and cell lines.

In our protocol MN-FACS assay was performed on a BD Biosciences FACS Canto II flow cytometer. The blue laser provided excitation at 488 nm for PI and the violet laser provided excitation at 405 nm for DAPI. The gating strategy was designed using FACS Diva version v6.1.3 software (BD Biosciences) and 50,000 events of DAPI range were analysed for each sample. MN were distinguished using several parameters including, size (forward scatter), granularity (side scatter), DNA content (DAPI), and negative PI (non-apoptotic/necrotic). In this chapter, two cell lines used are MAVER-1 and HeLa cells. In addition, we used freshly obtained primary patient derived CLL cells for experiments.

The first optimisation step for our MN-FACS protocol was to use PI to stain apoptotic and necrotic cells to allow exclusion (gated out) of these cells in the analysis. Once stained with PI, lysis of cells is an important step required to rupture the cytoplasmic membrane and facilitate binding of DAPI stain with DNA of live cells (nuclei and MN). A final critical step is the multi-gating strategy for analysis and identification of MN based on size discrimination.

3.2 Methods

3.2.1 MN enumeration using Flow cytometry on HeLa cells

The flow cytometry based assay was designed to identify and enumerate MN. The technique relies on critical steps to exclude debris, apoptotic bodies and necrotic cells from the analysis, followed by staining for nuclear DNA and MN in live cells. Finally, the DNA from MN is separated according to size. After irradiation with 3Gy and 5Gy cells were seeded at a density of 3×10^5 cells/ml in 6-well plates and harvested at 10 mins, 24 and 48 hrs. For adherent cell lines (HeLa cells) trypsinisation was required before harvesting. The cells were washed once with PBS and then re-suspended in 500µl of Propidium Iodide (PI; 1 mg/ml stock solution) diluted in PBS (1:400), vortexed and then incubated for 5min in the dark. The cells were then centrifuged at 500g for 5min, and after discarding the supernatant, re-suspended in 500µl of 'lysis buffer 1' (1 µg/ml DAPI (Sigma-Aldrich, UK), 0.584 mg/ml NaCl (Melford, UK), 1 mg/ml Sodium Citrate (Sigma-Aldrich, UK), 0.3 µg/ml IGEPAL-630 (Sigma-Aldrich, UK) and 250 µg/ml RNase A (Invitrogen, UK)). After incubation in the dark for 90mins 500µl of 'lysis buffer 2' (1 µg/ml DAPI, 85.6 mg/ml Sucrose (Sigma-Aldrich, UK) and 15 mg/ml Citric Acid (VWR, UK); pH 8-10) was added to the cells, and the sample incubated in the dark for a further 30 mins. The whole sample was then analysed immediately by flow cytometry. **Figure 3.4** summarises the protocol steps of the MN-FACS assay.

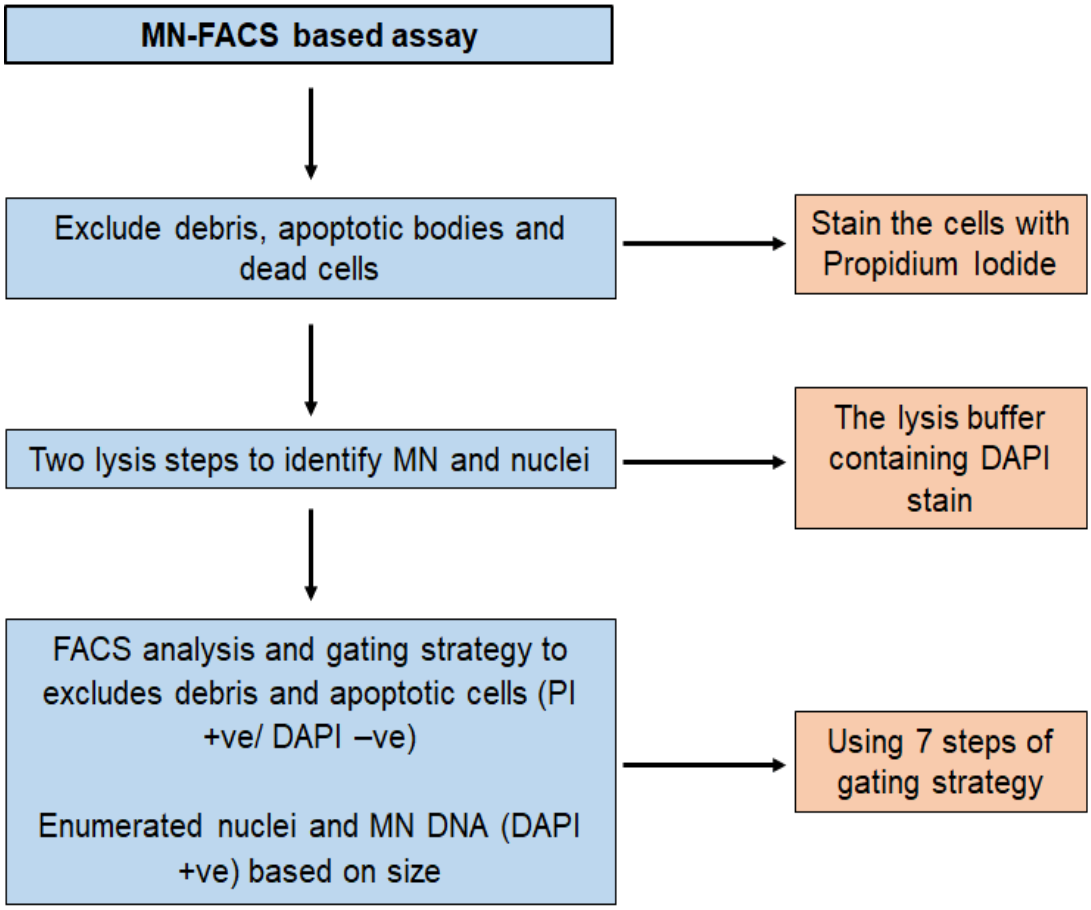

Figure 3. 4: A flowchart for MN-FACS assay protocol.

3.2.2 The gating strategy for assessment of MN frequency using Flow cytometry

Figure 3.5 highlights the sequential gating strategy used for measuring MN frequency in flow cytometry. The strategy incorporates 7 gating steps to exclude debris/chromatin from apoptotic/necrotic cells, and eventually scoring MN and nuclei from live cells based on size.

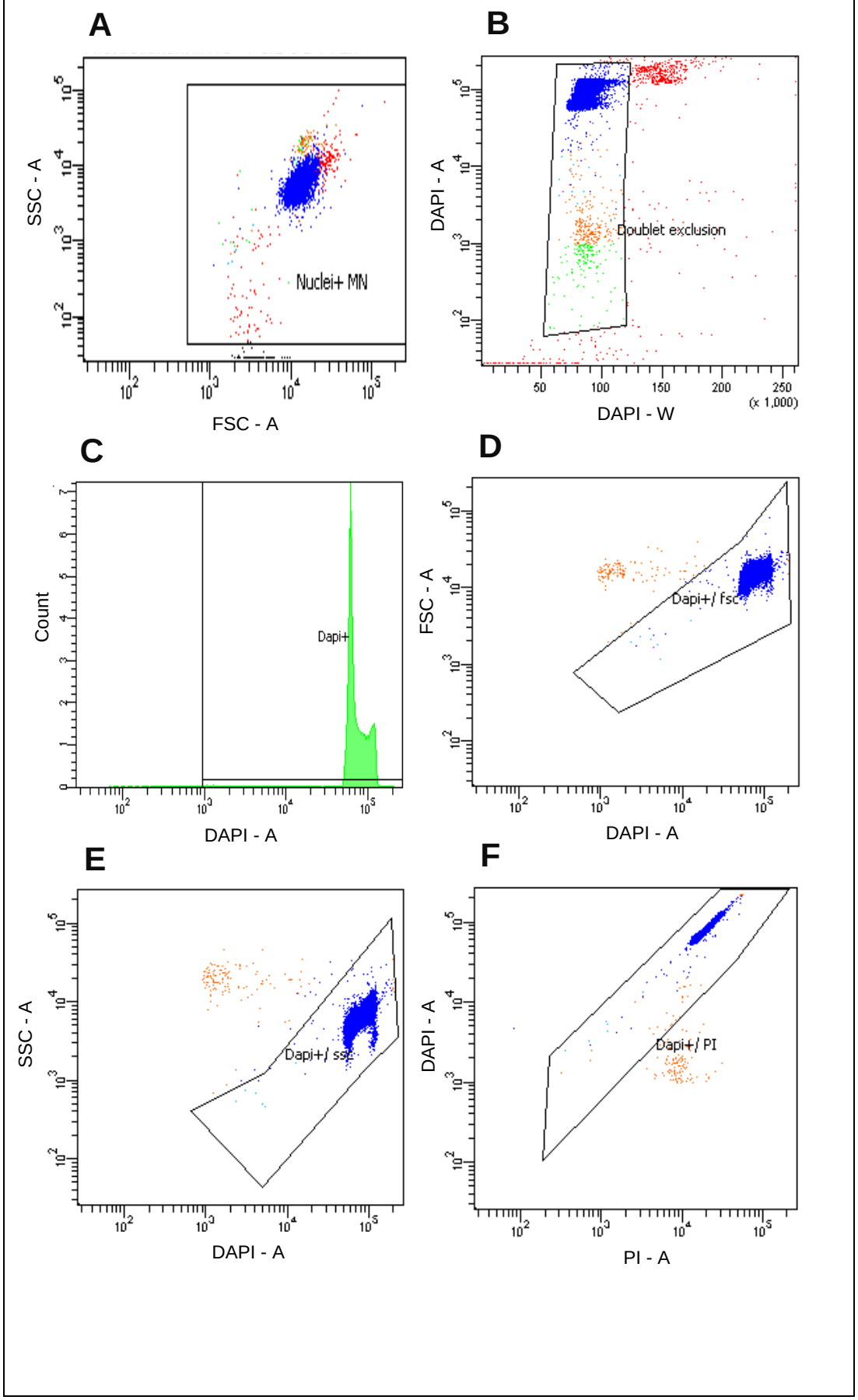
A
SSC - A
FSC - A
Nuclei+ MN
B
DAPI - A
DAPI - W
Doublet exclusion
(x 1,000)
C
Count
DAPI - A
Dapi+
D
FSC - A
DAPI - A
Dapi+/ fsc
E
SSC - A
DAPI - A
Dapi+/ ssc
F
DAPI - A
PI - A
Dapi+/ PI

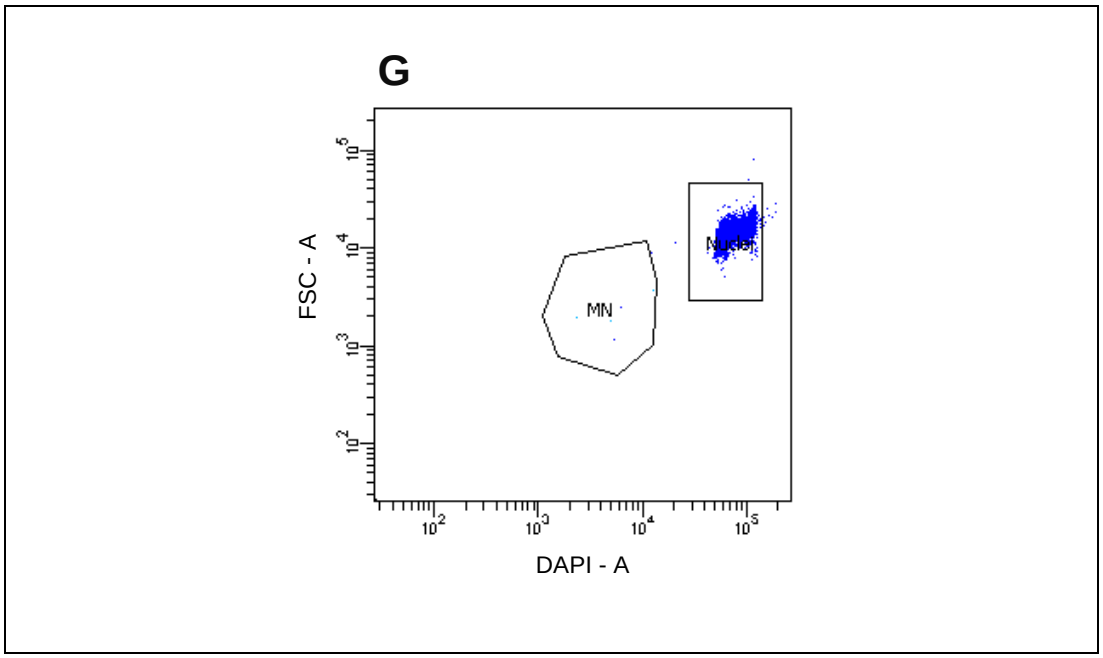

Figure 3. 5: Sequential gating strategy for MN-FACS assay based on FSC, SSC, DAPI fluorescence, and PI stain.

● **Doublets;** ● **DAPI range;** ● **Live cells (Nuclei) (+DAPI);** ● **Micronuclei (MN);**

● **Dead cells (+PI).**

Plots (**A-G**) show the sequential gating strategy;

A): Differentiation of events based on forward scatter (FSC; for size) and side scatter (SSC; for granularity). The gated events include most of the nuclear material but should exclude some dead cells.

B): The gated events are then re-analysed to exclude doublet cells (two or more cells sticking together) which fall outside of the rectangular selection.

C): Identification of DAPI stained single cells in different phases of the cell cycle.

D): DAPI-Area (DAPI-A) plotted against forward scatter-area (FSC-A). This includes all nuclei and events based on size within the DAPI range.

E): DAPI-Area (DAPI-A) against side scatter-area (SSC-A). This includes all nuclei and events based on the granularity within the DAPI range.

F): PI-Area (PI-A) against DAPI-Area (DAPI-A). This helps in excluding all PI positive cells to remove any residual events derived from necrotic/ apoptotic cells from the final analysis.

G): DAPI-A against FSC-A- All DAPI +ve/ PI -ve populations from D, E, and F are included (nuclei or MN from live cells) and finally gated to discriminate MN from whole nuclei.

3.3 Results

For the MN-FACS assay, we first needed to ensure that the machine has the ability to detect MN, before proceeding to protocol optimisation.

3.3.1 Qualitative and quantitative of beads by Flow cytometry

In the first instance, we focused on three important aspects of MN detection by flow cytometry.

1. The flow cytometry should ideally be capable of accurately detecting particles similar to MN in size.
2. The FACS strategy should provide reliable and accurate quantitation of particles.
3. The impact of the wash and lysis steps within the protocol on MN loss and quantitation needed assessment.

These experiments were performed using commercial 'rainbow calibration beads' (BD Biosciences, UK). The beads are roughly 3.0-3.4 μm in diameter, and hence smaller than a nucleus (5 – 10 μm) and roughly reflect the size of

a MN which is variable but approximately 1/3 – 1/4 of the size of a nucleus [186].

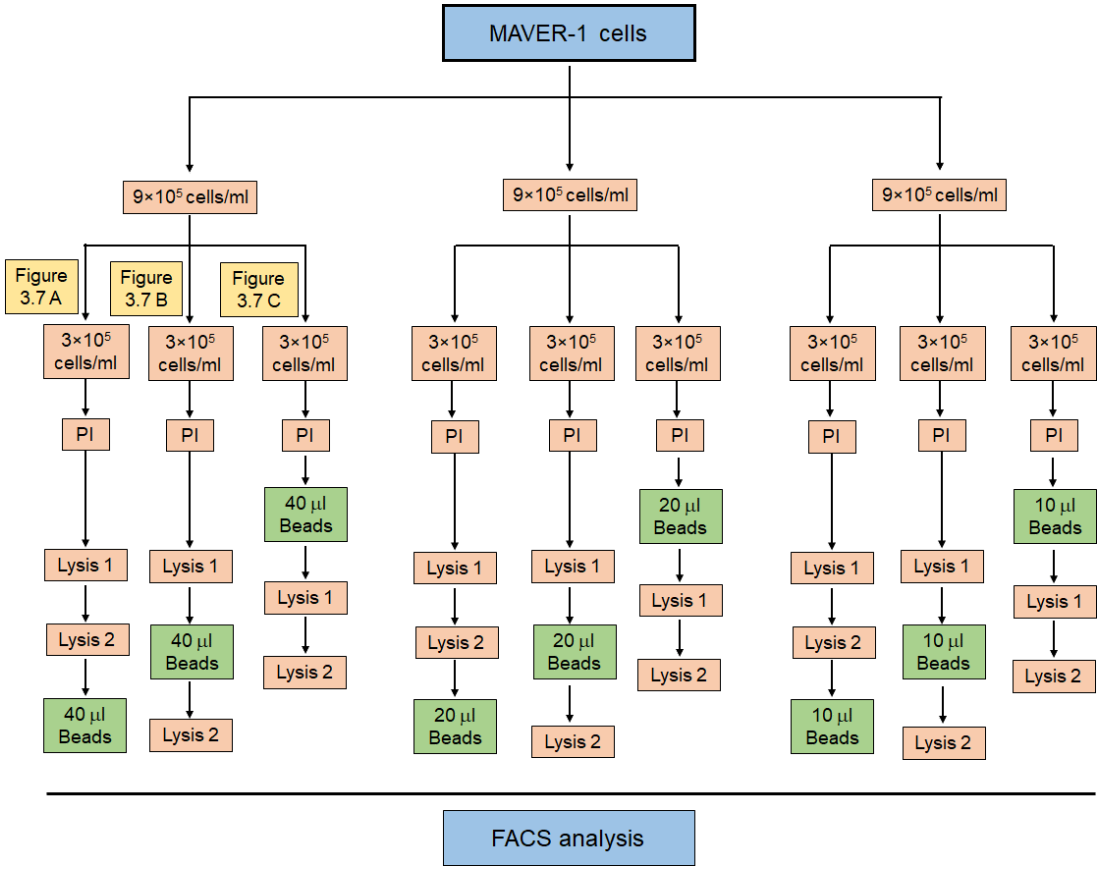

Figure 3. 6: Experimental plan for qualitative and quantitative assessment of beads by flow cytometry. This schematic diagram summarises the experimental plan for addressing the aims summarised in Section 3.3.1. Varying amount of beads were added to MAVER-1 cells at different stages of the MN-FACS assay protocol.

Increasing volumes of the bead suspension were added (**10, 20 or 40 µl**) to equal numbers of MAVER-1 cells (3×10^5 cells/ml) as shown in the experimental plan in **Figure 3.6**. Flow cytometry based assay was used for detection and analysis of the beads added to MAVER-1 cells at three different stages of the protocol to investigate the beads detected in the **R1** gate and for estimation of their loss at specific steps as shown in **Figure 3.7**

(**A, B, C**). MAVER-1 cells were separated into three separate tubes. In the first tube the beads were added after 'lysis buffer 2' step (**Figures 3.6 and 3.7 A**). This served as a control as the amount of the measured beads should be at the maximum compared with other conditions as the sample is analysed immediately by FACS without additional manipulations. To the second aliquot of MAVER-1 cells, beads were added after treatment with 'lysis buffer 1' (**Figure 3.7 B**). In the third instance, the beads were added to the cells after PI stain but prior to lysis steps (**Figure 3.7 C**). All tubes were analysed simultaneously by FACS and 50,000 events collected in the DAPI range.

In our 7-step gating strategy, the beads were serially tracked to ensure that they can be detected by the machine. The gating strategy is as follows:

1) Gating for all live cells using Forward scatter (FSC-A) vs Side scatter (SSC-A) in **R2** and to include the beads in **R1**

2) **R3** gating involves excluding doublet cells (two or more cells joined together) within the **R2** gate in the DAPI Area (DAPI-A) vs DAPI Width (DAPI-W) plot

3 a, b and c) Identify live cells based on the size (DAPI-A vs FSC-A), granularity (DAPI-A vs SSC-A) and exclusion of the apoptotic/ necrotic events (PI+ staining) (DAPI-A vs PI-A) – **R4**

4) Identification of nuclei (**R5**) and micronuclei (and beads) (**R6**)

Comparison of the R6 gate in Figures 3.7 A, B and C suggests that beads are progressively lost with each additional lysis step as reflected by the

intensity of the beads in the gate (A > B > C). The relative percentages of the beads in the **R1** gate in the three separate conditions (A, B and C) are shown in graph form in Figure 3.7 D. The results depicted are for experiments done on three different occasions. The beads detected in A (10, 20 or 40 μl) are set at 100% as they were added just before FACS analysis without any further manipulation of the sample. When the beads were added after lysis buffer 1 and prior to the 2nd lysis step, the bead loss was negligible (0 – 2%). The loss of beads was maximal and significant in condition C when the beads were added after PI staining and before both lysis steps. Irrespective of the volume of beads added the final loss was close to 60% ($p < 0.0001$; mean ± SEM; n= 3). The events in the R6 gate (in A, B and C) clearly indicate that the beads and MN co-localise within this gate due to their similarity in size. As all three conditions are put through the same number of protocol steps the percentage of micronuclei (within the R6 gate) for A, B and C are very similar (~0.2%). The Rainbow Particles have been detected in R6 gate in all three conditions as they have emission spectra compatible with many common fluorophores used for immunofluorescent staining with flow cytometric analysis.

The colours in the below plots (Figure 3.7 A, B, C) indicate: ● DAPI range; ● Doublets; ● Live cells (Nuclei) (+DAPI); ● Micronuclei (MN); ● Dead cells (+PI).

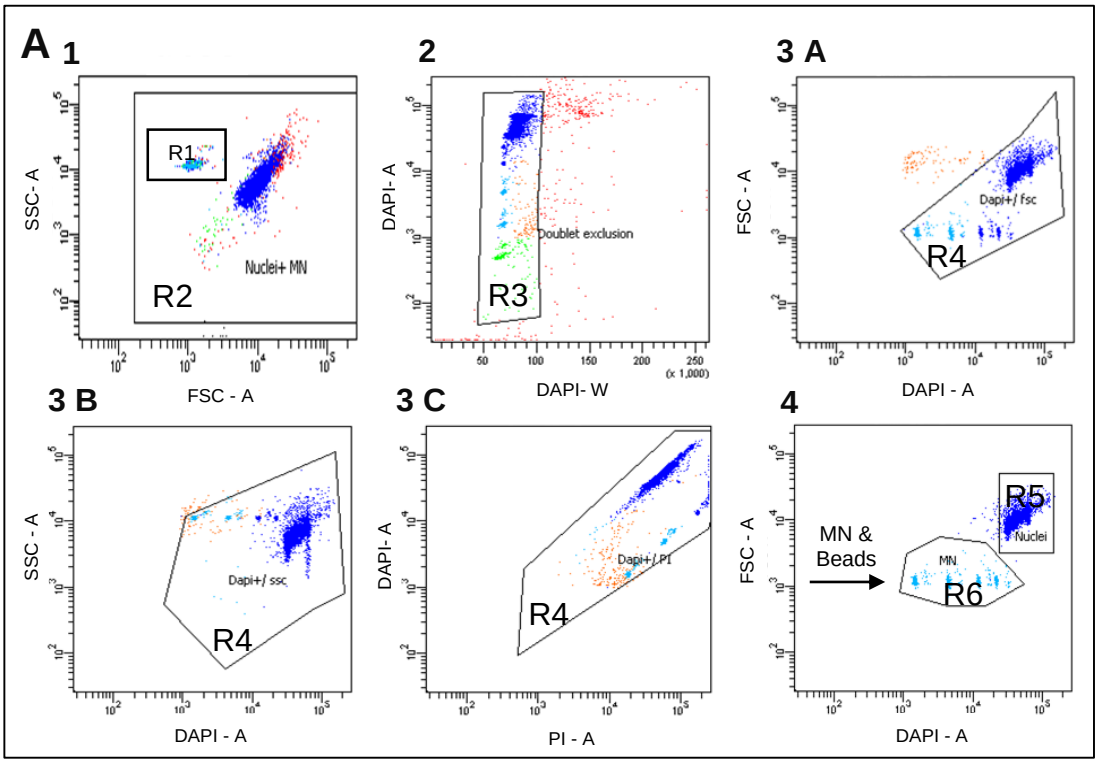

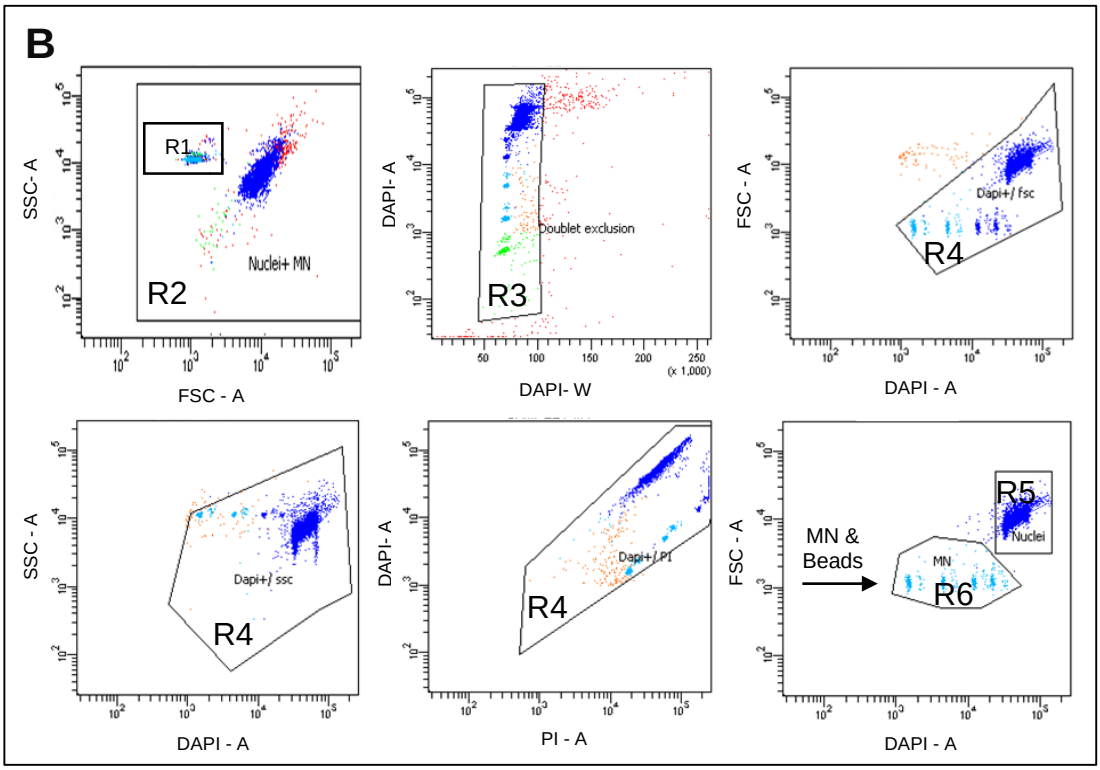

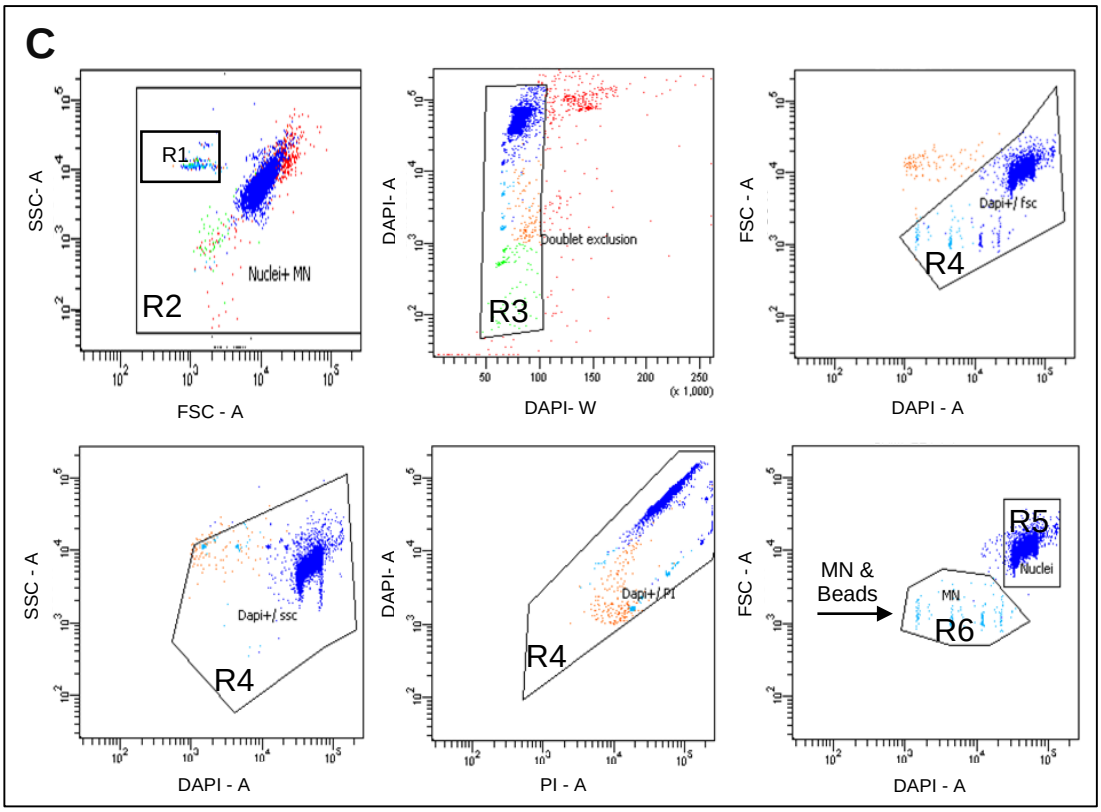

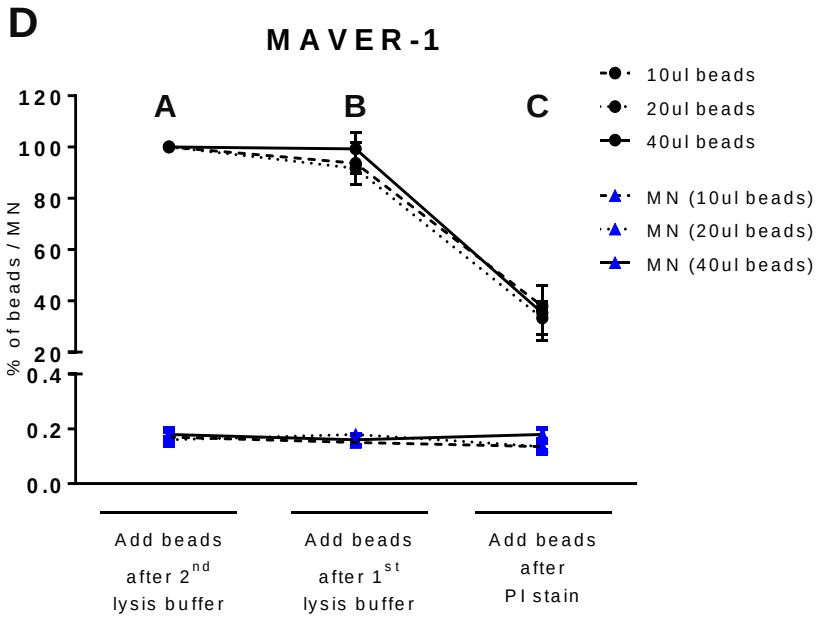

Figure 3. 7: Qualitative and quantitative of beads to ensure the detection of MN by Flow cytometry. The flow cytometry (FCM) plots and bar graph showed the percentage of beads detected by flow cytometry. **Figure 3.7** (**A, B, C**) have shown the amount of beads after added in three different stages of MN-FACS assay protocol**; 1)** Shown the beads population (R1) and all the collected events using

(FSC) for the size and (SSC) for the granularity detected by the machine; **2)** Doublet discrimination; **3 a, b and c**) FSC versus DAPI discriminate based size and fluorescence, SSC versus DAPI include all events show granularity and the fluorescence, DAPI-A vs PI-A to exclude apoptotic and necrotic cells; **4**) presented nuclei and MN. The data represented in **Figure 3.7 D** shown the percentage of beads and the MN count after exclude the beads population from the plot (4). The beads that added after the 2nd lysis buffer is the highest amount among others. The result obviously showed that **62%** of the beads were lost after PI stain without affecting the MN count, whereas the amount of beads added in the last two lysis steps were almost the same. One-way ANOVA- Dunnett's test was used to determine statistically significant differences in the volume of the beads between A vs B and C (**p< 0.001). (mean ± SEM; n= 3).

3.3.2 The effect of a final centrifugation step on MN enumeration by the FACS based assay.

As discussed above, it seemed reasonable for samples to be analysed immediately after the 2nd lysis step without further manipulation. Despite this it was felt essential to assess if an additional centrifugation step (13,000 for 10 mins) could provide a more accurate estimate of MN frequency by potentially ensuring that all debris is removed. For this experiment either MAVER-1 cells (a mantle cell lymphoma cell line) or primary CLL cells were employed.

MAVER-1 cells were subjected to irradiation to induce MN formation and assessed with and without centrifugation. Cells were irradiated (3 Gy) and re-cultured at a density of 3×10^5 cells/ml. Non-irradiated cells were included as control for the experiment. Untreated and irradiated cells were then harvested after 24 and 48 hours, processed, and analysed for MN frequency using the MN-FACS assay. The results are summarised in **Figure 3.8**. The irradiated cells did show greater numbers of MN at 24 hrs with a further increase at 48 hrs compared to untreated control cells. The results show that the additional centrifugation step does consistently decrease the numbers of MN as assessed by the FACS assay (blue vs the red bars; **Figure 3.8 A**) in triplicate experiments (indicted by the error bars). There was no difference in MN frequency in the untreated cells when compared at the 24 and 48 hr time points. The results suggest that the additional centrifugation step does compromise the assessment of MN frequency.

In parallel, the experiment was repeated with three fresh CLL samples. The samples were obtained fresh analysed without further manipulation (i.e. irradiation). Primary CLL cells (1×10^6 cells/ml) were processed and analysed in the stepwise MN-FACS assay with the aforementioned multi-gating strategy. As shown in **Figure 3.8 B**, the basal levels of MN were variable and likely reflect prior treatment or disease status. As with MAVER-1 cells the estimation of MN frequency was compromised by the additional centrifugation step in all three cases.

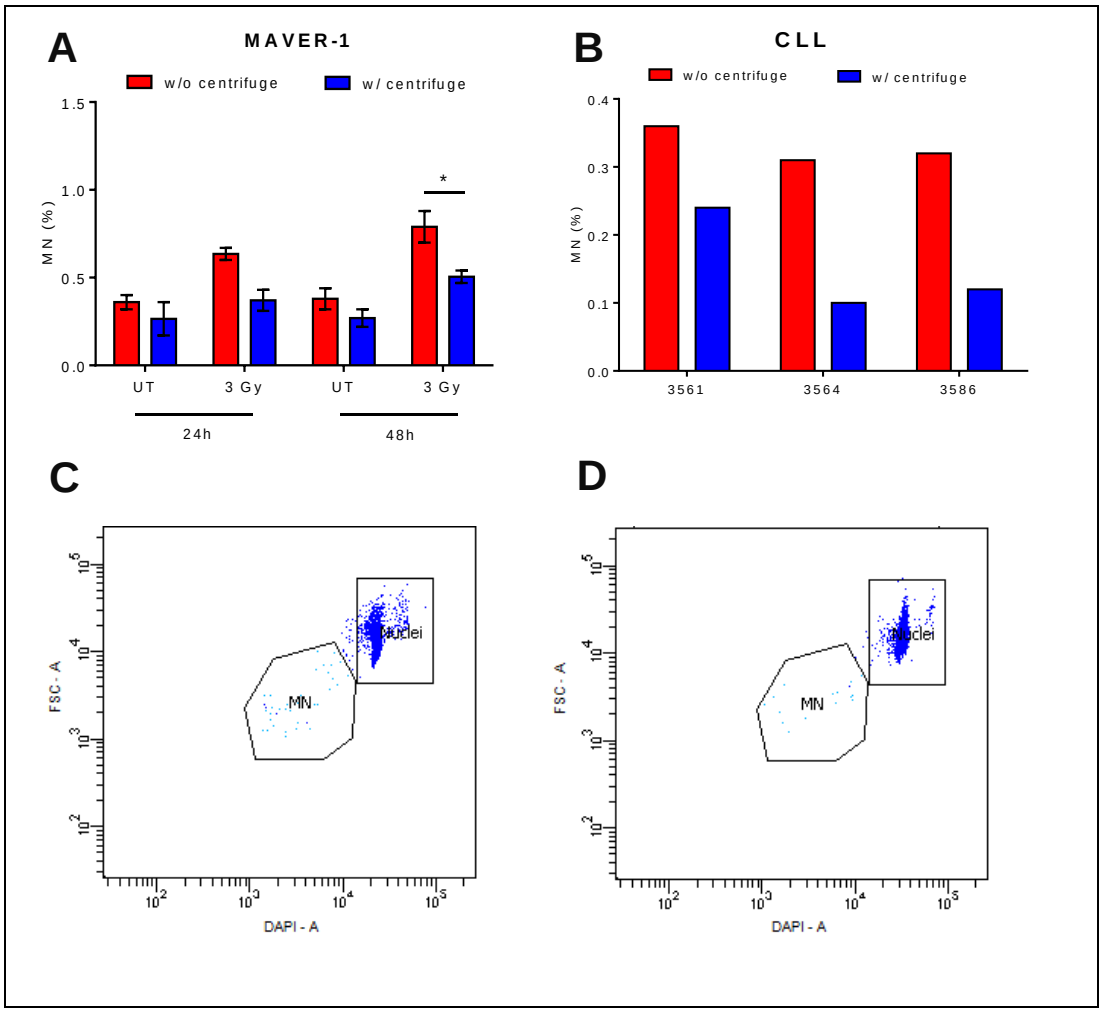

Figure 3. 8: Comparison of MN frequency with or without a final centrifugation step using MAVER-1 and CLL samples. A) Untreated or irradiated (3 Gy) MAVER-1 cells were assessed for MN percentage (y-axis) at 24 and 48 hrs with and without incorporation of an additional centrifugation step. **B)** Unmanipulated and fresh CLL patient samples were analysed for MN frequency (with and without centrifugation). **C+D)** The MN-FACS assay blots for the irradiated MAVER-1 cells w/o and w/ centrifuge after 48 h. The MN frequency as assessed by the MN-FACS assay is consistent higher in MAVER-1 cells and patient samples without an additional centrifugation step. Two-way ANOVA- Sidak's multiple comparisons test was used to determine statistically significant differences between the spin and without spin at 24 and 48 hrs. The irradiated cells with 3Gy after 48 hrs showed a significant difference. (*p< 0.05). (mean ± SEM; n= 3).

3.3.3 Optimization of the MN-FACS assay for HeLa cells

The HeLa cell line has been widely used for analysis of DNA damage with techniques such as the Comet assay [187] as they are susceptible to increasing doses of radiation or other genotoxic manipulations. For establishment of the MN-FACS assay as a robust technique we would need to benchmark the technique against other established assays. Hence, an important first step was to assess the performance of the MN-FACS in HeLa cells subjected to increasing doses of irradiation.

Towards this end, we first examined HeLa cells for the effects of increasing doses of irradiation. HeLa cells were first subjected to irradiation (3 or 5 Gy, 50 or 84 seconds). After irradiation HeLa cells were re-plated at a density of 3×10^5 cells/ml in 6-well plates. Apoptosis was measured at defined time points (10 mins, 24 and 48 hrs) by Annexin V/ PI staining followed by FACS analysis. The results are summarised in **Figure 3.9 A**. Irradiation resulted in a dose-dependent increase in apoptosis levels at 24 and 48 hrs compared to untreated controls. As expected, the levels of apoptosis were more marked with 5 Gy of radiation.

We next examined MN frequency in HeLa cells, with the same experimental conditions, using the MN-FACS assay. Untreated and irradiated (3 or 5 Gy) HeLa cells were plated at a density 3×10^5 cells/ml in 6-well plates. The cells were trypsinised and harvested after 24 and 48 hours and compared to cells immediately after irradiation (10 mins) for MN frequency by the MN-FACS assay.

Figure 3.9 B depicts a bar graph of MN frequency with escalating irradiation and at the specified time points. At baseline, the untreated cells (UT) and treated cells had similar MN counts (~2%). MN counts were subsequently also measured at 24 and 48 hours. At 24 hours, there were no significant differences between the 3 groups. At 48 hours, however, differences in MN frequency were more apparent. In UT cells, the count dropped to 0.5% MN, whereas cells exposed to 3 Gy showed MN frequency of 1.3%. Significantly, cells exposed to 5 Gy and harvested at 48 hrs showed the highest percentage of MN (2.9%). Given the increased levels of apoptosis seen with 5 Gy it is difficult to rule out the possibility that apoptotic debris may contaminate the micronuclei gate especially if the final centrifugation step is omitted. Hence, treatment of HeLa cells with 3 Gy and harvesting at 48 hrs was thought to be a reasonable condition further studies on HeLa cells to assess DNA damage by various methods for comparison.

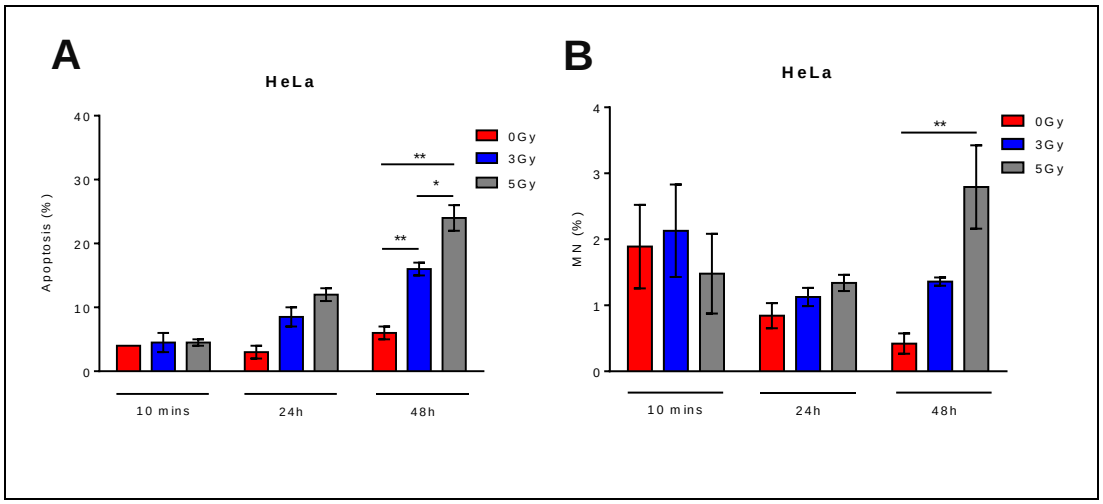

Figure 3. 9: Assessment of apoptosis MN frequency in HeLa cells. A) The bar graph depicts percentage levels of apoptotic cells as assessed by Annexin V/PI staining and FACS analysis. **B)** MN frequency assessed by the MN-FACS assay. Comparing untreated or irradiated cells (3 or 5Gy) at 10 mins, 24 or 48 hrs after treatment. Two tailed paired t-test showed significant statistical difference in cell apoptosis when compared between UT vs 3 and 5 Gy at 48 hrs (**$p < 0.01$). One-way Anova –Dunnett's test showed significant statistical difference in MN formation when compared between UT vs 5 Gy at 48 hrs (**$p < 0.01$). (mean ± SEM; n= 3).

3.4 Discussion

The aim of this chapter was to establish and optimise a flow cytometry based micronucleus enumeration assay using cell lines and CLL patient samples. MAVER-1 and HeLa cell lines were chosen for MN enumeration and to observe the changes in MN frequency after mutagenic radiation exposure. As previously stated, Nusse & Kramer (1984) have reported an MN-flow cytometry assay to measure the levels of DNA damage and genomic instability in cells [181], but significant issues needed to be addressed which could potentially impact accurate estimation.

In this chapter, we have explored the use of Propidium iodide (PI) as an alternative to Ethidium monoazide (EMA) to identify cells destined for apoptosis and with compromised cell membranes for several reasons. Firstly, PI is unable to penetrate the membrane of viable cells (metabolically active cells) with intact membranes and only for staining the DNA of the apoptotic bodies. Secondly, PI stain has double positive charge comparing with the EMA stain with a single charge and this has a role in improving the signal from PI stain. Finally, EMA can cross the membranes of intact cells more readily than PI. This is because EMA occasionally may permanently stain metabolically active cells even without membrane damage as the mechanism to expel the dye out of the cells is inactive [188]. These features make PI stain an excellent probe for identifying dead cells. In practice, an added benefit of the PI stain is the much shorter incubation time compared to EMA. Reducing the time needed to prepare the samples for FACS analysis make the MN-FACS assay much useful and applicable for the clinical purpose.

In our improved assay, we have used DAPI stain to identify nuclei and micronuclei within live cells. DAPI binds strongly to A-T rich regions of double-stranded DNA, with an excitation of 358 nm and an emission of 461 nm on flow cytometry [189]. In our protocol, DAPI added to the lysis buffers in combination PI and DAPI enable the enumeration of MN based on size and differentiation from apoptotic bodies and debris by exclusion in our multi-step gating strategy.

Other nucleic acid stains have used such as; 7-AAD and SYTOX red. We found that after the staining the two populations nuclei and micronuclei are attached and difficult to separate or differentiate between them based on size.

Using commercial beads, we were able to verify that our in house FACS Canto II Flow Cytometer can detect MN, which are similar in size. In addition, the FACS assay can detect MN even at low frequency (<1-2 %) and this high sensitivity make the technique suitable to use in the clinic. This step is important as it allows detecting low number of particles from the samples, which help in performing several tests in the clinic such as minimal residual disease (MRD) or in monitoring the diseases such as Myelodysplastic syndrome.

The two-lysis buffers contain DAPI stain, which binds to the DNA of the lysed live cells. The aim of using two lysis buffers is to ensure that both the cell membrane and the nuclear membrane of the cells were lysed. The step is essential in order to stain all the chromosomes for nuclei and MN.

The impact of an additional and final centrifugation step (13000g, 10mins) was also investigated. It was thought that this step could help to further remove cell debris that might mistakenly count as a MN. However, the results suggest that some MN were lost because of this step as some of the MN might be floating in the supernatant.

The centrifugation step suggested for future experiment to design a technique based on cellular precipitation using a grading column in order to separate the cell contents based on size including; micronuclei, endosomes, and mitochondria.

Our experiments on HeLa cells have further helped to test the MN-FACS assay and to establish reasonable conditions for further studies described in the chapters that follow.

Based on the levels of apoptosis a dose of 3 Gy and studies at 48 hrs after radiation was thought to be suitable as a positive control in future studies. The cells exposed to 5Gy showed a higher percentage of apoptotic cells, therefore it was decided that a 5Gy dose of irradiation may be too high and that some MN could be lost due to cell death. As a result of the described experiments, a robust and reliable FACS based MN assay incorporating a multi-step gating strategy to improve sensitivity and specificity was established for downstream studies.

In the next chapter, we are aiming to validate this technique through correlating MN-FACS assay results with traditional DNA damage assays in **chapter 4**.

Chapter 4: Evaluating the performance of MN-FACS Assay to assess DNA damage

4.1 Introduction

Developing a robust, reproducible and reliable assay to study genetic material and assess DNA damage on exposure to a variety of genotoxic agents, environmental factors, drugs, UV light or industrial chemicals can be useful for downstream applications [190]. DNA misrepair can lead to altered nucleotide sequence or structure and these 'DNA lesions' may result in potentially harmful genetic aberrations [191]. Established techniques are largely subjective and time consuming. An automated technique in this context may be more objective, require shorter time and enable a higher throughput assay that allows examination of a greater number of cells. In the previous chapter, we described the establishment and optimisation of a FACS based MN assay that does address some of these issues.

Results described in this chapter aim to prove that our MN-FACS assay is a reliable and accurate technique and compares favourably to existing DNA damage assays. Towards this end, we first established a few standard techniques in house and then compared them with the MN-FACS assay. We chose three assays for the comparative studies.

1. The cytokinesis-block micronucleus (CBMN) assay, which is the current gold standard for quantifying MN.

2. The Comet assay that is widely used for the study of DNA damage by many researchers.
3. Lastly, induction of H2AX phosphorylation (γH2AX) that is a marker of sites of DNA damage within cells.

We investigated the relationship between parallel results generated in the MN-FACS based assay and traditional DNA damage assays by correlation analyses.

4.1.1 The CBMN Assay

The CBMN assay is the current gold standard technique for quantifying and measuring MN that are surrogate markers for genotoxic insults and resultant DNA damage in mammalian cells.

DNA damage can cause cells to become genetically unstable. Following DNA damage and during mitosis fragments or entire chromosomes lag behind and are not incorporated into the daughter nuclei leading to formation of small nuclear bodies known as micronuclei. Other mitotic abnormalities also considered markers of DNA damage, are nucleoplasmic bridges (NPBs) and nuclear buds (NBUDs) (**Figure 4.1**). NPBs form when centromeres migrate towards opposite poles of the cell whereas NBUDs form due to elimination of amplified DNA or misrepaired DNA from daughter nuclei [192, 193].

The CBMN assay is currently used as a test for assessing chromosome breakage, DNA misrepair, chromosome loss, non-disjunction, necrosis, apoptosis, and cytostasis [194]. An essential step of this assay is to block

cytokinesis, the step where cytoplasm of the parent cell divides into the two daughter cells causing bi-nucleated (BN) cells. MN form and are best identified in bi-nucleated cells that are primed to undergo cytokinesis. In vitro treatment of cells with Mytotoxin or Cytochalasin B leads to the cell cycle arrest of bi-nucleated cells at the cytokinesis stage and helps in formation and measurement of MN. The CBMN assay is widely used to predict the sensitivity of normal to radiation and also for prediction of cancer risk [195]. The main drawbacks of the CBMN assay are that it requires cell culture and entails multiple laborious steps [196]. In addition, the number of cells that can be examined is small, time consuming and subjective.

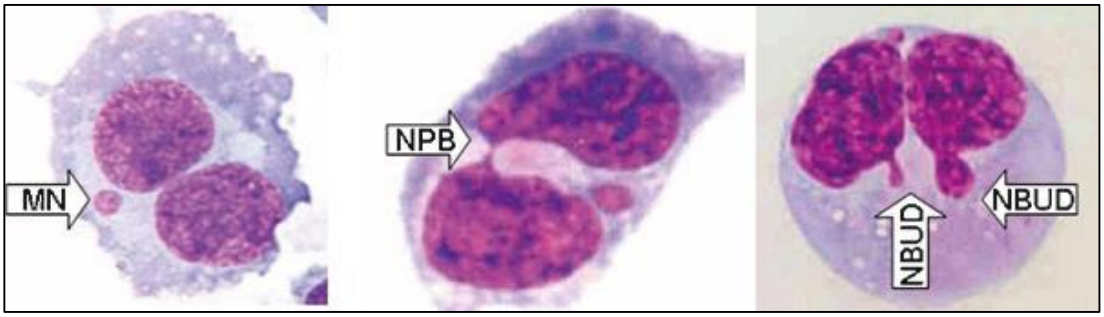

Figure 4. 1: The cells scored in the CBMN assay under microscope. The pictures show a cytokinesis blocked bi-nucleated cell with a micronucleus (MN); and similar cells with other genetic abnormalities such as nucleoplasmic bridges (NPBs) and nuclear buds (NBUDs) [194].

4.1.2 The Comet Assay

Ostling and Johanson (1984) originally established the Comet assay (or single cell gel electrophoresis (SCGE)) to detect and visualise DNA strand breaks in individual eukaryotic cells [197, 198]. This method is widely used to evaluate DNA damage that results from various genotoxic insults [199]. Initially the Comet assay was used mainly for measuring DNA single-strand

breaks (alkali Comet assay). Subsequent modifications have expanded the use of Comet assay for measurement of DNA double-strand breaks (neutral Comet assay), repair capacity, and cross-links (failure to identify single-strand breaks) [200]. The assay relies on the appearance of a ‘comet tail’ upon DNA gel electrophoresis and serves as an indicator of damaged DNA within the cell. The length of the ‘comet tail’ is directly proportional to the amount of damaged DNA in each cell. Special software is required to examine and assess several cells for the presence and absence of tails, as well the length of the tails, to get a sense of the extent of damage within a cell population.

4.1.3 H2AX phosphorylation

H2AX, a histone variant of H2A, is incorporated into nucleosomes at sites of DNA damage within cell nuclei. H2AX accounts for 2-25% of the total H2A protein family in the cell. Phosphorylated H2AX (serine 139) plays an important role in recruiting DNA repair proteins to sites of damage and can be used as a biomarker of DNA damage. H2AX, incorporated into the relevant nucleosomes, undergoes rapid phosphorylation (termed **γ-H2AX**) following DNA single-strand (SSBs) or double-strand breaks (DSBs) [201, 202].

Having established and optimised that the MN-FACS assay is a reliable automated technique for MN enumeration and can also be used to study the effects of DNA damaging stimuli [175], we hypothesise that the MN-FACS assay can be more accurate and less time consuming when compared to

traditional assays especially those described above. **Table 4.1** summarizes the potential advantages of the FACS based assay over other techniques.

Table 4. 1: The potential advantages of the MN-FACS assay over existing methods.

MN-FACS ASSAY	OTHER ASSAYS
Quick	Time consuming
Robust	Multiple steps
Automated	Labour intensive
High throughput	Low throughput
Not user dependent	Subject to bias

Thus, the **aims** of this chapter are:

1- To establish CBMN and comet assays to assess levels of DNA damage following irradiation of HeLa cells.
2- To investigate MN frequency by the FACS based assay following irradiation.
3- Correlation and comparison of the results obtained with MN-FACS, CBMN and Comet assays.

To address the aims of the chapter, the HeLa cell line was exposed to increasing doses of ionizing radiation (3Gy and 5Gy) and resultant DNA damage was measured at various time points (0, 24 and 48 hours) using the three above mentioned assays.

4.2 Methods

4.2.1 MN count using CBMN assay on HeLa cells

HeLa cells were harvested and re-suspended at a density of 3×10^5 cells/ml in 6mls of DMEM medium, supplemented with L-Glutamine, 1% penicillin/streptomycin, and 4.51µg/ml Cytochalasin B to block cytokinesis and generate bi-nucleated cells. After exposure to irradiation (0, 3 or 5 Gy), the cells were seeded in 6-well plates. Cells harvested at 24 and 48 hours were subjected to cytospin (800g/ 5 min) to spread the cells on to a slide for fixation and staining (May Grunwald's and Giemsa) (and compared to cells analysed immediately after irradiation). MN and other nuclear abnormalities were visualised by light microscopy for identification and counting. In total 500 bi-nucleated cells were scored and the frequencies recorded as percentages.

4.2.2 Assessing DNA damage using the Comet assay

The Comet assay, based on gel electrophoresis, detects and quantifies DNA fragmentation associated with DNA damage. HeLa cells, seeded at a density of 3×10^5 cells/ml in 6-well plates, were irradiated using 3 Gy or 5 Gy (50 and 84 seconds) and incubated at 37°C for 24 or 48 hours. Untreated and baseline samples (10 mins immediately after irradiation) were included for comparison. For the gel electrophoresis, HeLa cells were mixed with low melting agarose gel (~35°C) and quickly embedded in pre-coated slides with normal melting agarose. The cell and agarose mix was then covered with a coverslip (22 mm × 50 mm). The slides, with the cells and agarose mix, were placed on ice for 2-3 minutes to solidify the gel. The

cells were then transferred to a humidified incubator (37°C) for 20 min to enable DNA repair to occur and then the cover slip removed. The cells were then lysed for 1 hour to detach the cellular membrane whilst preserving the DNA and also to stop further DNA repair. The slides with the cells were transferred to an electrophoresis tank and covered with appropriate buffer (300mM NaOH, 1mM EDTA, and 1% DMSO) for 30 minutes in the dark to promote DNA unwinding and to reduce supercoiling. This allows the negatively charged DNA to migrate towards the anode (on electrophoresis at 300 mA for 25 min) and improves the yield of DNA fragments within the comet tail [203]. As the frequency of DNA breaks increases, the resultant DNA fragments migrate faster than intact DNA (undamaged) to form and give the appearance of a comet with a tail. On completion of electrophoresis, slides were washed with neutralisation buffer (three times for 5 minutes each) and dried overnight. The following day, slides were rehydrated with dH_2O for 30 minutes before staining with 1ml of SYBR Gold (1:10,000 dilution in PBS of a 10,000X concentrate in DMSO) for 30 minutes. Slides were then dried again prior to observation by fluorescent microscopy. Ten pictures taken for each slide were analysed using Image J 1.48 software. The percentage of DNA within the tail was calculated for each cell and the values transferred to an excel sheet for further analysis.

4.2.3 Synchronisation of HeLa cells in the cell cycle

To compare the three DNA damage assays (CBMN vs MN-FACS and Comet vs MN-FACS), synchronisation of HeLa cells to harmonise cell cycle status was thought to be essential and hence cells were cultured in serum free medium. Growth in serum free medium promotes cell cycle arrest at G0/G1 phase and ensures that the vast majority of the cells are at the same stage of the cell cycle when serum and growth is restored. Cell cycle analysis performed using flow cytometry confirmed that up to 80% of the cells were at the G0/G1 stage 24 hours after culture in serum free medium (data not shown).

HeLa cells were trypsinised, centrifuged at 500g for 5 minutes and re-suspended in complete medium (DMEM with serum) prior to irradiation. Irradiated cells were cultured in 6-well plates at a density at 3×10^5 cells/ml for two days.

4.2.4 Detection of H2AX phosphorylation

The expression of H2AX phosphorylation marks sites of DNA repair after exposure to DNA damaging agents. HeLa cells (1.5×10^6 cells/ ml) were harvested and exposed to 3Gy of radiation. The cells were incubated at 37˚C for 0.5, 1, 2, 6, 24 hrs in an incubator (5% CO_2) and a control sample was processed 10 minutes after irradiation. At each time-point the cells were trypsinised and harvested prior to PBS washes. Ice-cold methanol was added to the cell suspension dropwise and the cells were fixed for 1 h. The cells were then washed with PBS and re-suspended with 1.4 ml (PBS + 0.25% Triton X-100) and incubated on ice for 25min. The cells were then

centrifuged and re-suspended in 100 μl PBSBA (PBS containing 1% bovine serum albumin and 0.02% sodium azide) along with 0.75 μg Rabbit anti-Phospho Histone H2AX (Ser139) or an isotype control. The tubes were incubated at room temperature for 2-3 hours and inverted every 15 mins. After further centrifugation, the pellet was re-suspended in 100 μl PBSBA containing secondary antibody (Alexa - labelled donkey anti-rabbit) and incubated for 30min at room temperature in the dark with gentle mixing. Finally, before FACS analysis the cells were washed and re-suspended in 500 μl PBSBA.

4.3 Results

The following section describes the optimisation of each technique. In addition, comparative data obtained for each technique performed alongside the MN-FACS assay was examined for correlations.

4.3.1 Effect of Cytochalasin B (with and without irradiation) on HeLa cell division and numbers

Before optimizing the CBMN assay, we examined the effect of Cytochalasin B (Cyt-B) on HeLa cells. HeLa cells (3×10^5 cells/ml) were first synchronized for 24h, harvested, and treated with irradiation (3 or 5Gy). The cells were then re-suspended in serum containing DMEM medium with and without Cyt-B (4.51µg/ml) and incubated in 6-well plates for 24 or 48 hrs and compared to cells immediately after irradiation (10 mins). The cells were then harvested stained with trypan blue and counted (Nexcelom apparatus). Treatment of cells with Cyt-B alone (no irradiation) resulted in decreased cell numbers (see **Figure 4.2**). When the cells were irradiated with 3 Gy there was not an additional effect of Cyt-B in decreasing cell numbers as the cells are on the base line. The cell numbers did not change at 24 hrs following 5 Gy irradiation, but seems to be decreased more after 48 hrs.

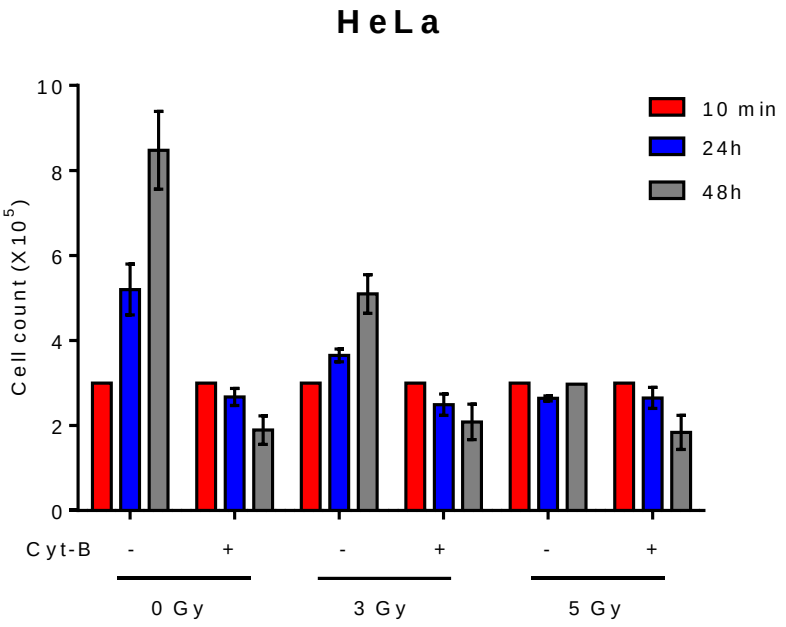

Figure 4. 2: The effect of Cytochalasin B on HeLa cells. After synchronisation 3×10^5 cells/ml HeLa cells were harvested, irradiated, and cultured in 6-well plates for 24 and 48 h with and without Cyt-B. The results show that Cyt-B does have an effect on the number of cells in both untreated and irradiated cells. Results of triplicate experiments are shown. (mean ± SEM; n= 3).

4.3.2 Induction of bi-nucleation in HeLa cells by Cyt-B

To ensure that the Cyt-B induces bi-nucleation 2000 HeLa cells were counted after the conditions described above. The results indicate that with Cyt-B treatment bi-nucleated cells increased over time in non-irradiated cells when compared to control cells. With increasing radiation (3 or 5 Gy), the number of bi-nucleated cells decreased in the cells treated with Cyt-B, indicating that irradiation is likely affecting cell cycle progression. However, with each dose irradiation the number of bi-nucleated cells did increase with time (48 hrs > 24 hrs). The cells not treated with Cyt-B treatment showed lesser numbers of bi-nucleated forms.

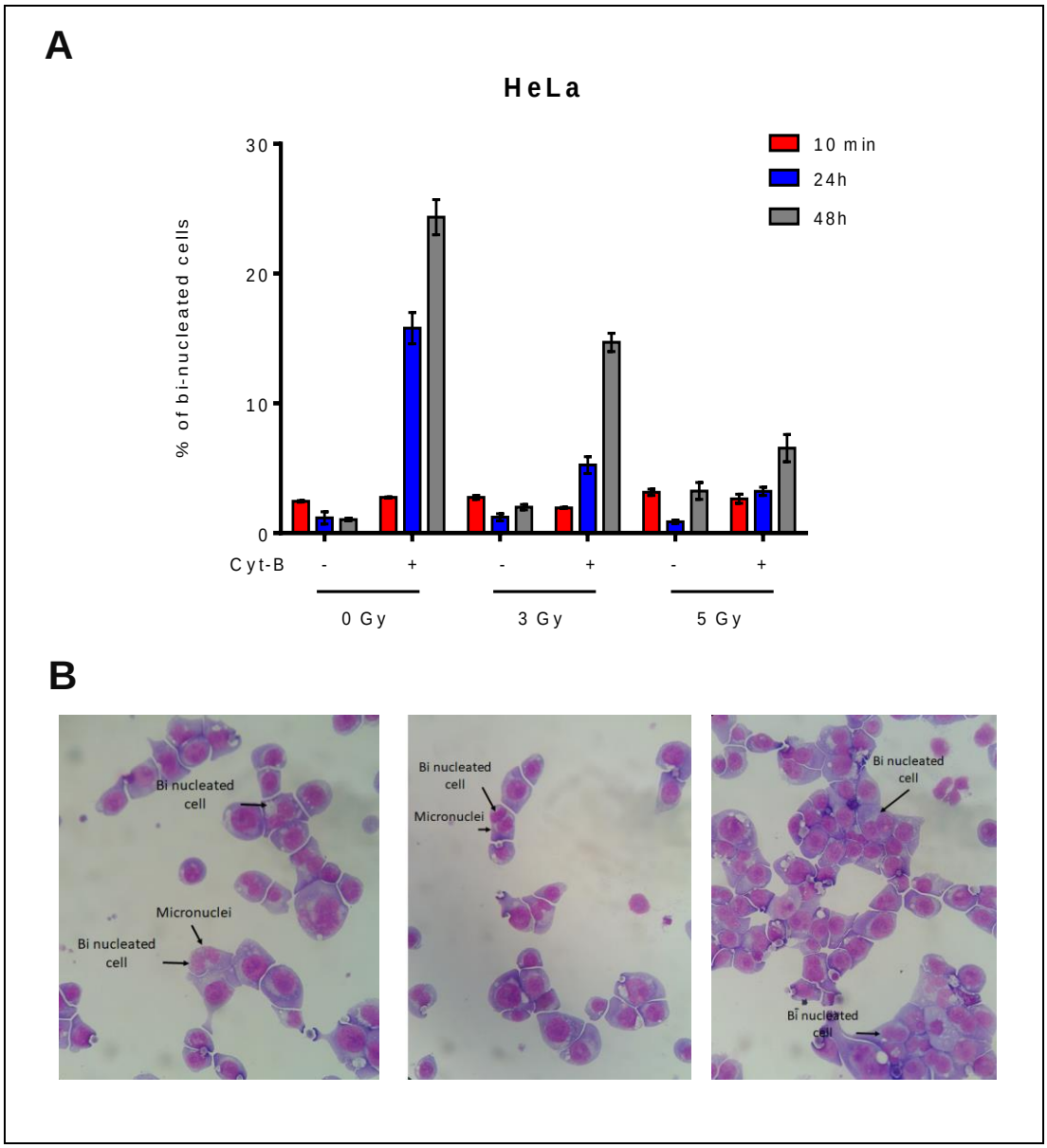

Figure 4. 3: Induction of bi-nucleation in HeLa cells by Cytochalasin B. A) The percentage of bi-nucleated cells in the UT and irradiated HeLa cells w/o and w the treatment of Cyt-B. **B)** Pictures taken from the same experiment showing bi-nucleated cells and MN. HeLa cells were serum starved for 24h and synchronized. Next day the cells were re-suspended with complete medium with and without Cyt-B and exposed to irradiation. After 24 or 48 hrs the cells trypsinised and cytospun on to slides and compared to cells immediately after irradiation (10 mins). For counting cells were fixed and stained with Gay Grunewald's and Giemsa stains and examined by light microscopy. The results show that Cyt-B does increase the number of bi-nucleate cells especially without irradiation. (mean ± SEM; n= 3).

4.3.3 Optimization of CBMN assay in HeLa cells

We next measured the number of induced MN in cells with or without irradiation. After synchronisation for 24 hrs, HeLa cells were centrifuged, re-suspended in serum containing medium. The cells were then irradiated with 3 or 5Gy and cultured for 24 or 48 hrs in the presence of Cyt-B. After each time point cells trypsinised, harvested, cytospun, stained with Giemsa and may-Grunewald's. After washing with PBS, the slides observed under light microscopy. The frequency of MN increased with radiation dose when compared to non-irradiated cells at both time points.

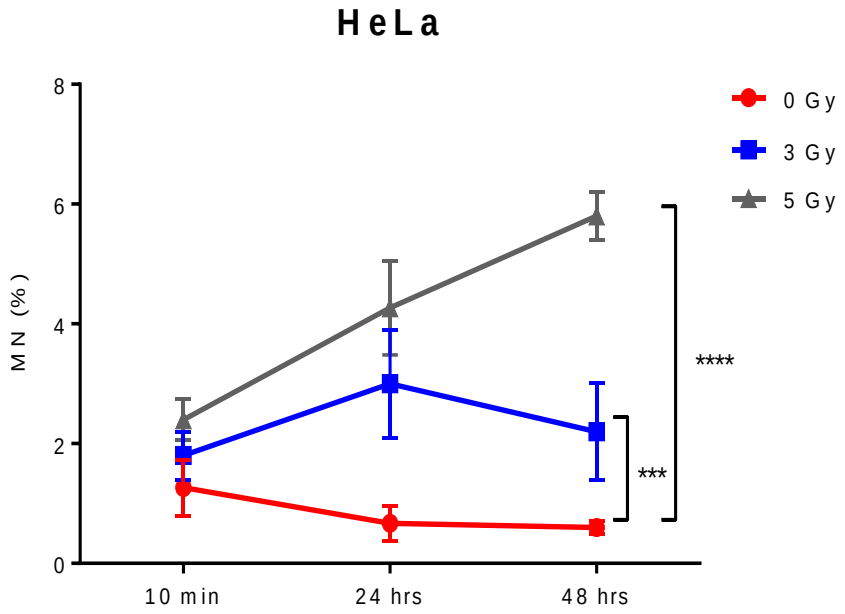

Figure 4. 4: Optimization of CBMN assay in HeLa cells. Irradiated HeLa cells (3 or 5 Gy) were examined for MN frequency at specified time points. The graph shows 'percentage' MN counts for each 500 bi-nucleated cells for each condition and time point. Two-way ANOVA- Dunnett's multiple statistical comparisons were performed and statistically significant differences from UT were found for all time points (0 Gy vs. 3 Gy ***p<0.001; 0 Gy vs. 5 Gy ****p<0.0001. (mean ± SEM; n= 3).

4.3.4 Correlation analysis between MN-FACS and CBMN assays

Having optimised the CBMN and MN FACS assays, we next performed a correlation analysis of results obtained with both techniques performed in parallel on the same cells.

HeLa cells were treated and harvested as above (see **Section 4.2.1**) and aliquots subjected to CBMN or MN FACS assays. For the MN-FACS assay 50,000 cells were counted. The assay, however, measures MN frequency but does not provide any information regarding the frequency of bi-nucleated cells within the whole sample. As this may impact the results and compromise comparison to CBMN assay (which relies on counting MN frequency in a pure population of bi-nucleated cells) we developed a strategy to correct for this variable within the two assays to get a better sense of the results obtained. Here, we observed that previous published reports of MN FACS assay have not provided this refinement and did not express MN numbers as a function of bi-nucleated cell frequency.

As the studies were performed in parallel, we first determined the percentage of bi-nucleated cells in 2000 cells when performing the CBMN assay (**see Figure 4.3**). This allowed us to apply a correction to the MN frequency that was measured by the MN-FACS assay. In summary, we normalized MN frequency measured by the FACS assay to the percentage of bi-nucleated cells within each sample (differing radiation doses and time points). The relevant equations and calculations are shown below and MN count was adjusted to represent frequencies in 100 bi-nucleated cells. The experiment was performed in triplicate to check for reproducibility.

No. of bi-nucleated cells/ 2000cells= **A**

(A × 50,000)/ 100= **B**

(MN-FACS value/ B) × 100= **C (=MN count/100 bi-nucleated cells)**

Table 4.2 shows the values obtained in the CBMN assay and the adjusted values generated by the MN-FACS assay (in each case normalised for a 100 cells) that were then examined for correlations.

Table 4. 2: Summary of 'adjusted' CBMN (100 cells) and MN-FACS results (corrected for bi-nucleated cell frequency and in a 100 cells) in three biological replicates.

Experiment (1)				
		10 min	24 hrs	48 hrs
0 Gy	CBMN	2.2	1.2	0.8
	FACS	0.04	0.07	0.003
3 Gy	CBMN	2.6	4.8	3.8
	FACS	0.4	0.07	0.02
5 Gy	CBMN	3	5.8	6.2
	FACS	0.042	0.19	0.13

Experiment (2)				
		10 min	24 hrs	48 hrs
0 Gy	CBMN	0.8	0.2	0.4
	FACS	0.184	0.009	0.004
3 Gy	CBMN	1.4	2	1.2
	FACS	0.41	0.05	0.016
5 Gy	CBMN	1.8	3.8	6.2
	FACS	0.035	0.07	0.07

Experiment (3)				
		10 min	24 hrs	48 hrs
0 Gy	CBMN	0.8	0.6	0.6
	FACS	0.168	0.002	0.004
3 Gy	CBMN	1.4	2.2	1.6
	FACS	0.16	0.03	0.019
5 Gy	CBMN	2.4	3.2	5
	FACS	0.185	0.056	0.068

The results are graphically summarized in **Figure 4.5**. At the 10 minutes time point we did not see any significant correlation between results obtained by the CBMN and MN-FACS assays (**Figure 4.5 A**). This could be because the Cyt-B is unlikely to have had sufficient time to induce bi-nuclearity. In contrast, after 24 or 48 hours the results obtained by the MN FACS Assay (and adjusted as described above) did show significant correlations with results obtained by the CBMN assay (Figures 4.6 B and C). The percentages of MN increased with irradiation at 24 hrs with both 3 and 5 Gy. Although this trend and correlation was also seen at 48 hrs there was no further increase in MN frequency at 48 hrs despite an increase in bi-nucleated cells as previously described (**Figure 4.4**). One explanation may be the onset of apoptosis and subsequent disappearance of cells with damaged DNA.

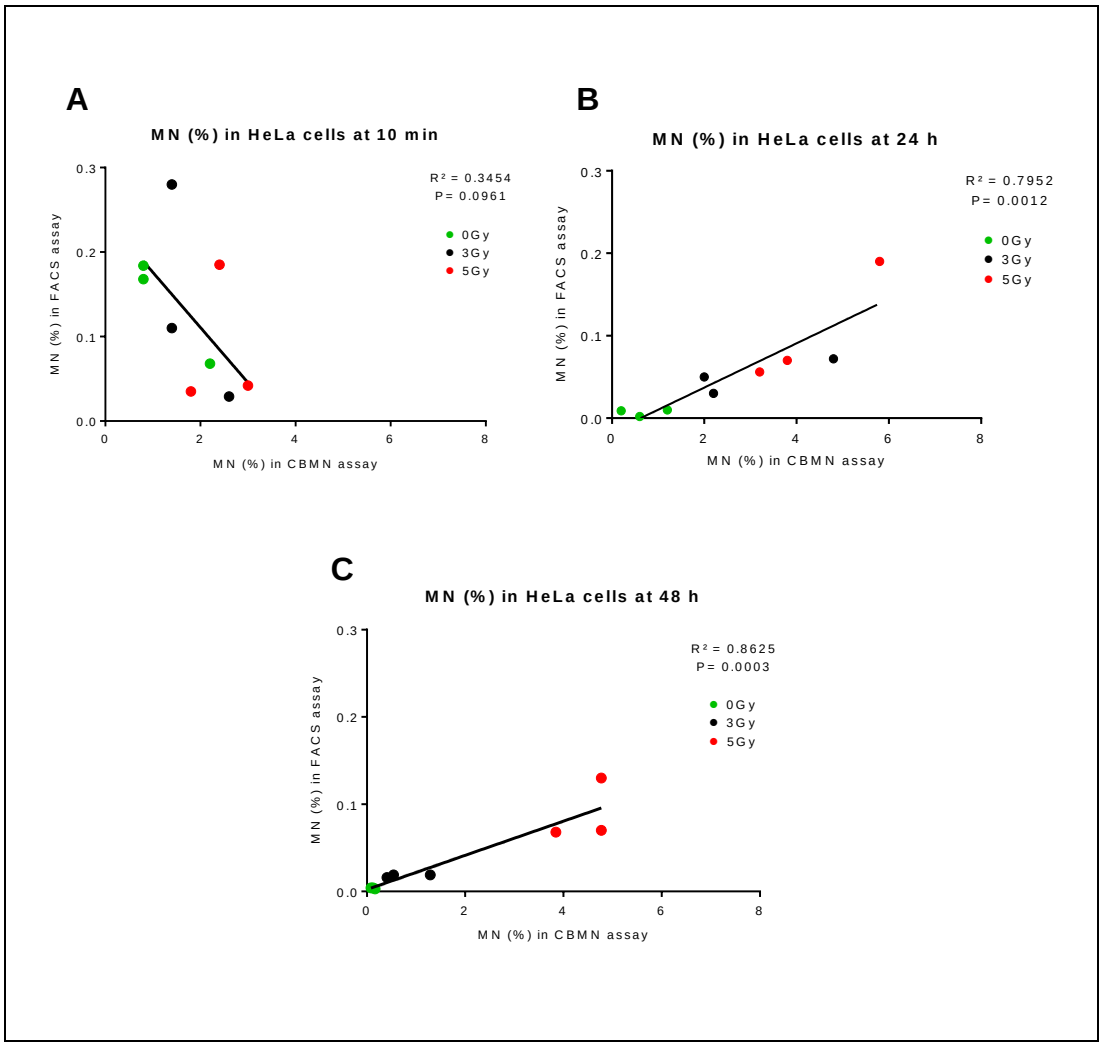

Figure 4. 5: Correlation analysis between MN-FACS and CBMN assay. HeLa cells were treated with irradiation (3 and 5Gy) and MN frequency was assessed using MN-FACS and CBMN assays in parallel. The dot plots show results obtained at 10 mins (A), 24 hrs (B) or 48 hrs (C). The specific values are shown in **Table 4.2** and represent adjusted counts (per 100 cells and bi-nucleate cell frequency). The values showed significant correlations between the MN-FACS and CBMN assays (for 0, 3 or 5Gy) at 24 and 48 hrs but not at 10 minutes. (A: p = 0.095, R^2= 0.3454; B: p< 0.01, R^2= 0.7952**; C: p< 0.001, R^2= 0.8625***). (Mean ± SEM; n= 3).

4.3.5 Optimization of Comet assay in HeLa cells

The Comet assay is a well-established technique to assess DNA damage and has previously been used for studies on cell lines and peripheral blood lymphocytes (PBL) [204]. We followed a modified protocol, which was recently published [161]. The advantages of this modified protocol established at the North West Cancer Research Centre in the University of Liverpool are that it is less expensive, all the reagents and gels can be made in the lab, and the protocol uses SYBR gold as an alternative stain to published methods that improves the detection of 'Comet tails' by the software. After analysis the Comet slides can be stored for extended periods (up to two years) without affecting the results.

We first examined the effects of irradiation on DNA integrity of HeLa cells using previously described conditions and time points (10 mins, 24 or 48h). Synchronised and revived HeLa cells were exposed to irradiation (3 or 5 Gy) and harvested after 24 or 48 hrs and examined by the Comet assay. The percentage of DNA sequestered within the 'comet tail' within individual cells was measured as described in the methods section (see **section 4.2.2**).

As shown in **Figure 4.6 A** (representative images of cells and comet tails for each condition and time point)**,** and as expected, increasing radiation dose resulted in greater DNA damage and generation of fragments which constitute the comet tails. The average of ten random images was taken for each comet slide. **Figure 4.6 B** represents the values obtained by the image J software upon counting 100 cells per slide (10 cells per image). The Comet tails were most prominent immediately after irradiation (10 mins). As

expected, increasing irradiation caused greater DNA damage immediately after irradiation. It is clear from Figure 4.7 B that there is a consistent decrease in the damaged DNA measured by the Comet assay at later time points (24 and 48 hrs) for 0, 3 and 5 Gy. This is most likely due to elimination of cells with damaged DNA by apoptosis (as seen in **Figure 4.6 B** with 5 Gy and 48 hrs where a 'hedgehog comet' represents an apoptotic cell) or due to the onset and completion of DNA repair.

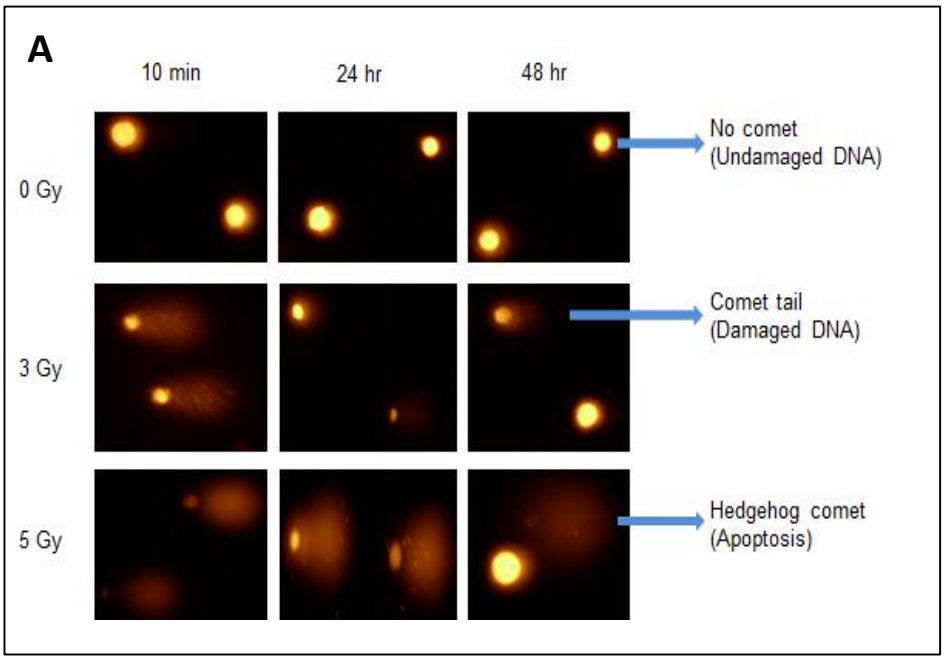

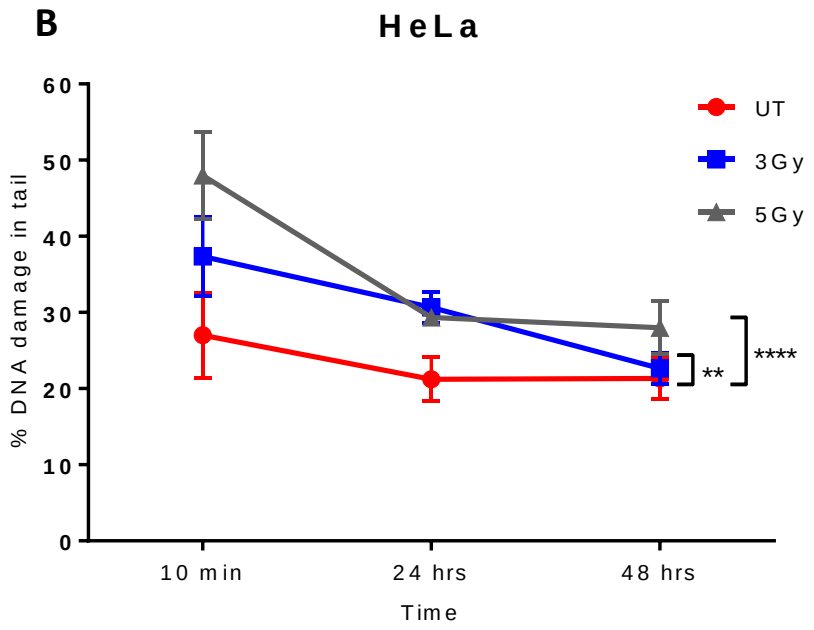

Figure 4. 6: A) The effect of exposing HeLa cells to different doses of irradiation (3Gy and 5Gy); B) Optimization of Comet assay in HeLa cells. HeLa cells were synchronized, harvested and irradiated (3 or 5 Gy). The cells were harvested at indicated time points (24 and 48 hrs) and examined using the Comet assay. Slides were analysed using ImageJ software. Two-way ANOVA- Dunnett's multiple comparisons were performed and statistically significant differences from UT were found for the irradiated samples (0 Gy vs. 3 Gy ** p<0.01; 0 Gy vs. 5 Gy **** p<0.0001. (mean ± SEM; n= 3).

4.3.6 Correlation analysis between MN-FACS and Comet assays

HeLa cells were examined by MN-FACS and Comet assays in parallel in three biological replicate experiments to determine whether there is a relation between the measurements. For these analysis, induction of bi-nucleated cells by Cyt-B was not necessary or used. Hence, the MN-FACS assay values generated do not take into account the percentage of bi-nucleated cells within the whole population. At 10 mins (**Figure 4.7 A**) the results showed that there is no significant correlation of findings in the MN-FACS assay and Comet Assay. The MN FACS assay did suggest that there was more cellular debris and dead cells at this time point.

Similarly, there was a lack of correlation at later time points (24 or 48 hrs) as well (**Figure 4.7 B and C**).

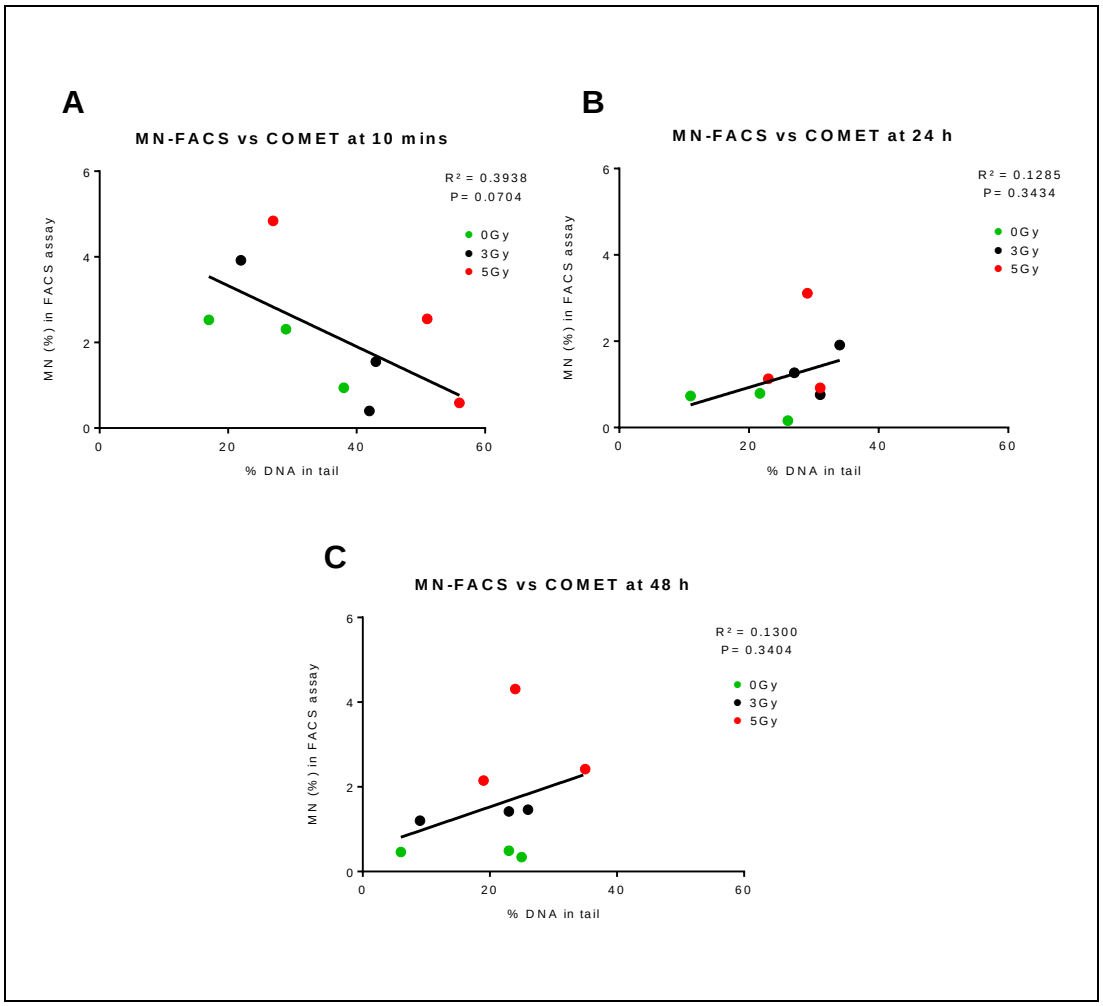

Figure 4. 7: Correlation analysis between MN-FACS and Comet assay. HeLa cells were treated with two doses of irradiation (3 or 5Gy) and correlation analysis was performed at 3 different time points (10min, 24h or 48h) (**A-C**). Regression analysis was used to determine statistically significant differences between MN-FACS and Comet assay (UT, 3, 5Gy). A: p= 0.0704, R^2= 0.3938; B: p= 0.3434, R^2= 0.1285; C: p= 0.3404, R^2= 0.1300. (Mean ± SEM; n= 3).

We next sought to understand the lack of correlation between the Comet assay and the MN-FACS at each time point. Given that the level of DNA damage at the later time point as assessed by the Comet assay does not significantly increase from the earlier points, it is likely that either apoptosis or DNA repair may be playing a role. In contrast, any repaired DNA incorporated into the genome is likely to yield increased number of MN at later time points. Hence an obvious avenue of investigation was to look for correlations between the Comet and MN-FACS assays from different time points. Taking the logical next step to the hypothesis outlined above we sought to examine any link between the findings from the Comet assay at an early time point, when the evidence for increased fragments is higher, to a MN enumeration by FACS at a later time point. In other words, the level of DNA damage at early time point (10 mins) might affect the MN count at later time points (after 24 hrs). Conversely, correlating findings from a later time point in the Comet assay with MN counts at an early time point may not be logical step as MN formation is likely to be late effect whereas early DNA damage is more likely to better appreciated in the Comet assay.

Hence, a correlation analysis was performed between late MN-FACS (24 and 48 hrs) and early Comet assay (10 mins) counts. The results in **Figure 4.8 (D and E)** suggest that MN-FACS assay findings at 48 hrs (but less so at 24 hrs) do correlate with the Comet assay results at 10 minutes.

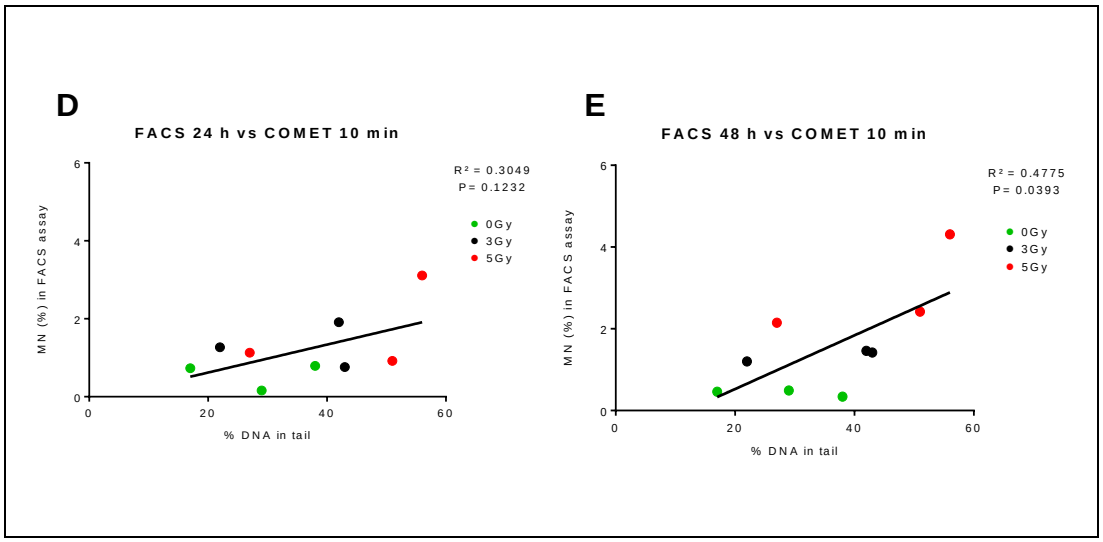

Figure 4. 8: Correlation analysis between MN-FACS and Comet assay. HeLa cells were treated with two doses of irradiation (3 or 5Gy) and the correlation analysis was performed between MN-FACS assay at 24 or 48 hrs and Comet assay at 10 mins (**D and E**). A regression analysis test was used to determine statistically significant differences at 24 hrs (D: p= 0.1202, R^2= 0.3090) or 48 hrs (E: p< 0.05, R^2= 0.4815*). (Mean ± SEM; n= 3).

4.3.7 The expression of γH2AX on HeLa cells

We next focused on γH2AX expression as this is another assay that is used to study the sites and extent of DNA damage. The aim of this experiment was to examine early and late expression of γ-H2AX in HeLa cells by FACS analysis to determine the levels of DNA damage after irradiation (3Gy) and to see if this mirrored the results seen with the Comet assay. HeLa cells, synchronized and harvested at a density 1.5×10^6 cells/ml, were exposed to irradiation (3Gy) and incubated for 0.5, 1, 2, 6 or 24 hrs in 6-well plates and compared to cells immediately after irradiation (10 mins) prior to the protocol for γH2AX antibody staining of the cells. At each time point, cells were trypsinised, harvested, and washed with PBS and fixed with ice cold methanol for 1h at -20˚C. After a further PBS wash, the cells were re-suspended in 1.4 ml of PBS (containing 0.25% Triton X-100) and incubated on ice for 25 mins. Equal aliquots of the cells were re-suspended in 100 μl PBS-BA with 0.75 μg of anti-phospho Histone H2AX (Ser139) or an isotype control. The tubes were incubated at room temperature for 2-3 hrs and inverted every 15 mins. Finally, pelleted cells were re-suspended in 100 μl PBS-BA containing secondary antibody (Alexa - labelled donkey anti-rabbit antibody) and incubated for 30min at room temperature in the dark with gentle mixing. After a final wash, the samples were subjected to FACS analysis.

The results show that the highest levels of phosphorylated γH2AX (serine 139) were noticeable at 30 mins after irradiation. The γH2AX expression was maintained up to 2 hrs, followed by a steady decline (**Figure 4.9**). Expression returned to basal level after 24 hrs. We conclude from the findings that the

expression of γH2AX reflects the findings of the Comet assay which is more likely to show evidence of DNA damage at early time points.

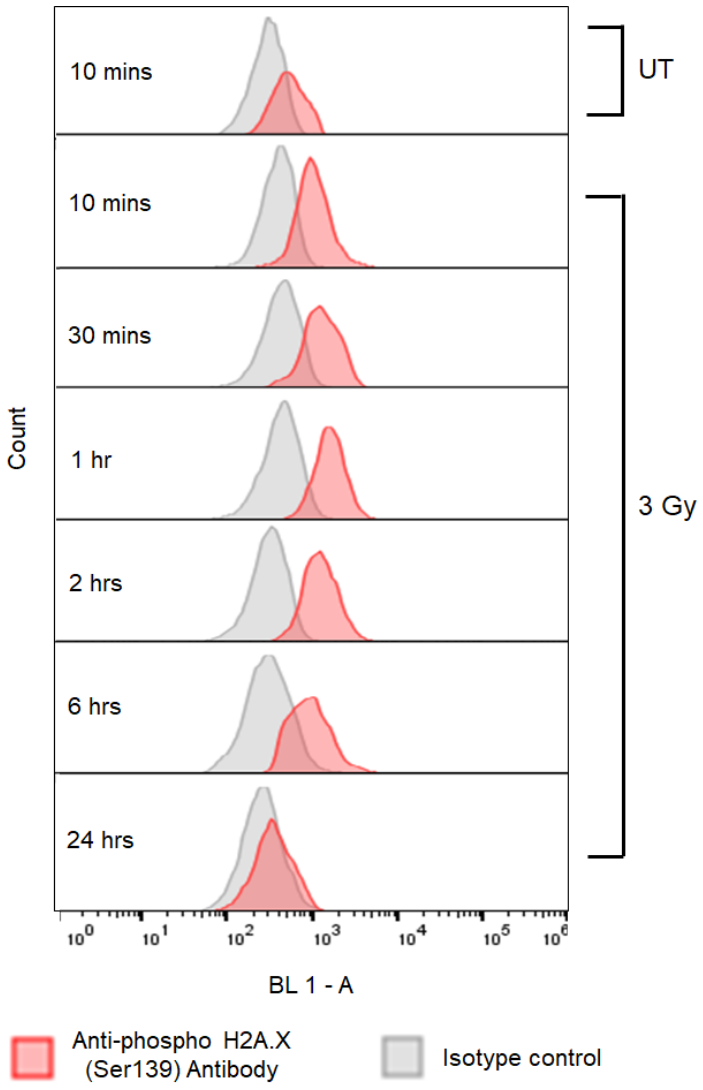

Figure 4. 9: The expression of γH2AX on HeLa cells (Histogram). HeLa cells were irradiated (3 Gy) and collected at indicated time points 10, 30 mins, 1, 2, 6, 24 hrs. Cells were stained with primary and secondary antibodies (rabbit anti γH2AX followed by Alexa labelled donkey anti-rabbit secondary antibody) or isotype control. H2AX phosphorylation peaked at 30 min and was maintained until 2h. The levels of H2AX phosphorylation then gradually decreased and returned to basal levels at 24 hrs. These images are representative n=3.

4.3.8 Investigation of Mitomycin C as a DNA damaging agent

In all the experiments described above, we primarily employed irradiation to induce DNA damage. We felt that it would be useful to have a more readily accessible chemical alternative for future planned studies. Not all labs may have access to a source of radiation and certain cell types such as primary cells may be more susceptible to apoptosis after irradiation thus compromising the detection of genotoxicity especially with the MN FACS assay. One such agent that has previously been used for such studies is the cytotoxic agent Mitomycin C (MMC) is a cytotoxic agent causes different types of DNA damages to the cells [205].

Synchronised HeLa cells (3×10^5 cells/ml) were incubated with increasing concentrations of MMC (0.025, 0.05, 0.1, 0.5, 1 μg/ml) at 37˚C for 3 hours in 6-well plates. The cells were then trypsinised, washed and re-plated for 24 or 48 hrs. Harvested cells were then subjected to the MN-FACS assay. The results (**Figure 4.10**) show that there is a dose dependent relationship between the amount of MMC used and the number of MN detected by the assay. Based on the results, we opted to use an MMC concentration of 0.5 μg/ml (3 hrs treatment) and incubation for 48 hrs for future studies.

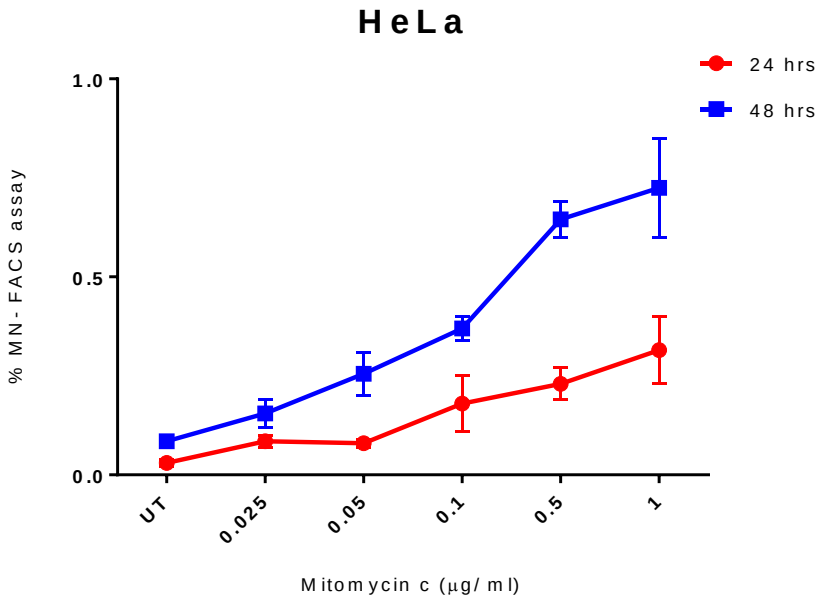

Figure 4. 10: Investigation of Mitomycin C (MMC) as a DNA damaging agent in HeLa cells. Synchronized HeLa cells were treated with increasing concentrations of MMC (0.025 – 1 µg/ml) for three hours and incubated for 24 or 48 hrs. An untreated sample was included for control. The MN-FACS assay was used to enumerate MN numbers. The results suggest that MMC can be used to induce DNA damage and MN formation. (Mean ± SEM; n= 3).

4.4 Discussion

The main aim of this chapter was to benchmark the MN-FACS assay against other established assays traditionally used to study DNA damage (i.e. CBMN and Comet assays). We compared results obtained with the three assays and performed correlation analysis. For these experiments, we employed HeLa cells and used irradiation for induction of DNA damage.

In all the described experiments there was evidence of DNA damage within irradiated HeLa cells compared to untreated controls and hence justified the used of this cell line for our studies and for comparative studies.

To achieve this, we first established and optimised the CBMN and Comet assays. We then performed parallel MN- FACS and CBMN assays at defined time points (10 mins, 24 or 48 hrs) to see if the results correlated. The results show that the MN count in the MN-FACS assay was less than that in the CBMN assay. The main reason for this discrepancy is that MN counting in the CBMN assay is restricted to bi-nucleated cells, whereas in the MN-FACS assay the MN count is reflective of the whole population of cells. The MN-FACS assay does not have steps to ascertain the number of bi-nucleated cells within a given cell population. Although, there was a quantitative difference in the MN count between the two assays, the results show a consistent correlation at both 24 and 48 hrs. The comparison between MN-FACS and CBMN assays has investigated in the literature using different DNA damaging agents and the results did show a variation between both assays but the pattern was the same for both assays [175, 206].

Another explanation for getting less MN count in MN-FACS assay comparing with the CBMN assay that the used genotoxic stress 3Gy is not enough to be detected by the MN-FACS assay.

The main advantages of the MN-FACS assay are that it is faster and allows objective exclusion of apoptotic bodies when compared to the CBMN assay. Not surprisingly, at 10 mins there was no correlation between the two assays, as the radiation treatment would not have had sufficient time to manifest itself. In addition, induction of bi-nucleation by Cyt-B would not have had enough time to occur. Nevertheless, these results suggest that the MN-FACS assay is as reliable as the CBMN assay in estimating induced differences in MN counts with treatments that cause DNA damage.

We next decided to compare the MN-FACS assay with another type of DNA damage assay not based on MN enumeration. Here, we investigated the relationship between the results obtained with the Comet and MN-FACS assays. The results showed that there was no correlation when both assays were compared at each specific time point. It is likely that at 10 mins after irradiation the Comet assay is able to detect DNA fragments whereas as previously stated sufficient time has not elapsed to induce MN formation. Similarly, at later time points the level of DNA damage as assessed by the Comet assay is either static or declines likely due to elimination of fragments either via apoptosis or DNA repair. In contrast, the MN-FACS assay is more likely to inform on mis-incorporated DNA by increase number of MN. Interestingly, when we compared the results at 10 mins by the Comet assay to MN counts at later time points (24 or 48 hrs) using the MN-FACS assay

there does seem to be a correlation. Conversely, there was no correlation between an early time point measurements by the MN-FACS assay with results at later time points with the Comet assay. In our hands, some disadvantages of the Comet assay include the time taken to complete the assay and the unreliability of the software in accurately identifying comet tails.

Finally, we studied the induction of H2AX phosphorylation upon DNA damage by irradiation. As with the Comet assay, the levels of γH2AX expression were highest at early time points. Although we have not attempted this, it may be theoretically possible to include γH2AX analysis within the MN-FACS protocol to get additional information regarding the levels of DNA damage and their relationship to MN counts within cell populations. In addition, improve the MN-FACS assay allows us to understand the time that takes the DNA damage to cause the chromosomal breaks e.g. DNA double strand breaks, which leads to MN formation.

The MN-FACS assay does lend itself well to the study of other cell types and cell lines. As the MN-FACS assay cannot estimate the number of binucleated cells within a sample as our protocol does not include a Cyt-B step. A compromise may be to treat cells in parallel with Cyt-B to enumerate the number of binucleated cells and apply a correction as shown within the results section. All our experiments using the MN-FACS assay required fresh cells. We have not investigated whether freeze-thaw cycles affect the assay. Such treatment is certainly likely to increase the levels of apoptosis. Such studies were beyond the scope of this project.

In addition to irradiation as a modality to induce DNA damage we have successfully explored the use of Mitomycin C (MMC) as an alternative DNA damaging agent for future studies, especially when using cells or cell lines that may be resistant to radiation-induced damage.

In **Chapter 5,** we would like to investigate the effect of the sequential treatment on the formation of MN.

Chapter 5: The effect of sequential exposure to therapeutic genotoxic interventions on DNA integrity

5.1 Introduction

Patients with lymphoid malignancies such as CLL, MCL, FL etc. frequently require sequential courses of chemotherapeutic agents as the disease course in each is characterised by remissions and relapses. In addition, some patients may also need radiotherapy for disease control. The impact of such exposure to potentially toxic chemotherapeutic agents (e.g. Chlorambucil, fludarabine, bendamustine, cyclophosphamide etc.) and/or radiotherapy on genome integrity of cancerous and non-cancerous cells within the individual is clinically relevant.

It is likely that such exposure may lead to accumulation of DNA damage within cancerous cells and could influence disease behaviour. Understanding accumulated DNA damage in cells due to prior treatments is important for understanding long-term effects of therapies in patients. As MN formation is a surrogate marker of DNA damage within the genome, the effect of sequential genotoxic treatments on MN frequencies may provide useful insights.

Although not addressed in this chapter, the use of MN-FACS assay and indeed other DNA damage assays for serial and sequential screening of primary patient samples for accumulated DNA damage may help in establishing the long term effects of standard treatments, novel agents such

as kinase inhibitors (ibrutinib, idelalisib etc) and indeed immunotherapies (rituximab etc.).

In this chapter, we examine the effects of sequential drug exposure and/or radiotherapy on MN frequencies within cancer cells using cell line models. For these studies, we have used a panel of CLL and MCL cell lines, exposed them to chemotherapeutic agents and irradiation in sequence, and assessed them by the MN-FACS assay. Given the findings in the previous chapter that suggest an influence of cell divisions and cell cycle status on MN frequencies some additional observations of potential relevance are included.

In the event of irreversible DNA damage, cells undergo apoptosis and cell death. If the cumulative DNA damage is sub-lethal, cells will continue to accrue harmful mutations/lesions that lead to genome instability [207].

It is well known that a major complication of cytotoxic chemotherapy is therapy-related myelodysplasia and/or acute myeloid leukaemia (t-MDS/AML). Furthermore, a study investigating the effects of doxorubicin on mechanical properties of cancer cells using human AML blast cells showed that the drug impacts and reduces the stiffness (increase cell death) of leukemic cells and impairs drug bioavailability within the target cells [208, 209]. Cytotoxic therapies induce chromosomal aberrations and mutations of genes essential for haematopoiesis [210].

Antimetabolite drugs such as Fludarabine, cytarabine and 5-fluorouracil, are nucleoside analogues that incorporate into DNA during the S-phase of the cell cycle and subsequently trigger apoptosis. These drugs are also known to cause t-MDS/AML [211].

In a published study on mesenchymal stem/stromal cells (MSCs) within the bone marrow (BM) exposed to the chemotherapeutic agent cyclophosphamide, an increase in DNA damage was demonstrated using the CBMN assay. In parallel, HS5 cells treated with the cyclophosphamide show DNA damage in a Comet assay. Interestingly, despite drug wash-out there was evidence of persistent DNA damage in subsequent generations [212].

DNA-damaging agents can increase mutation rates within cancerous and non-cancerous cells. A study on de novo versus relapsed acute myeloid leukaemia showed an increase in transversions that are associated with DNA damage caused by cytotoxic chemotherapy [213].

It has been shown that mutation rates increase even when cells are treated with low doses of DNA-damaging agents [214]. The levels of DNA damage vary between individual cells and can depend on tumour DNA damage response, cell cycle status or functional status of TP53 [215].

Adaptation and survival following drug treatments in cancer is driven by genetic heterogeneity and genomic instability. Sequential treatments likely lead to sub-clones with accumulated DNA damage that are potentially more evolved and resistant to subsequent therapies. There has been a lot of interest in recent years to understand clonal heterogeneity to improve therapeutic outcomes [216]. It is likely that such clonally evolved tumours have ‘scars’ of accumulated DNA damage that may be appreciated in assays such as the Comet assay or by MN frequency enumeration.

Previous studies have shown that overall copy number alterations (CNAs), which also correlate with the genomic instability index (GII), impact

proliferative potential in cancer [217]. Other studies show that DNA-damaging therapies increase somatic copy number alterations (SCNA). For example, DNA damage sensitivity in neuroblastoma is associated with increased DNA content, arising from aneuploidy or duplication events within the cancer genome [218].

Chemotherapy and mutagens may increase genomic instability and proliferation rates. Drugs that enhance chromosomal instability (CIN) can potentially increase the level of genomic instability which may lead to more aggressive behaviour in cancer cells [219] (**Figure 5.1**).

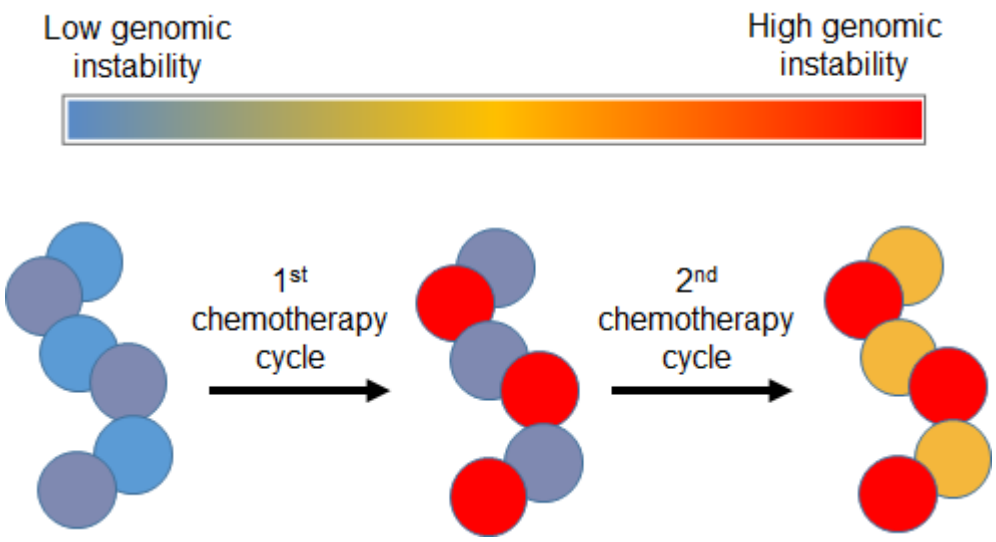

Figure 5. 1: The figure illustrates increasing genomic instability partly due to sequential chemotherapeutic treatments that could affect proliferation rates and behaviour of cancer cells. The circles indicate heterogeneous cancer cells containing sub-clones of variable genomic instability (see colour bar). Figure adapted from [213].

A study in Acute Lymphocytic leukaemia (ALL) patients has shown increasing micronuclei counts throughout the treatment period [220]. The frequency of MN in peripheral blood lymphocytes (PBL) of patients with small cell lung cancer (SCLC) and ovarian carcinoma (OC) undergoing chemotherapy (combination of cisplatin and etoposide) reached their peak after 2 to 3 cycles [221].

In this chapter, we hypothesise that cancer cells surviving sequential treatments (such as chemo-radiotherapy) harbour increasing levels of genomic damage and instability. It is, hence, interesting to see if exposure to repeated genotoxic treatments affects the frequencies of MN within cancer cells. To address this, we measured MN frequencies in CLL and MCL cell lines (HG3 and JeKo-1) after 'sequencing' chemotherapeutic agents (such as Fludarabine or Bendamustine) +/- irradiation (3Gy).

We chose Fludarabine and Bendumustine for these experiments as the two agents are frequently used for the treatment of CLL and indeed other low grade NHLs.

The **aims** of this chapter are to:

1. Determine the effect of sequential exposure to Fludarabine and Bendamustine +/- irradiation on MN frequencies.
2. Examine the influence of apoptotic rates and cell cycle status on MN formation within these conditions.

5.2 Results

5.2.1 Effects of Fludarabine on CLL and MCL cell lines

We first assessed the effect of increasing doses of Fludarabine on the viability of 3 CLL cells lines (MEC1, EHEB, HG3), and 2 MCL cell lines (MAVER-1 and JeKo-1). Cells were cultured at a density 3×10^5 cells/ ml in 6-well plates, treated with drug, and harvested at 24, 48 and 72 hrs. Apoptosis assays were performed at each time point using Annexin V/ PI staining and FACS analysis.

Figures 5.2 A-E show the effects of Fludarabine (0, 0.1, 0.3, 1, 3, or 10 μM) for three days on the mentioned cell lines. The results show that MEC1 and EHEB cell lines are resistant to Fludarabine at all concentrations. In contrast, HG3, MAVER-1 and JeKo-1 cell lines did show sensitivity to Fludarabine at concentrations above 0.3 μM. For experiments involving MN frequency enumeration we chose to use two different concentrations for each cell line; a) one that does not affect cell viability and b) another that is at the cusp of affecting viability without profound effects on apoptosis but is likely to have sustained DNA damage that may be reflected in the MN-FACS assay. Therefore, the concentrations chosen for HG3, MAVER-1 and JeKo-1 were 0.3 & 1 μM, 0.1 & 0.2 μM and 0.1 & 0.2 μM respectively.

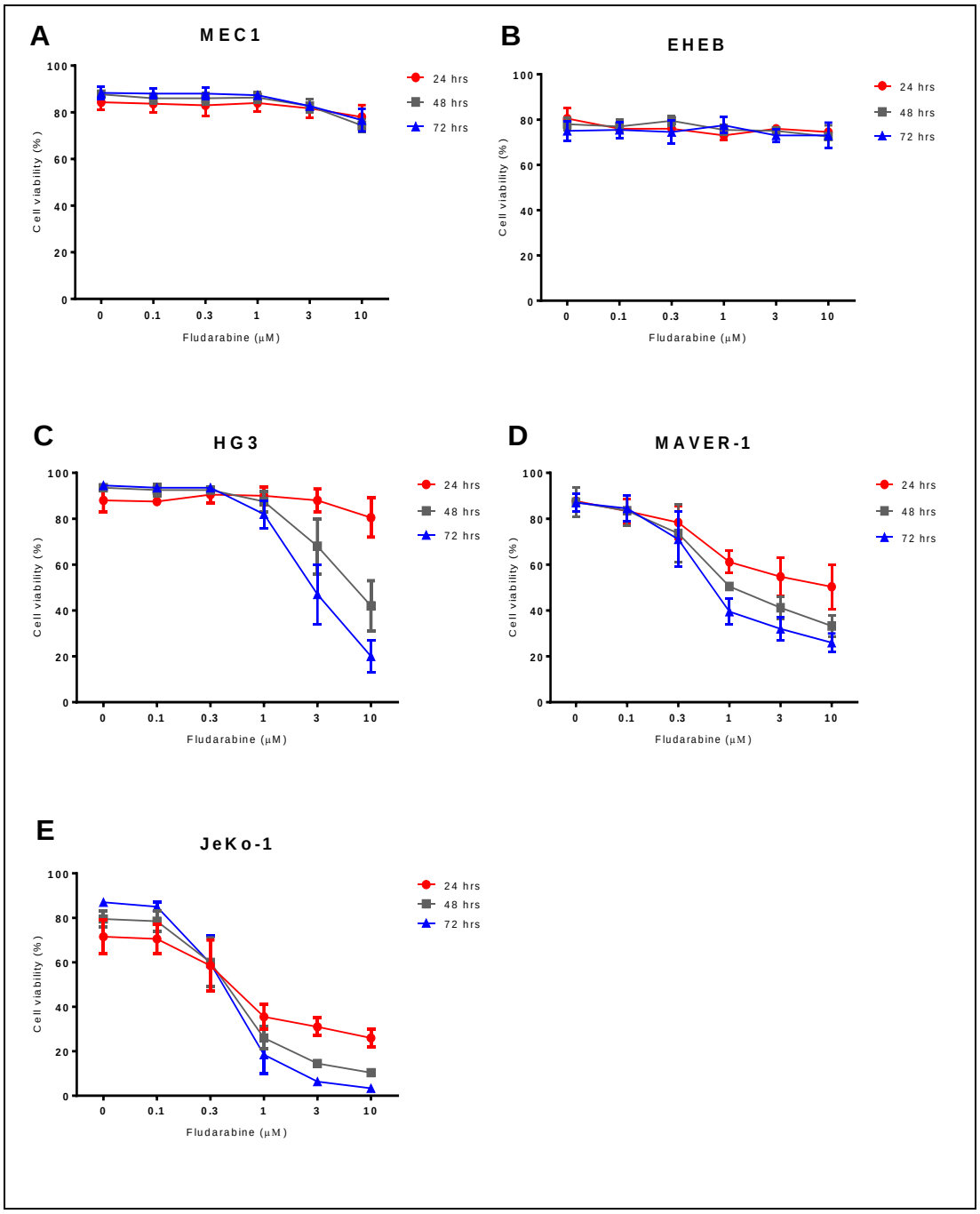

Figure 5. 2: Effects of Fludarabine on cell viability using FACS. The treated cell lines are; **A.** MEC1; **B.** EHEB; **C.** HG3; **D.** MAVER-1; **E**. JeKo-1. HG3. Cell lines were treated with escalating doses of Fludarabine (0.1 μM to10 μM) for 72 hrs. Cell viability was measured after 24, 48 or 72 hrs of treatment using Annexin V/ PI staining. The y-axes show percentages of viable cells. (Mean ± SEM; n= 3).

5.2.2 Effects of Bendamustine on CLL and MCL cell lines

As for Fludarabine, the effects of Bendamustine were studied on the same 5 cell lines using similar conditions.

Figures 5.3 A-E show the effects of increasing concentrations of Bendamustine (0, 0.1, 0.3, 1, 3, 10 μM) for three days on the cell lines. In essence MEC1, EHEB and HG3 are resistant to Bendamustine, while MAVER-1 and JeKo-1 are sensitive at higher concentrations. We selected 1 and 2 μM to treat MAVER-1 and JeKo-1 cell lines in the MN enumerations experiments. As these two cell lines only represent MCL we have included experiments on HG3 cells (a CLL cell line) at 1 and 2 μM concentrations.

As the main purpose and aim of our experiments was to study the effects of sequential exposure to chemotherapeutic agents on MN frequency we devised a drug exposure schedule with Fludarabine followed by Bendamustine (or vice versa) with built in drug holidays. For these experiments, we chose a CLL and MCL cell line each (HG3 and JeKo-1). **Figure 5.4** shows a flow chart outlines the sequential treatment strategy for HG3 and JeKo-1.

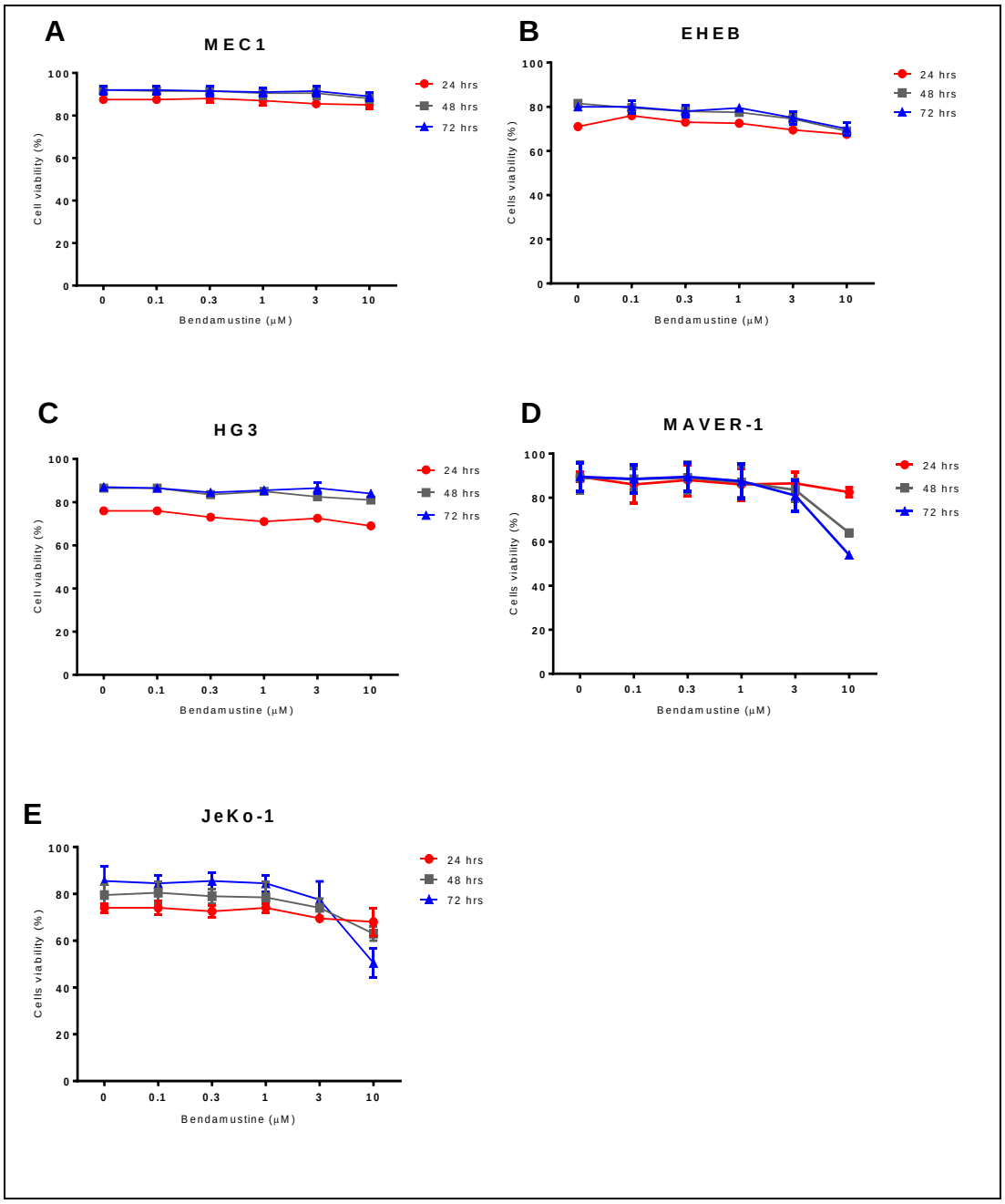

Figure 5. 3: Effects of Bendamustine on cell viability using FACS. Five cell lines (**A.** MEC1; **B.** EHEB; **C.** HG3; **D.** MAVER-1; **E.** JeKo-1) were treated with Bendamustine (0.1 μM to 10 μM) and assessed for cell viability after indicated time points (24, 48 or 72 hrs). (Mean ± SEM; n= 3).

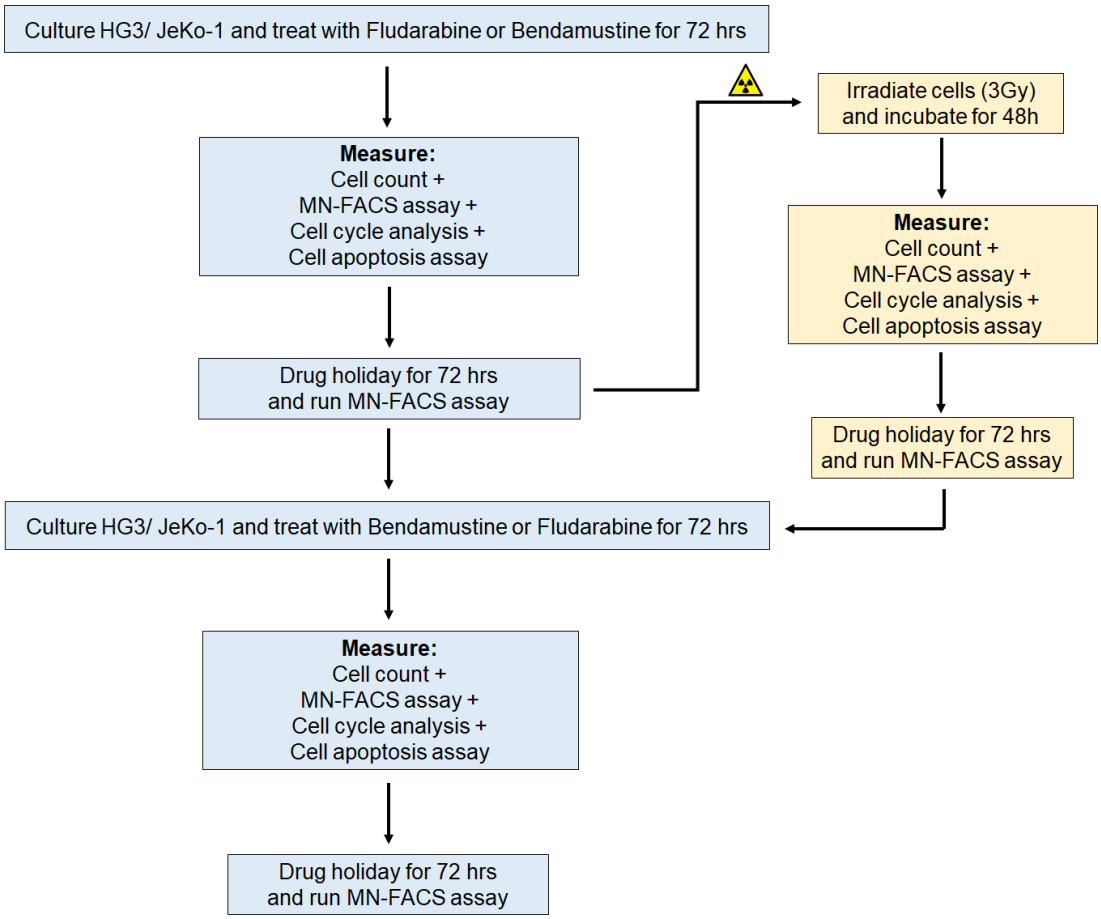

Figure 5. 4: A flow chart summarising the sequential treatments and assays of indicated cell lines.

We decided this treatment strategy by starting with chemotherapy first, followed by irradiation based on the published studies in the literature, which recommended this way for treating cancer. Also the clinical trials found that starting treatment with chemotherapy had better overall results compared with treating the patients first with irradiation [222].

5.2.3 Sequential treatment of HG3 cell line with Fludarabine (F) and Bendamustine (B)

The aim of this experiment was to assess the effect of Fludarabine and Bendamustine on MN formation in HG3 cells. Two parallel experiments were performed using two different sequences of the chemotherapy drugs. Two concentrations of each drug were chosen as previously discussed (see Section 5.2.1). After each treatment, MN frequencies were measured using the MN-FACS assay. Cell viability and cell cycle status were assessed at defined time points as indicated in **Figure 5.4**.

The results for cells treated with Fludarabine followed by Bendamustine or vice versa in **Figure 5.5 A1 and B1** show that there were no significant differences in MN frequencies with untreated and lower concentrations (0.3 μM F and 1 μM B). There was tendency to slightly increased MN frequencies at the higher dosages (1 μM F and 2 μM B). Cell viability appears to decrease with the higher concentrations as expected (**Figures 5.5 A2 and B2**). The changes in cell cycle status with the different conditions were also not significant (**Figures 5.5 A3 and B3**).

The results suggest that fludarabine at a higher dose (1μM) does increase MN frequency. A further conclusion is that bendamustine followed by fludarabine, rather than the other way around, is more likely to increase MN frequency even after a drug holiday. There is a suggestion that frequent passage may also contribute as some increase is observed in the untreated samples.

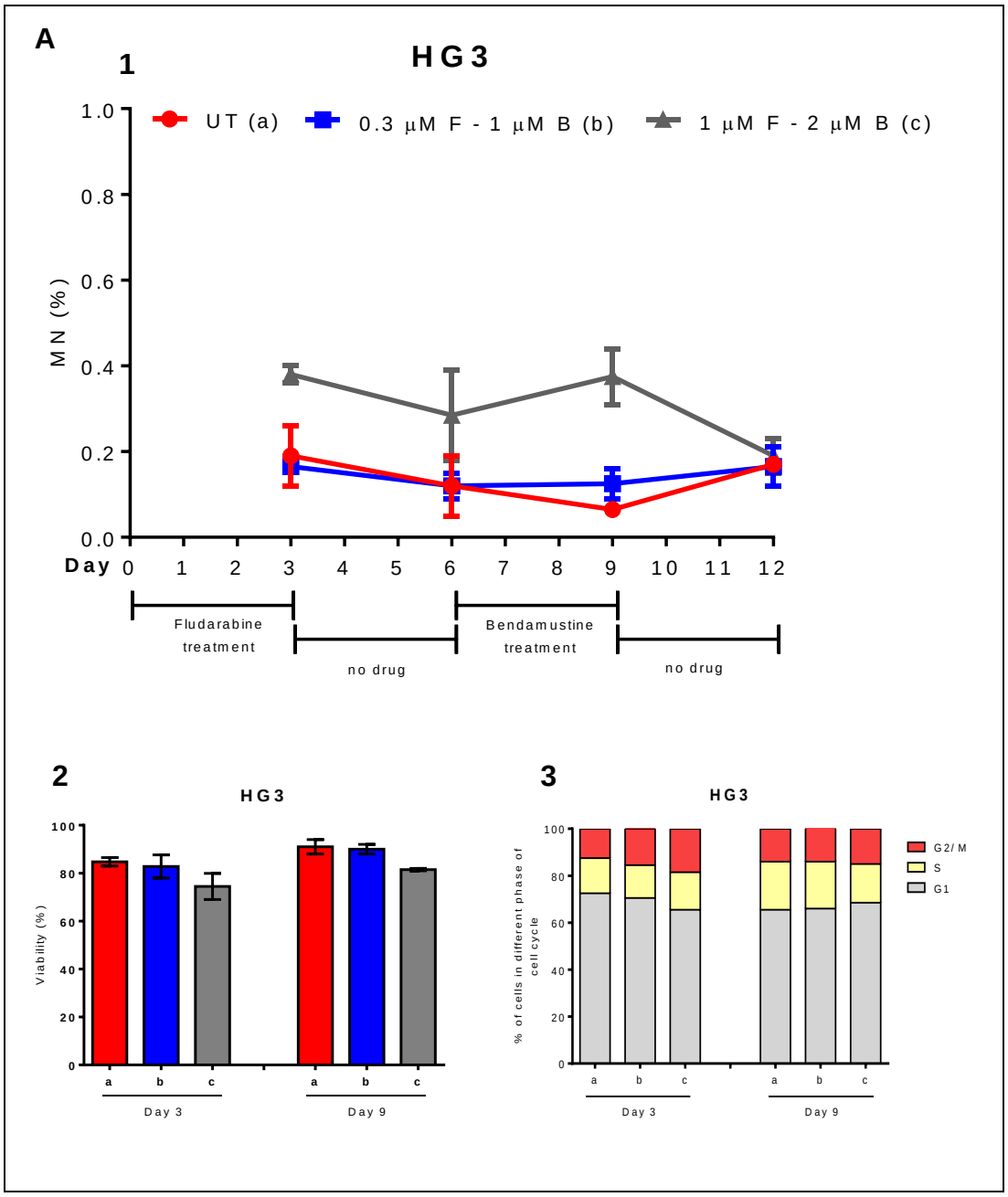
A
1
HG3
UT (a)
0.3 µM F - 1 µM B (b)
1 µM F - 2 µM B (c)
MN (%)
Day
Fludarabine treatment
no drug
Bendamustine treatment
no drug
2
HG3
Viability (%)
Day 3
Day 9
3
HG3
% of cells in different phase of cell cycle
G2/M
S
G1
Day 3
Day 9

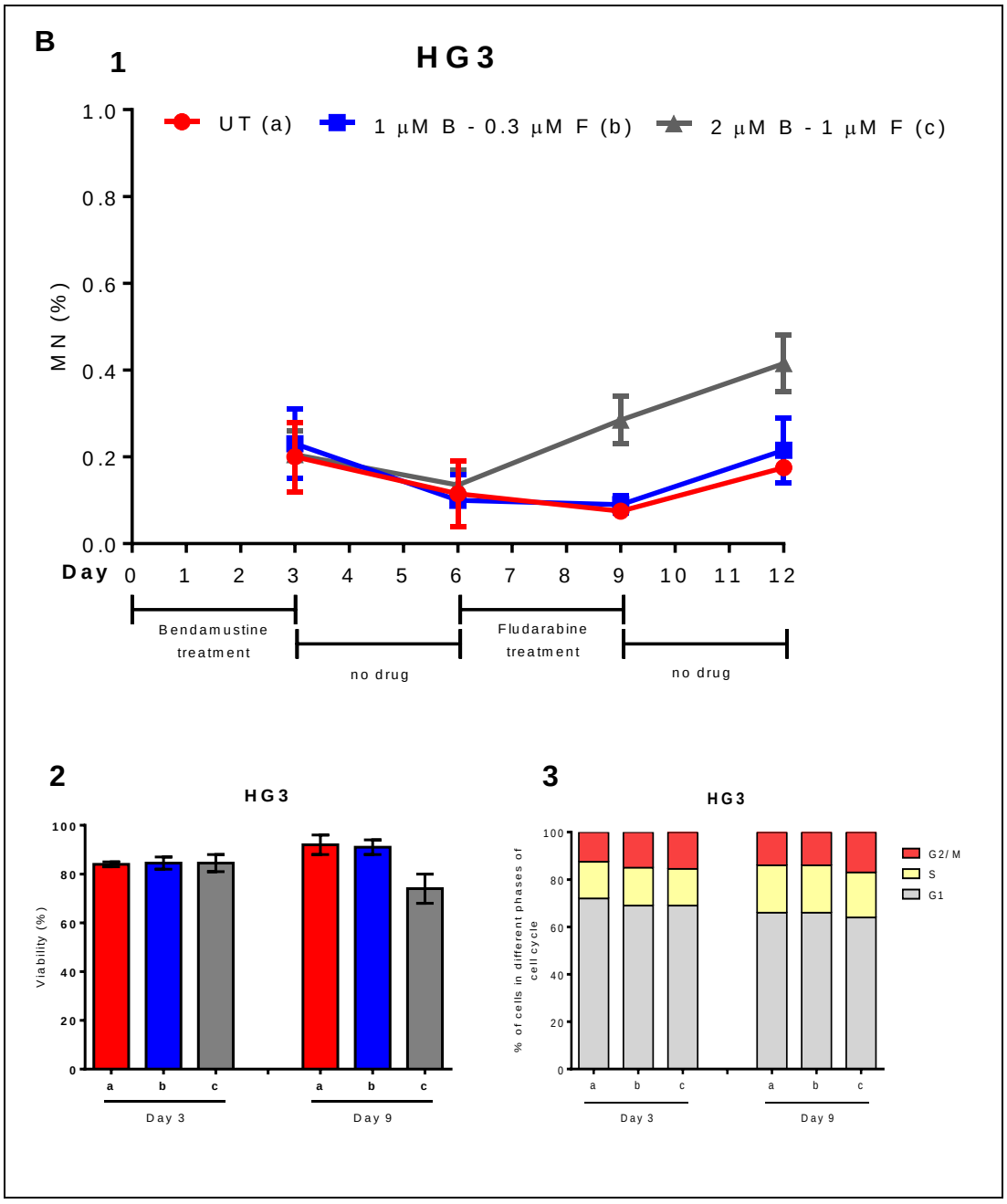

Figure 5. 5: Sequential treatments of HG3 cell line: A) Fludarabine followed by Bendamustine; **B)** Bendamustine followed by Fludarabine. The concentrations of the two drugs and the sequencing are indicated (blue or grey) as are the time points of each assessment MN frequencies (A1 and B1), Viability (A2 and B2) and Cell cycle status (A3 and B3). The results summarise the findings of n=3 experiments and error bars represent S.E.M.

5.2.4 Sequential treatment of HG3 cell line with Fludarabine (F) followed by irradiation and Bendamustine (B)

This experiment was conducted to assess the effect of Fludarabine followed by irradiation (3Gy) and finally Bendamustine on MN frequencies in HG3 cells at specified time points. As in the previous section, parallel experiments with different order of F and B (and two doses of each drug) were used with an intermediate irradiation step. The experimental plan is as shown in **Figure 5.4**.

The results summarised in **Figure 5.6 A1** (F followed by IR followed by B) suggest that when treated with the higher dose of fludarabine followed by radiotherapy there is a marked increase in MN frequency after Day 8 which increases further by Day 11. This is sustained until day 17 but the treatment with bendamustine does not seem to have an additional effect. The combination of fludarabine followed by irradiation do have an effect on cell viability and cells in G2/M at the higher doses of fludarabine and bendamustine. It is difficult to draw any definite conclusions regarding the effects of cell viability (**Figure A2**) and cell cycle status (**Figure A3**) on MN frequencies.

Figures 5.6 B1, 2 and 3 show the results obtained when the order of the drugs was reversed (Bendamustine first and fludarabine second). The only significant changes were seen at the higher concentrations of the 2 drugs (see grey line in Figure 5.6 B1). At day 11 there did not seem to be any difference in MN frequency after the use of F or B with irradiation (see Figures 5.6 A1 and B1, grey lines). The use of fludarabine after

bendamustine and irradiation (compared to bendamustine after F and IR) seems to cause a significant increase (at least 2-fold) in MN frequency at day 14 with the higher concentrations of the drugs. Again, the impact of cell viability and cell cycle status on MN frequencies were not apparent. At day 17 in (**Figure 5.6 B**) the MN formation dramatically decreased to the 5%, which could be due to cell apoptosis or MN engulfed by the nucleus.

It is important to take into account the earlier finding (see section 5.2.2) that HG3 cells are resistant to Bendamustine at the drug concentrations used and hence the predominant effects are only seen with Fludarabine. Despite this the combined treatments do seem to have effects on MN frequency suggesting more cumulative DNA damage especially when fludarabine is used after bendamustine and even more so when there is an intermediate irradiation step.

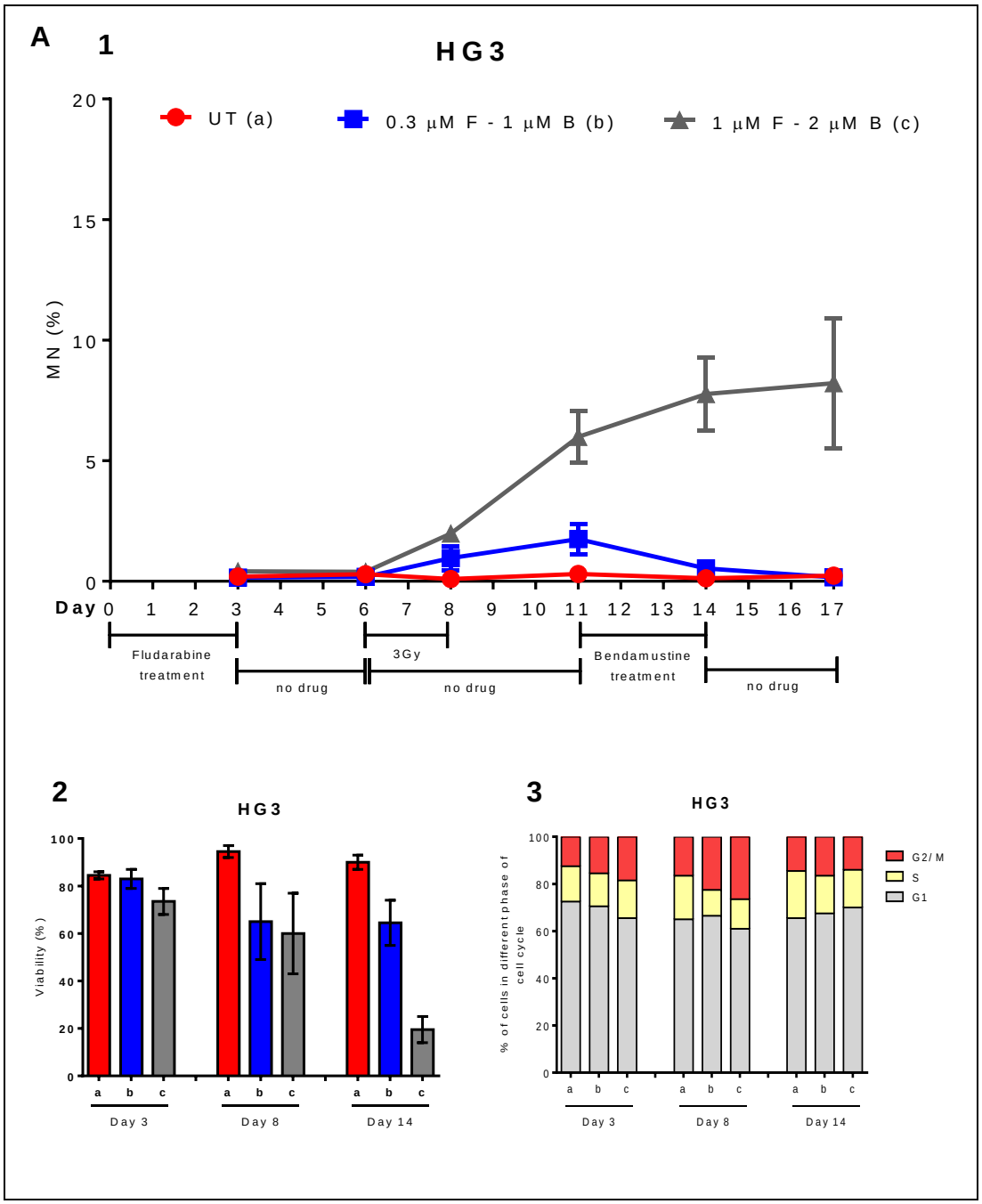
A
1
HG3
UT (a)
0.3 µM F - 1 µM B (b)
1 µM F - 2 µM B (c)
MN (%)
Day
Fludarabine treatment
no drug
3Gy
no drug
Bendamustine treatment
no drug
2
HG3
Viability (%)
Day 3
Day 8
Day 14
3
HG3
% of cells in different phase of cell cycle
G2/M
S
G1
Day 3
Day 8
Day 14

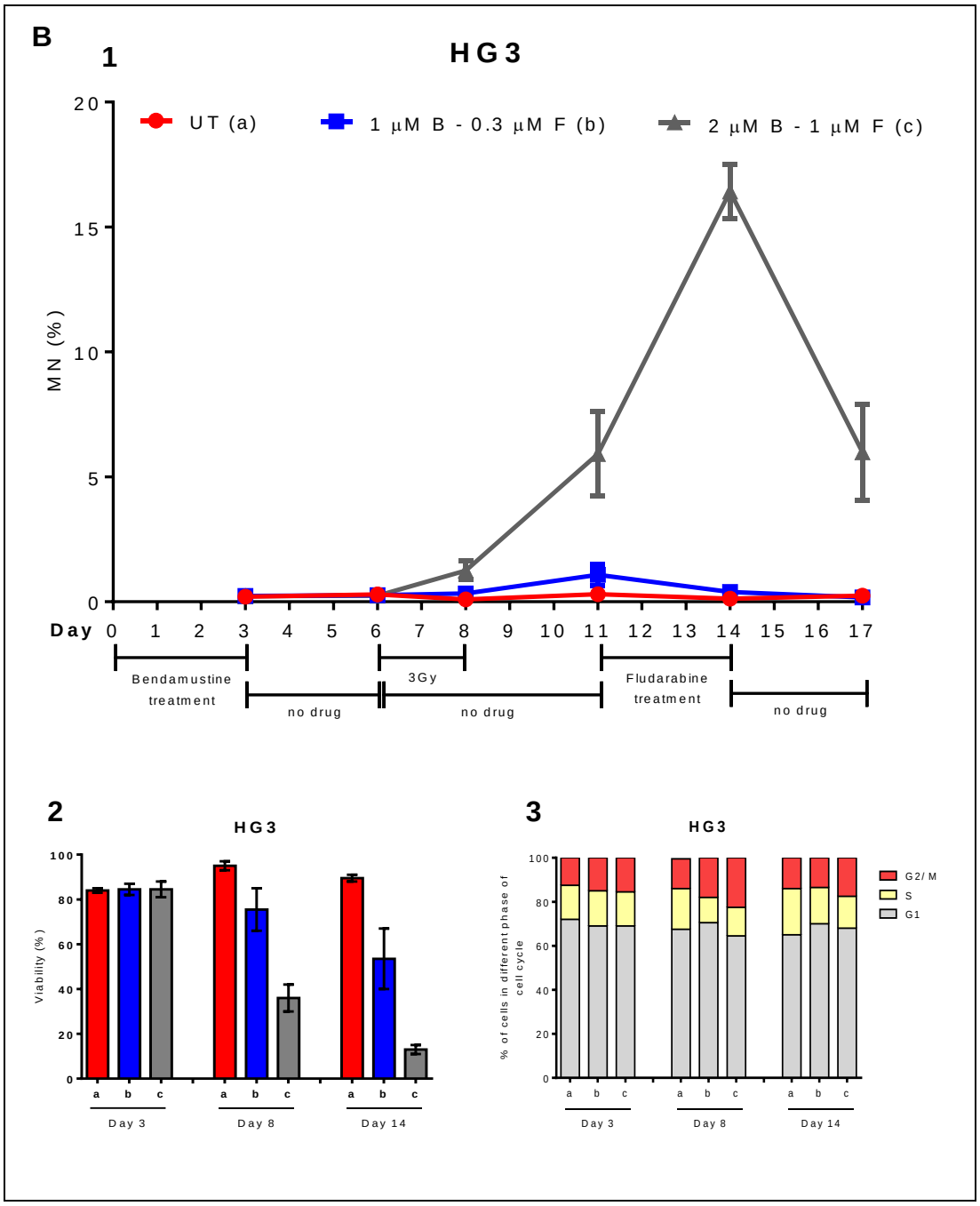

Figure 5. 6: Effects of combined chemo-radiotherapy on HG3 cells: A) Fludarabine followed by irradiation (3Gy) and Bendamustine; **B)** Bendamustine followed by irradiation (3Gy) and Fludarabine. Effects on MN frequencies (A1 and B1), cell viability (A2 and B2) and cell cycle status (A3 and B3) are shown. The specific days on which the assays were performed are also indicated in the X-axes.

Results summarise the results of 3 independent experiments and error bars represent S.E.M.

5.2.5 Sequential treatment of JeKo-1 cell line with Fludarabine (F) and Bendamustine (B)

The aim of this experiment is to investigate the effect of Fludarabine and Bendamustine on MN frequencies in JeKo-1 cells. The experiments were performed and described exactly as with HG3 cells in the preceding sections.

Figure 5.7 A1 and B1 show that immediately neither the sequence nor concentration of either drug leads to any significant differences in MN frequencies. Similar to HG3 cells there were no clear differences in cell viability or cell cycle status with each of the conditions (**see Figures 5.7 A2, A3, B2 and B3**) and there is no clear impact on MN frequencies.

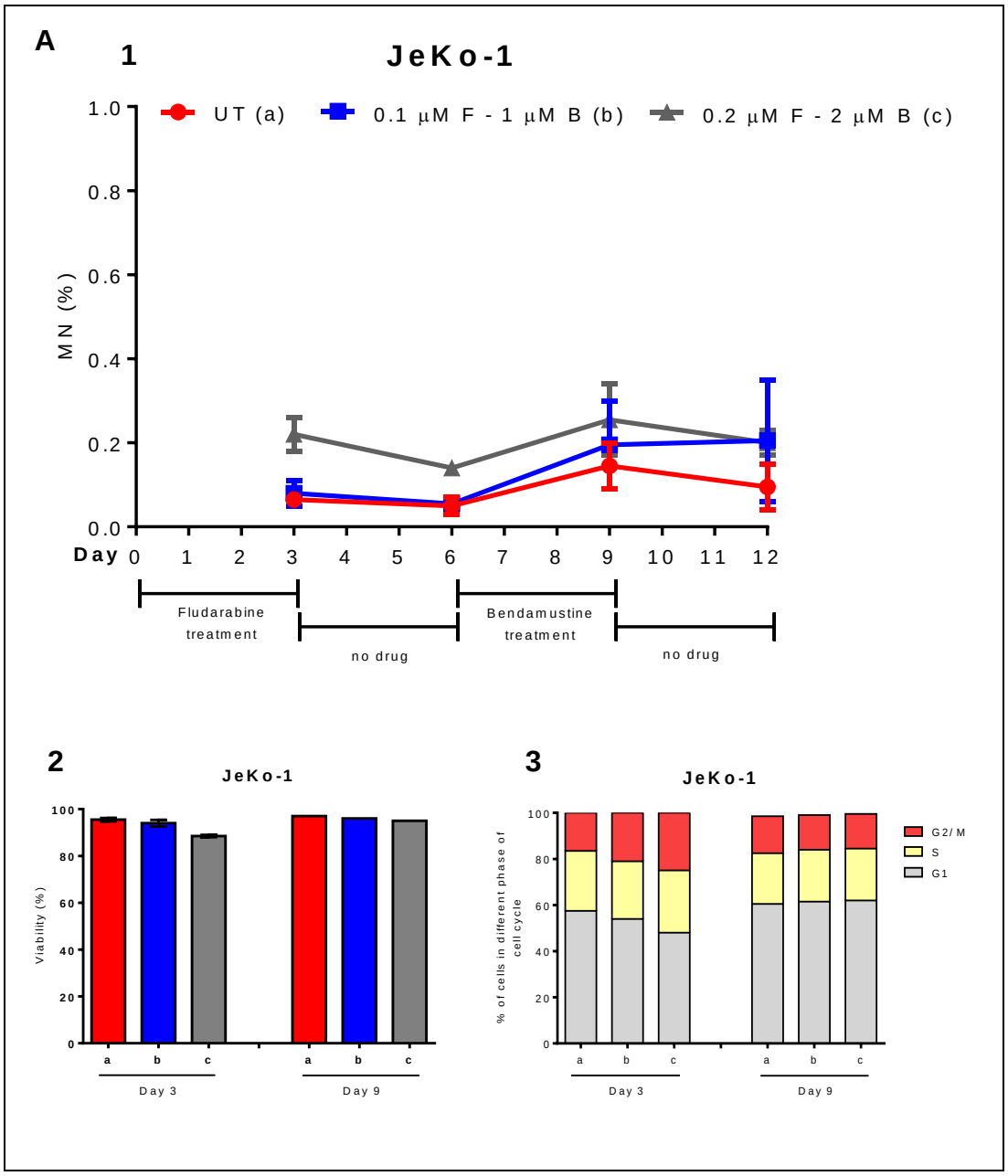
A
1
JeKo-1
UT (a)
0.1 µM F - 1 µM B (b)
0.2 µM F - 2 µM B (c)
MN (%)
Day
Fludarabine treatment
no drug
Bendamustine treatment
no drug
2
JeKo-1
Viability (%)
Day 3
Day 9
3
JeKo-1
% of cells in different phase of cell cycle
G2/M
S
G1
Day 3
Day 9

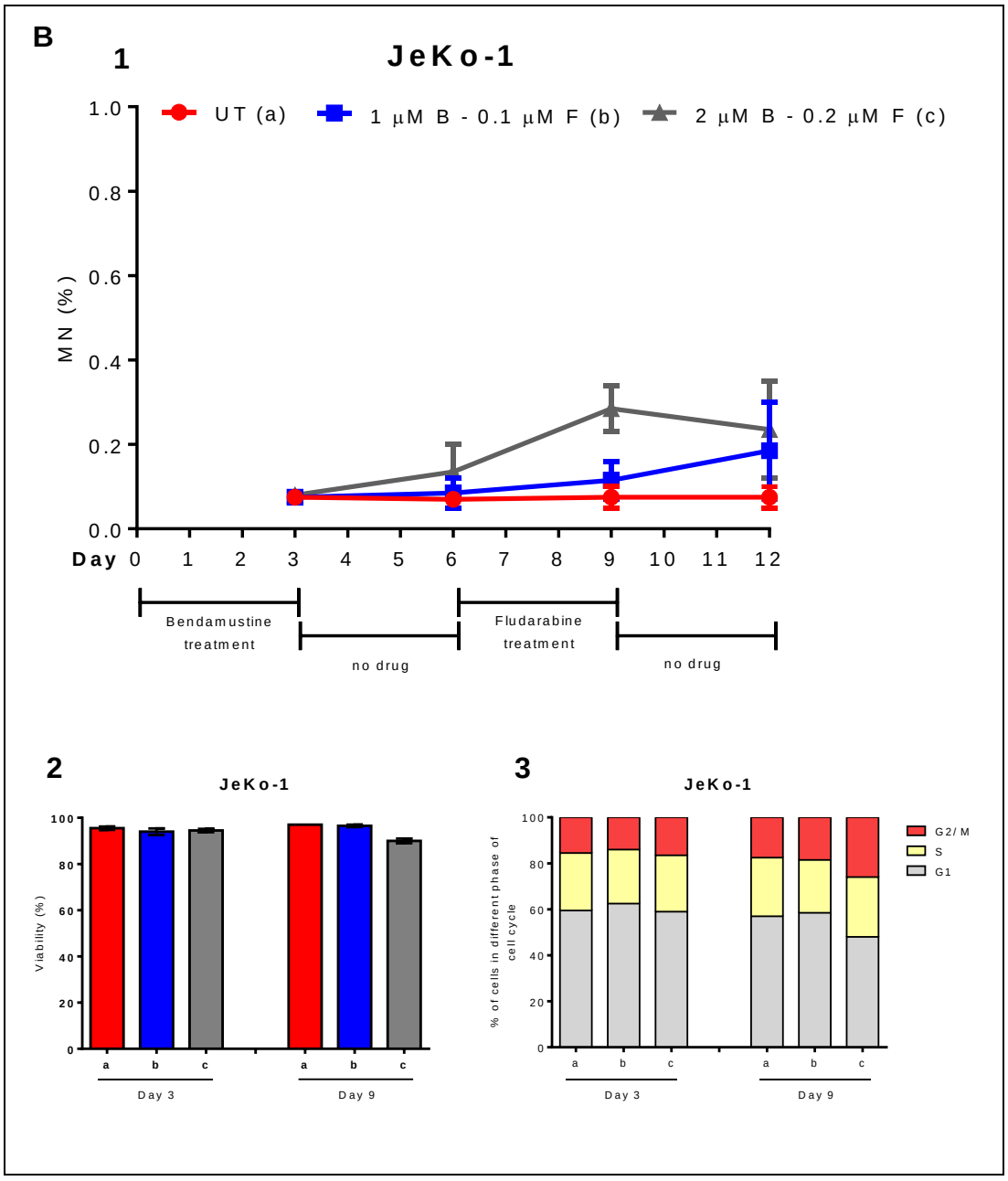

Figure 5. 7: Effects of sequential treatment of JeKo-1 cells: A) Fludarabine followed by Bendamustine; **B)** Bendamustine followed by Fludarabine. Cells were analysed on indicated days for MN frequencies (A1 and B1) cell viability (A2 and B2) and cell cycle status (A3 and B3). The results summarise the findings of 3 independent experiments and error bars represent S.E.M.

5.2.6 Effects of sequential Fludarabine, Bendamustine and irradiation on Jeko-1 cells

The experimental plan and the assays performed are exactly the same as with HG3 cells (Section 5.2.4).

As shown in **Figures 5.8 A1 and B1** there were no significant differences between the lower drug concentrations and untreated samples (red and blue lines). In contrast, at the higher concentrations (grey lines) there does seem to be a marked increase in MN frequency (see day 11 MN frequencies in **Figures A1 and B1**). This is despite the fact that cells in G2/M phase are comparable for both treatments (compare 'bars c' at Day 8 in **Figures A3 and B3**). This suggests that the effect is mainly attributable to bendamustine (at the higher dose) + irradiation and may reflect the immediate levels of retained DNA damage within the cells as the differences are also apparent at Day 17 (**Figures A1 and B1**). Similar to HG3 cells, the broader impact of cell viability for all time points is not very apparent, but the G2/M cell cycle arrest at day 8 can be a predictor of MN formation. This pattern of cell cycle arrest was also observed when we exposed MAVER-1 to the same sequential treatment (results not shown). This indicated that Mantle cell lymphoma cell lines are more susceptible to the irradiation compared with the HG3 cell line causing an increase MN formation.

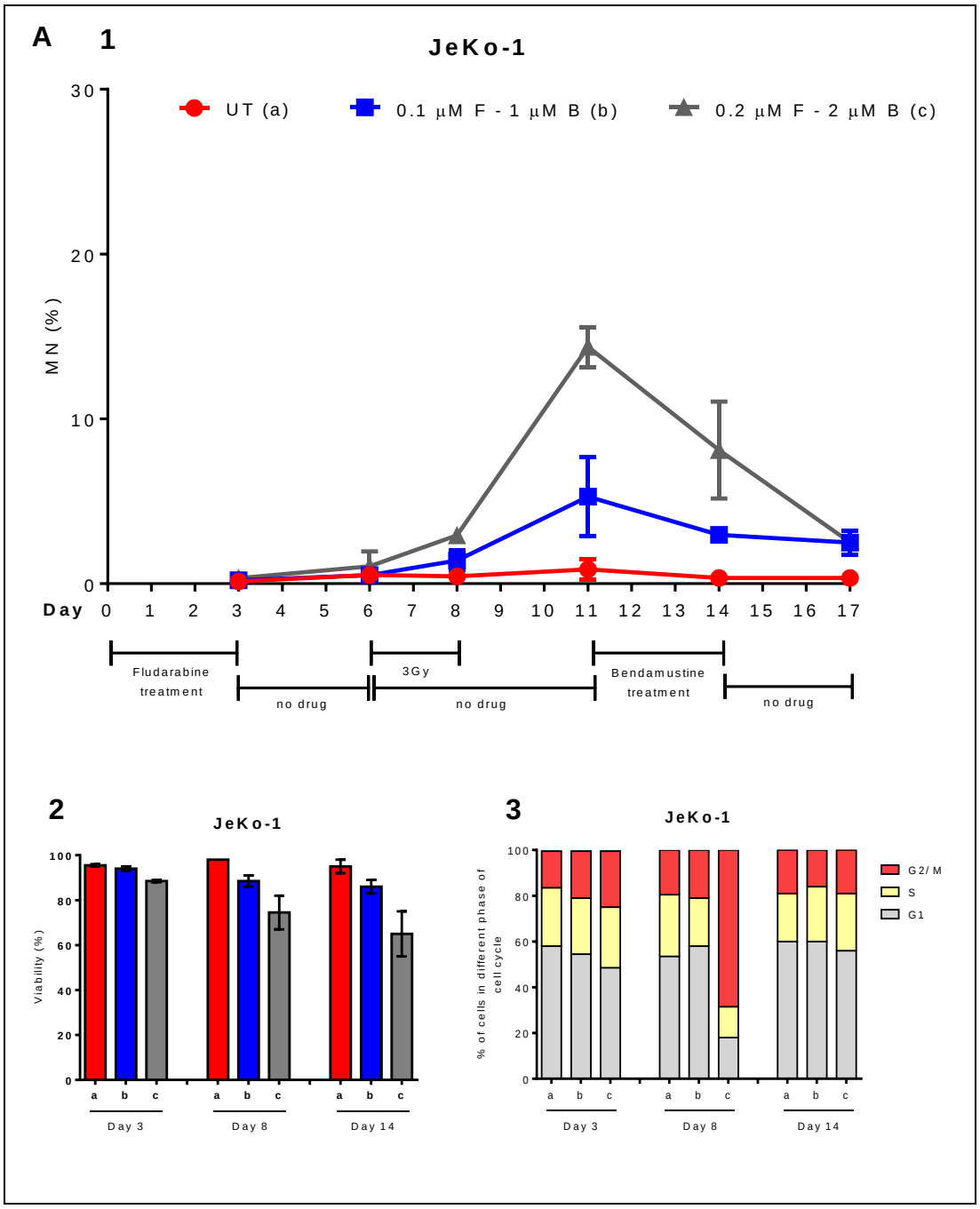
A 1
JeKo-1
UT (a)
0.1 µM F - 1 µM B (b)
0.2 µM F - 2 µM B (c)
MN (%)
Day
Fludarabine treatment
no drug
3Gy
no drug
Bendamustine treatment
no drug
2
JeKo-1
Viability (%)
Day 3
Day 8
Day 14
3
JeKo-1
% of cells in different phase of cell cycle
G2/M
S
G1
Day 3
Day 8
Day 14

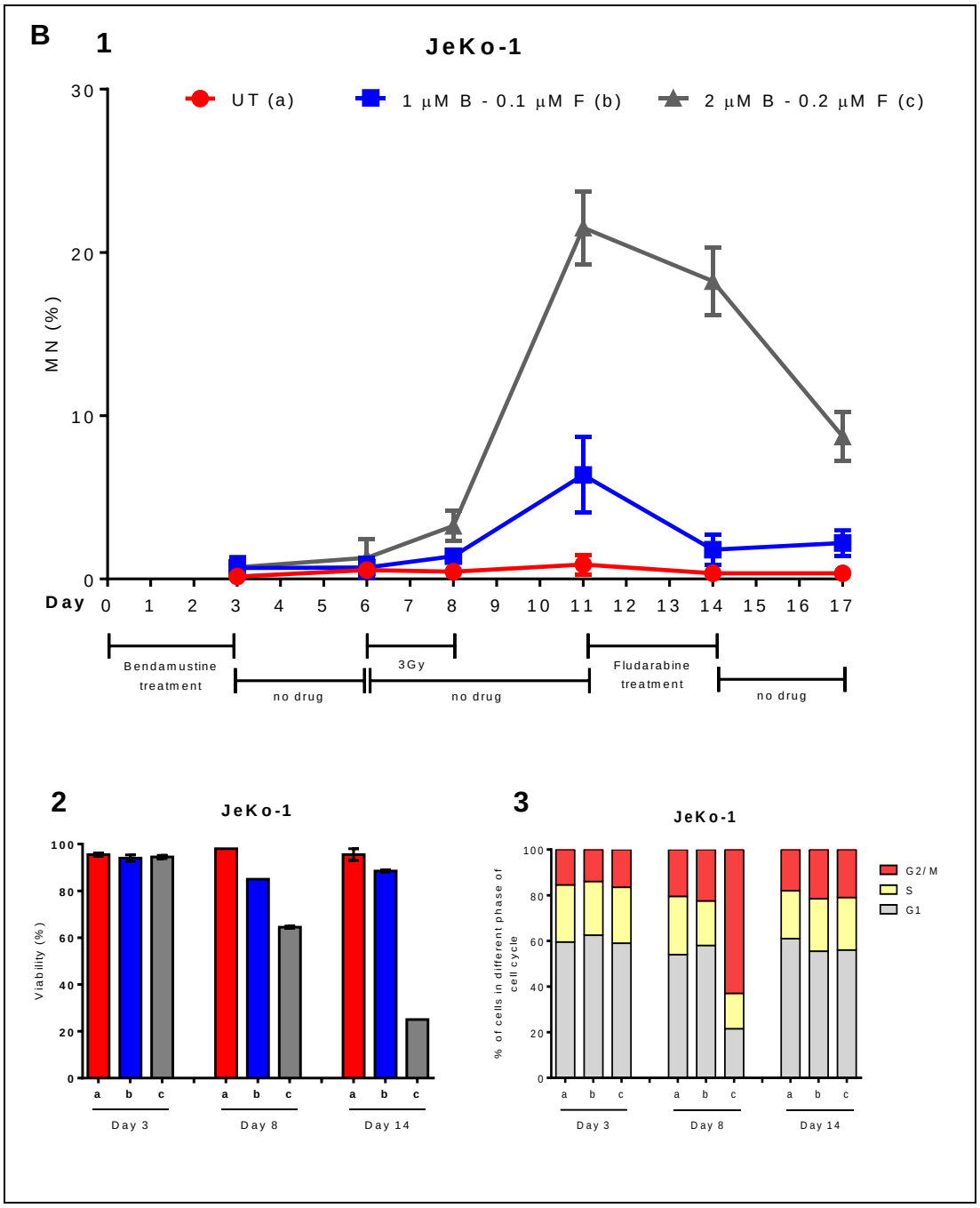

Figure 5. 8: Effects of combined chemo-radiotion treatment of JeKo-1 cells: A) Fludarabine + irradiation (3Gy) followed by Bendamustine; **B)** Bendamustine + irradiation (3Gy) followed by Fludarabine. Cells were analysed on indicated days for MN frequencies (A1 and B1) cell viability (A2 and B2) and cell cycle status (A3 and B3). The results summarise the findings of 3 independent experiments and error bars represent S.E.M.

The results for the higher concentrations of fludarabine and bendamustine +/- irradiation described in sections 5.2.3 – 5.2.6 are summarised in **Table 5.1**. Clearly, the most significant findings are seen with Jeko-1 cells when irradiation is included in the treatment schedule. This is more pronounced when bendamustine is used first. It is possible that the lack of activity/resistance of HG3 cells to bendamustine is likely influencing some of the specific findings. In addition, some of the changes are also a function of the concentrations of the drugs used.

Table 5. 1: Summary of MN frequencies with the various conditions described in this chapter (the numbers reflect the MN frequencies in the grey lines (A1 and B1) in Figures 5.5, 5.6, 5.7 and 5.8.

Chemotherapy +/- irradiation	HG3			JeKo-1		
	Day 9	Day 11	Day 14	Day 9	Day 11	Day 14
F → B	0.4			0.3		
F→ I → B	4	7.5	8	7.5	15	10
B → F	0.3			0.3		
B → I → F	3	6	17	9	24	19

5.3 Discussion

The main aim of this chapter was to understand the effects of sequential cytotoxic treatments on MN frequencies as a surrogate marker of cumulative DNA damage in cell line models of CLL and MCL. Fludarabine and bendamustine used for these experiments reflect clinical practice for the two diseases. An additional irradiation step was also included as this is used not infrequently in the clinical setting.

Although the concentrations of fludarabine and bendamustine used are arbitrary, they tilt the balance towards a scenario when cells survive despite DNA damage and to avoid the effect of significant apoptosis on MN frequencies. It is difficult to compare the results obtained with HG3 cells vs Jeko-1 cells, as the former was largely resistant to bendamustine treatment. Nevertheless, one can conclude that MN frequencies can be used as surrogate markers to monitor cumulative DNA damage of sequential treatments which likely impacts disease behaviour, course and therapeutic responses to subsequent treatments.

There is a suggestion from these results that the sequence of treatments may also have an impact on retained effects on DNA integrity within cancer cells that survive cytotoxic treatments. This experiment gives some insights into the clinical applications as it might help to avoid using a particular order of the sequential treatment that cause more cumulative DNA damage. The induction of DNA damage may indicate poor prognosis e.g. cell resistance to the treatment or evolution of more aggressive clones.

The results in this chapter do not show the direct relationship with cell viability and cell cycle status except in MCL cell lines, these cells were arrested in G2/M causing an increase in the MN formation. The MCL cell lines (JeKo-1 and MAVER-1) were arrested in G2/M cell cycle and the cell viability was low after combined irradiation with the chemotherapy treatment indicated that these cells are more sensitive to irradiation than the B-CLL cell line.

The cells, which exposed to irradiation in combined with chemotherapy showed that there is a decreased in MN frequency after day 11. This might happen due to cell apoptosis or absorption of the MN into the nucleus or due to the elimination of abnormal chromosomes out of the cells, which leads to exclude these chromosomal fragments (debris or apoptotic bodies) later from the gating strategy.

It is possible that the MN-FACS assay used for these experiments will be underestimating the true levels of DNA damage given that a step that promotes cytokinesis block is not included within the assay as currently established and optimised.

The experiments and results do suggest that serial examination of patient samples at different stages in their treatment journey is worth pursuing. This is particularly relevant when multiple lines of cytotoxic treatments are used in diseases such as CLL and low-grade lymphomas. It was not possible to address this within the time frame of this project, but may need to be planned over a longer time period in a larger cohort of patients with annotated demographics and outcomes. Ideally, this could be done with samples

collected before each next treatment when the cell counts (of CLL or MCL cells) are likely to be high. It may be useful to see if MN frequencies at each stage is predictive of subsequent therapy response.

Given the advent of novel therapies such as kinase inhibitors in CLL and MCL, the MN-FACS assay could also be used to examine the effects of sequential treatments that include these agents on long-term DNA integrity. This is likely very relevant because there is a suggestion of increased risk of high-grade transformations with agents such as ibrutinib and venetoclax especially after previous cytotoxic treatments when patients eventually relapse.

In **chapter 6,** we would like to enumerate MN within stimulated CLL cells and investigate the influence of repeated exposures to prior therapies and disease variables on MN formation.

Chapter 6: Micronuclei enumeration assay for assessment of genotoxicity in primary patient samples

6.1 Introduction

Historically, CBMN based MN enumeration has been widely used as a biomarker, to evaluate the genotoxicity of radiation or chemical exposures, to assess public safety. The assay has historically used blood or epithelial cells for investigations. Recent literature suggests that increased MN formation within human blood cells may in fact be predictive of cancer risk. Such studies support the use of MN enumeration as a predictive biomarker of carcinogenesis [223].

A number of studies have described the importance of MN enumeration as a predictive marker for both malignant and non-malignant diseases, such as breast and cervical cancers, Hodgkin's lymphoma, and diabetes mellitus [224-226]. MN formation is associated with genomic instability, which may lead to a condition called chromothripsis, characterised by DNA misrepair and accumulation of overwhelming double strand breaks [227, 228].

Studies of cells in pleural effusion samples have shown significantly increased numbers of MN in malignant versus benign effusions [229]. Cultured lymphocytes from patients with bladder cancer, show a greater frequency of MN compared to healthy controls [230]. Similarly, MN frequency may be a promising biomarker for detection of early stage colorectal cancer

(CRC). Peripheral blood lymphocytes (PBL) were used in this study to examine and compare the MN frequencies in patients with CRC to patients with colonic polyps or without intestinal lesions as controls [231].

It is widely accepted that exposure to chemotherapeutic agents results in cumulative DNA damage and genomic instability. Analysis of MN frequencies in solid tumours treated with chemotherapy have shown reduced MN formation in p53 wild-type (WT) tumours. In contrast, p53 mutated tumours display increased MN formation, potentially due to altered growth arrest or defective DNA repair mechanisms [232]. These studies also suggest that increasing MN frequency is associated with poor treatment response [233, 234].

Our lab is primarily engaged in research into lymphoid cancers such as Chronic Lymphocytic Leukaemia (CLL). CLL is primarily an indolent disease with heterogeneous behaviour. Most patients eventually require treatment and the current standard for frontline treatment is chemo-immunotherapy [235]. The disease is currently incurable and patients may require multiple lines of treatment during their lifetime. It is widely appreciated that the intervals between treatments progressively get shorter due to disease evolution as sequential treatments lead to phenotypes that are more aggressive. It is likely that such behaviour is due to increasing genomic instability either due to the disease itself or due to prior treatments. In addition, several prognostic factors (such as IgVH mutational status, chromosomal defects (11q-, 17p- etc.) and patient demographics) also influence disease biology.

Chemotherapeutic agents used for treatment of CLL include fludarabine + cyclophosphamide or bendamustine and are usually combined with monoclonal antibody therapies such as rituximab. It is well known that chemotherapeutic agents can cause irreversible DNA damage and sometimes lead to secondary malignancies. Novel agents are revolutionising the treatment of CLL and include Ibrutinib (a Bruton tyrosine kinase inhibitor), idelalisib (a phosphatidylinositol-3-kinase δ inhibitor) and venetoclax (a BCL-2 inhibitor) [236]. The long-term effects of these new treatments on genomic integrity is yet unknown.

In this chapter, we describe MN frequencies in primary CLL patient samples. We mapped MN frequencies to disease characteristics, prognostic factors and prior therapies to gain a better understanding of genomic integrity within patient samples. Such insights should lead to a greater understanding and prediction of the impact of prior treatments and disease behaviour.

As previously described, MN formation requires the cells to be in the G2/M phase of the cell cycle. A potential confounding issue identified relates to the fact that CLL cells are predominantly in the G0/G1 phase of the cell cycle. Hence, a critical first step is to find in vitro ways to stimulate proliferation of CLL cells and promote entry into the G2/M phase when MN formation is most relevant. Several studies, including those from our lab, have shown that culturing CLL cells on fibroblast layers expressing CD40, and treatment with cytokines such as IL-4 and 21, can prevent apoptosis in vitro and promote proliferation by recapitulating the CLL microenvironment in lymph nodes. This

co-culture system mimics the stimuli that CLL cells require for cell survival, growth and proliferation [237].

We obtained fresh primary cells from 21 CLL patients with diverse characteristics and treatment stages to enumerate MN frequencies.

We hypothesized that MN counts within stimulated CLL cells are influenced by disease variables and repeated exposures to prior therapies such as cytotoxic agents. Thus, MN frequency may be a surrogate marker for underlying genomic instability within patient samples and may help predict disease behaviour.

The **aims** of this chapter are as follows:

1. Establish and optimise methods to promote CLL cell proliferation using the CD40 co-culture system and/or cytokines.
2. Study MN frequency in primary CLL patient samples using the MN-FACS assay.
3. Consider the impact of prognostic variables and prior treatment on MN frequency.

6.2 Methods

Fresh CLL patient samples (n=21), at baseline and post-treatment, were obtained from the CLL /Lymphoma clinics at the Royal Liverpool Hospital and collected in BD Vacutainer® CPT™ (Lymphoprep) Cell Preparation Heparinised tubes after patient consent. Ethical approval for this part of the study is in place.

6.2.1 Stimulation of CLL proliferation on CD40 expressing fibroblasts

The aim of this method is to promote cycling and proliferation of CLL cells, as these cells are otherwise predominantly in the G0/G1 phase and dormant.

Primary blood samples from CLL patients were subjected to Lymphoprep and harvested mononuclear cells were enriched in clonal B-cells. The percentage of clonal CLL cells in the PBMCs was >90% in all cases. We ensured that at least 80% of fibroblast cells used for the experiments showed expression of CD40. CD40 expressing fibroblast cells were irradiated with 75 Gy to stop cell proliferation, and then 200 μl (4×10^5 cells/ml) was added per well in 96 well plate and incubated for 24 hrs to form a monolayer before plating CLL cells on top. CLL cells were counted and layered on CD40 expressing fibroblast monolayers at a density of 5×10^6 cells/ml for both MN enumeration and proliferation studies. Cells were plated in complete RPMI medium supplemented with recombinant human interleukin-4 (rhIL-4; 10 ng/ml) and recombinant human interleukin-21 (rhIL-21; 15 ng/ml), in accordance with a previously established protocol in our lab, to promote CLL cell proliferation and cell survival *in vitro* [238]. Equal numbers of cells were used for MN enumeration and cell proliferation tests. The cells for MN enumeration were

cultured in three different conditions for each time point: without mitogens, with mitogens (IL-4 + IL-21), and irradiated (3 Gy) as +ve control (as well as mitogens). Cells stained with 0.5 μM CFSE to assess cell proliferation were treated similarly. CFSE stained cells were harvested on a daily basis for measuring cell division rates. For MN enumeration, cells were collected on days 7 or 9 for MN-FACS analysis. Half of the medium was replaced with fresh medium containing rh-IL4 + rh-IL21 on days 4 and 7 (**Figure 6.1**). In order to perform both experiments (MN enumeration and cell proliferation), the total numbers of cells required were around 6.5×10^7 cells.

6.2.2 Staining cells with CFSE

The principle of CFSE staining is that the parent compound (CFDA-SE) has two acetate groups per molecule allowing this non-fluorescent compound to cross the cellular membrane. Upon entry into the cell, intracellular esterases remove the acetate groups, converting CFDA-SE into fluorescent CFSE. During mitosis, CFSE stained nuclear material distributes equally between the daughter cells, and allows appreciation of cell division by FACS analysis.

CLL Lymphocytes (3×10^6 cells/ml) were washed with PBS and stained with 0.5 μM of CFSE. Cells were incubated for 30 mins in a 37˚C water bath with agitation every 5 mins. They were subsequently centrifuged at 550g for 5 mins and re-suspended in complete RPMI medium and incubated at 37˚C in a CO_2 incubator for 15 mins. Following this, cells were washed twice with fresh medium and re-suspended at a density of 5×10^6 cells/ml, before layering on fibroblasts.

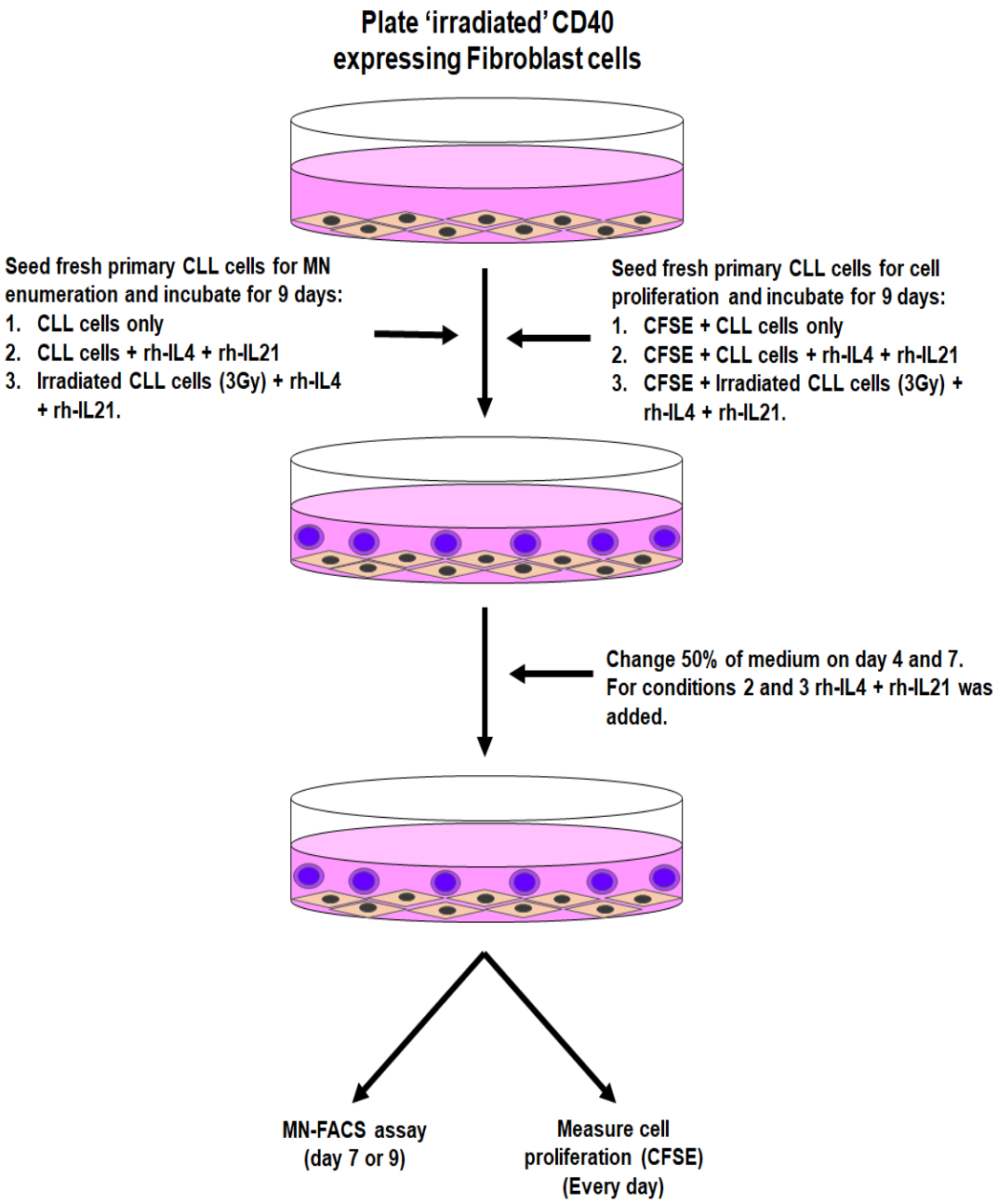

Figure 6. 1: Diagram illustrates the protocol for maintenance of primary CLL cells in culture for MN-FACS assay and CFSE assay.

6.3 Results

6.3.1 Optimization/ establishment of a co-culture system using CD40 expressing Fibroblast cells

The main purpose of using the co-culture system is to facilitate division of CLL cells, promote entry into the G2/M phase of the cell cycle and induce MN formation. Freshly obtained CLL cells were subjected to the protocol described in the methods section above.

The cohort of patient samples used included previously untreated or treated (FCR or Ibrutinib) cases. Samples from Ibrutinib treated patients are predominantly 4 weeks after commencement of treatment at the lymphocytosis stage. The results in **Figure 6.2** represent the three treatment categories (A=UT, B=FCR and C=Ibrutinib) and two representative cases are shown for each category. As evident from the figures, there is some variation in the results between cases and with specific treatments (UT vs IL4+ IL21 vs 3Gy + IL4+ IL21). In general, mitogen treatment without irradiation did promote cell cycle entry in CLL cells. This was less evident in samples subjected to irradiation prior to mitogen treatment. Progressively more cells had undergone cell divisions as seen from days 6 to 9 when multiple peaks appear to the left of the main cluster of cells and represent cells that have undergone cell division. Also apparent is the finding that Ibrutinib treated samples are more resistant to cell cycle entry. Some samples likely had more apoptotic rates accounting for the variations in peak sizes.

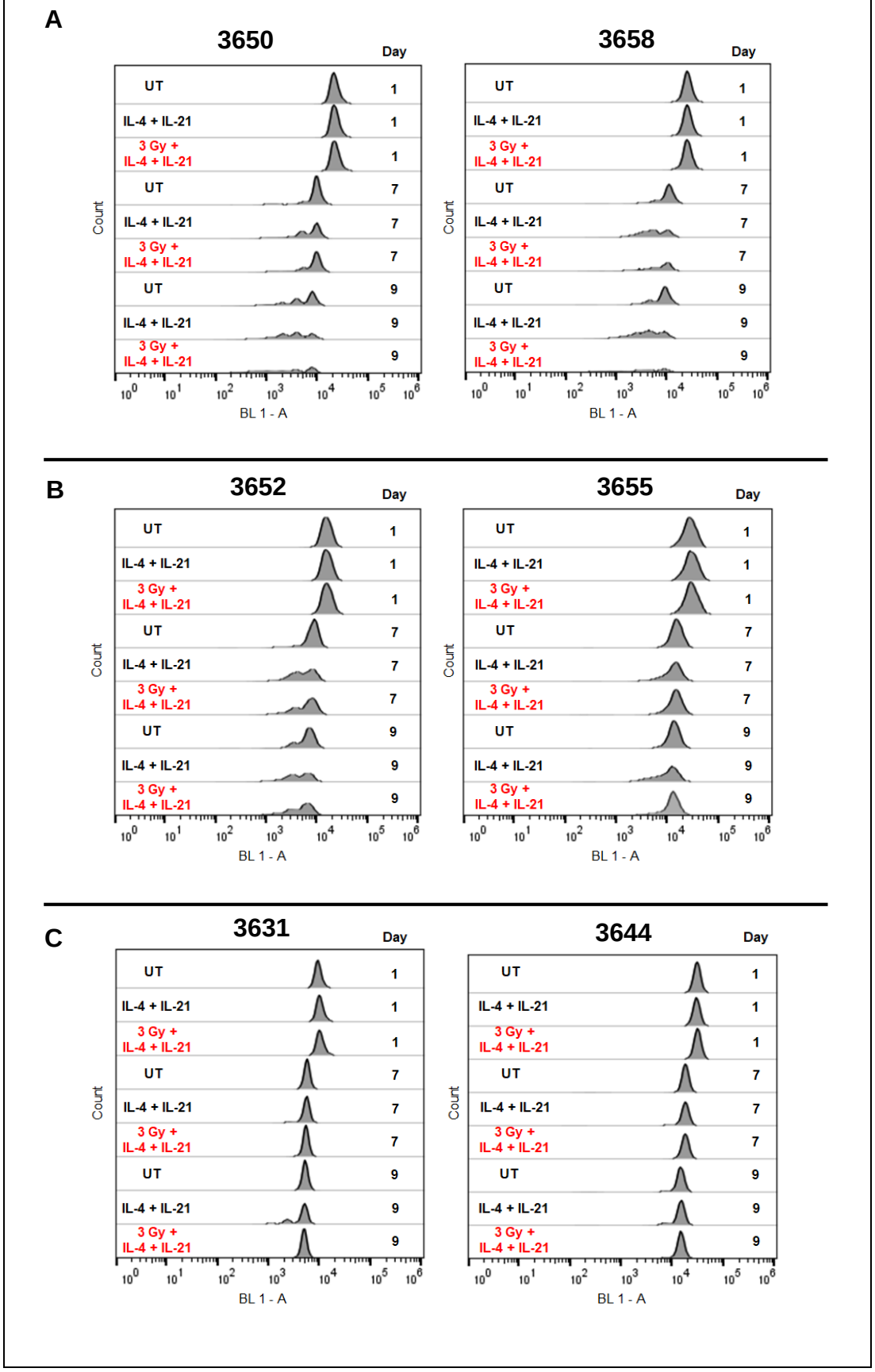
A
3650
Day
UT
1
IL-4 + IL-21
1
3 Gy +
IL-4 + IL-21
1
UT
7
IL-4 + IL-21
7
3 Gy +
IL-4 + IL-21
7
UT
9
IL-4 + IL-21
9
3 Gy +
IL-4 + IL-21
9
Count
BL 1 - A
3658
Day
UT
1
IL-4 + IL-21
1
3 Gy +
IL-4 + IL-21
1
UT
7
IL-4 + IL-21
7
3 Gy +
IL-4 + IL-21
7
UT
9
IL-4 + IL-21
9
3 Gy +
IL-4 + IL-21
9
Count
BL 1 - A
B
3652
Day
UT
1
IL-4 + IL-21
1
3 Gy +
IL-4 + IL-21
1
UT
7
IL-4 + IL-21
7
3 Gy +
IL-4 + IL-21
7
UT
9
IL-4 + IL-21
9
3 Gy +
IL-4 + IL-21
9
Count
BL 1 - A
3655
Day
UT
1
IL-4 + IL-21
1
3 Gy +
IL-4 + IL-21
1
UT
7
IL-4 + IL-21
7
3 Gy +
IL-4 + IL-21
7
UT
9
IL-4 + IL-21
9
3 Gy +
IL-4 + IL-21
9
Count
BL 1 - A
C
3631
Day
UT
1
IL-4 + IL-21
1
3 Gy +
IL-4 + IL-21
1
UT
7
IL-4 + IL-21
7
3 Gy +
IL-4 + IL-21
7
UT
9
IL-4 + IL-21
9
3 Gy +
IL-4 + IL-21
9
Count
BL 1 - A
3644
Day
UT
1
IL-4 + IL-21
1
3 Gy +
IL-4 + IL-21
1
UT
7
IL-4 + IL-21
7
3 Gy +
IL-4 + IL-21
7
UT
9
IL-4 + IL-21
9
3 Gy +
IL-4 + IL-21
9
Count
BL 1 - A

Figure 6. 2: Assessment of cell divisions CFSE stained and co-cultures CLL cells: A) Untreated CLL patients (3650, 3658); **B)** CLL patients previously treated with FCR (3652, 3655); **C)** CLL patients treated with Ibrutinib (3631, 3644). The cell division rates were assessed each day (Days 1 through to 9) by flow cytometric detection of CFSE staining of cells. For each case the histograms depict results obtained on Day 1, 7 and 9 using the three co-culture conditions described in the methods section (UT, IL4+ IL21, 3Gy + IL4 +IL21). The results suggest that the cell division was evident after 6 days of co-culture. Further cell divisions can be seen with IL4+ IL21 treatment but not when the cells are first irradiated.

6.3.2 MN enumeration in primary CLL cells

For these experiments, freshly obtained primary CLL cells were layered on CD40 expressing fibroblasts in the presence of IL4 and IL21 (with and without irradiation) for 7 days as previously described. Cells harvested on day 7 were then analysed by the MN-FACS assay and frequencies of MN noted. As MN formation requires the entry of cells into the G2/M phase of the cell cycle parallel analysis of cell cycle status for each sample was performed. In total 21 patient samples were analysed (UT=10; Previous FCR=4 and Ibrutinib=7). As shown in **Figure 6.3 A1** UT and FCR treated cases showed a spread of MN frequencies (0.4 – 1.6%). In contrast, Ibrutinib treated samples had very low levels of MN. None of the samples from Ibrutinib treated cases showed levels above 0.6%. Interestingly, the UT cohort seem to have undergone most cell divisions (and Ibrutinib treated cells the least) as shown in **Figure 6.3 A2** and may reflect the variation in MN frequencies between cases.

When the CLL cells were first subjected to 3Gy of radiation prior to co-cultures for 7 days there was a clear increase in MN frequencies in each case across all three patient cohorts as shown in **Figure 6.3 B1.** This was despite the fact that the number of cells that had undergone a cell division significantly decreased in all cases. We hypothesised that this may be in part due to cells undergoing G2/M cell cycle arrest especially after irradiation when MN are most likely to form and be detected. To test this, we estimated the number of cells in the different phases of the cell cycle for each case.

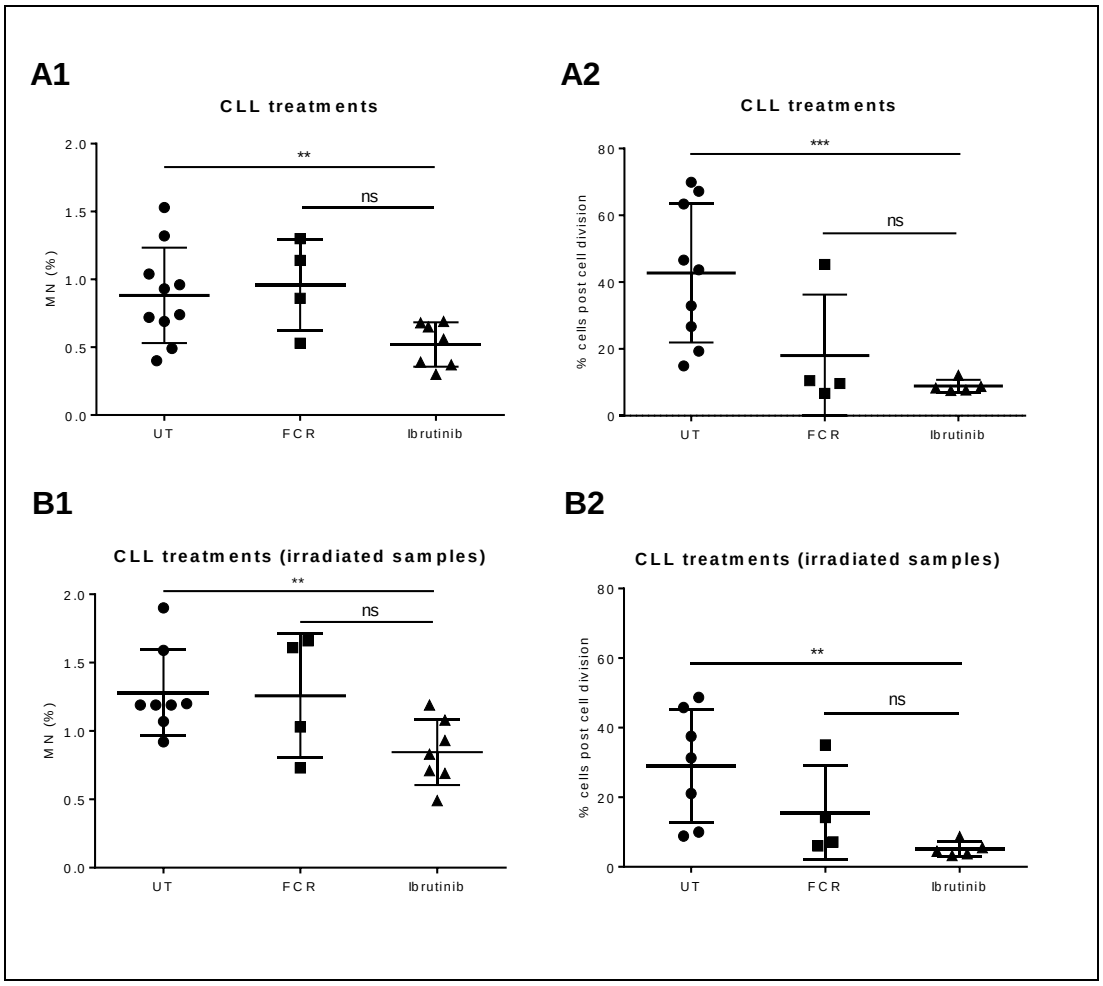

Figure 6. 3: MN enumeration and cell divisions in untreated and previously treated (FCR or Ibrutinib) CLL cases. A (1 and 2) MN count and cell division rates for three different CLL patient categories (UT CLL patients, CLL patients previously treated with FCR, and Ibrutinib). **B (1 and 2)** MN count and cell division rates when an irradiation step (3Gy) was included prior to mitogen exposure and co-culture in the same CLL patient categories mentioned above. The MN counts are roughly similar in the UT and FCR treated cases. This is despite lower cell division rates in the FCR cases. The MN counts and cell division rates in CLL patients treated with Ibrutinib were low. Two-way unpaired t-test non parametric Mann-Whitney for Figure 6.3 A showed a statistically significant difference in MN counts and cell division rates between UT and Ibrutinib cases but not in other comparisons (**p<0.01; ***p<0.001) respectively. This was true even when an irradiation step was included (**p<0.01 in both).

6.3.3 Dynamics of MN frequencies in the co-culture system

To understand the dynamics of MN frequencies with and without the inclusion of irradiation in the protocol we plotted values obtained on day 7 (see Figure 6.1). As evidenced in Figure 6.4 (panels A1, B1 and C1) in all 3 groups (UT, FCR and Ibrutinib) there was a consistent increase in the number of MN at the day 7 time point. There was also a suggestion that irradiation slightly increased the frequency of MN in each individual case. It is apparent that the increase in MN frequency is minimal in the Ibrutinib-exposed patients although irradiation did increase the levels in all cases to a small extent. The samples obtained from untreated cases and those from FCR treated cases did not suggest any major differences.

To see if there were any obvious differences between the UT + FCR cases vs Ibrutinib cases in cell cycle status that may impact MN frequencies, we plotted the G2/M frequencies at the same day 7 time point in all cases and these are shown panels A2, B2 and C2 in Figure 6.4. In general, there does seem to be an increase the number of cells in G2/M in UT + FCR cases (Figures 6.4 A2 and B2), whereas the induction of G2/M in the Ibrutinib group was very poor. Table 6.1 summarises the MN and G2/M frequencies in all the 21 cases and was the basis of the Figure 6.4.

A discussion regarding the impact of cell cycle status and cell divisions is included later in the chapter.

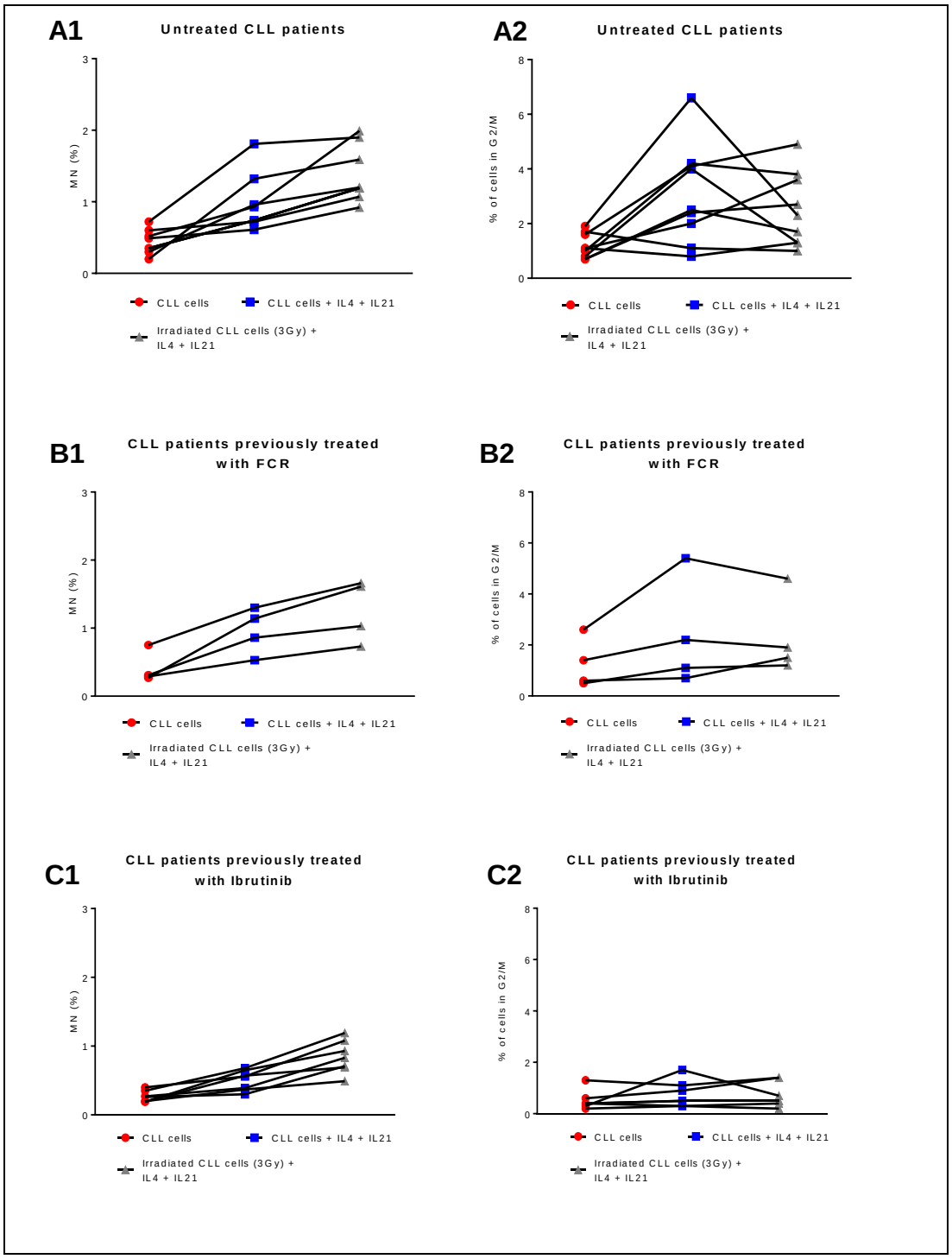

Figure 6. 4: Dynamics of MN frequencies after 7 days of co-culture in primary CLL cases. A1 (n=7), B1 (n=4) and C1 (n=7) show values of MN frequencies on day 7 (with and without an irradiation step. The panels on the right (A2, B2 and C2) show the dynamics of cells in G2/M in each individual case in parallel.

The cells in G2/M and MN frequency data for the 21 CLL patients, which studied in this chapter are summarised in **Table 6.1**.

Table 6. 1: The number of cells in G2/M and MN count in 21 CLL patients. The table provides a summary of the number of cells in G2/M and MN count in untreated CLL patient, CLL patients previously treated with FCR and CLL patients previously treated with Ibrutinib. In each case the cells were co-culture alone, with IL4 + IL21 or 3Gy + IL4 + IL21 and measured on day 7.

Patient no.	Treatment	7 days	
		G2/M	MN
Untreated CLL patients			
3620	Fibroblast + CLL	0.8	0.52
	Fibroblast + CLL + IL-4 + IL-21	4	0.93
	Fibroblast + 3Gy +IL-4 + IL-21	1.3	1.99
3637	Fibroblast + CLL	0.4	0.33
	Fibroblast + CLL + IL-4 + IL-21	1.1	0.40
	Fibroblast + 3Gy +IL-4 + IL-21	13.1	2.16
3640	Fibroblast + CLL	0.7	0.72
	Fibroblast + CLL + IL-4 + IL-21	2.5	1.53
	Fibroblast + 3Gy +IL-4 + IL-21	1.7	1.90
3645	Fibroblast + CLL	1.7	0.30
	Fibroblast + CLL + IL-4 + IL-21	1.1	0.96
	Fibroblast + 3Gy +IL-4 + IL-21	1	1.20
3647	Fibroblast + CLL	1.1	0.60
	Fibroblast + CLL + IL-4 + IL-21	0.8	0.72
	Fibroblast + 3Gy +IL-4 + IL-21	1.3	1.07
3650	Fibroblast + CLL	1.9	0.49
	Fibroblast + CLL + IL-4 + IL-21	6.6	0.61
	Fibroblast + 3Gy +IL-4 + IL-21	2.3	0.92
3656	Fibroblast + CLL	1.1	0.20
	Fibroblast + CLL + IL-4 + IL-21	2	1.32
	Fibroblast + 3Gy +IL-4 + IL-21	3.6	1.59
3658	Fibroblast + CLL	0.7	0.35
	Fibroblast + CLL + IL-4 + IL-21	2.4	0.74
	Fibroblast + 3Gy +IL-4 + IL-21	2.7	1.19
3661	Fibroblast + CLL	1.6	0.35
	Fibroblast + CLL + IL-4 + IL-21	4.1	0.74
	Fibroblast + 3Gy +IL-4 + IL-21	4.9	1.19
3663	Fibroblast + CLL	1	0.35
	Fibroblast + CLL + IL-4 + IL-21	4.2	0.74
	Fibroblast + 3Gy +IL-4 + IL-21	3.8	1.19
CLL patients previously treated with FCR			
3624	Fibroblast + CLL	1.4	0.31
	Fibroblast + CLL + IL-4 + IL-21	2.2	0.86
	Fibroblast + 3Gy +IL-4 + IL-21	1.9	1.03

3642	Fibroblast + CLL	0.6	0.75
	Fibroblast + CLL + IL-4 + IL-21	0.7	1.30
	Fibroblast + 3Gy +IL-4 + IL-21	1.5	1.66
3652	Fibroblast + CLL	2.6	0.29
	Fibroblast + CLL + IL-4 + IL-21	5.4	0.53
	Fibroblast + 3Gy +IL-4 + IL-21	4.6	0.73
3655	Fibroblast + CLL	0.5	0.27
	Fibroblast + CLL + IL-4 + IL-21	1.1	1.14
	Fibroblast + 3Gy +IL-4 + IL-21	1.2	1.61
CLL patients previously treated with Ibrutinib			
3621	Fibroblast + CLL	0.6	0.27
	Fibroblast + CLL + IL-4 + IL-21	0.9	0.39
	Fibroblast + 3Gy +IL-4 + IL-21	1.4	0.83
3623	Fibroblast + CLL	0.4	0.40
	Fibroblast + CLL + IL-4 + IL-21	0.3	0.56
	Fibroblast + 3Gy +IL-4 + IL-21	0.4	1.08
3627	Fibroblast + CLL	0.4	0.26
	Fibroblast + CLL + IL-4 + IL-21	0.5	0.30
	Fibroblast + 3Gy +IL-4 + IL-21	0.5	0.71
3631	Fibroblast + CLL	0.3	0.19
	Fibroblast + CLL + IL-4 + IL-21	1.7	0.57
	Fibroblast + 3Gy +IL-4 + IL-21	0.7	0.69
3639	Fibroblast + CLL	0.2	0.19
	Fibroblast + CLL + IL-4 + IL-21	0.3	0.65
	Fibroblast + 3Gy +IL-4 + IL-21	0.2	0.93
3644	Fibroblast + CLL	0.4	0.20
	Fibroblast + CLL + IL-4 + IL-21	0.5	0.37
	Fibroblast + 3Gy +IL-4 + IL-21	0.5	0.49
3660	Fibroblast + CLL	1.3	0.35
	Fibroblast + CLL + IL-4 + IL-21	1.1	0.68
	Fibroblast + 3Gy +IL-4 + IL-21	1.4	1.19

6.3.4 Correlation analysis between cell divisions and G2/M

As it was possible that the number of cell divisions and cells in different phases of the cell cycle may have an impact on MN enumeration in our MN-FACS assay, we were curious to see if we could get more insights from our data in primary CLL samples. To explore this we performed a correlation analysis between cell division rates and the number of cells in the G2/M phase in each case from all three treatment categories (UT, FCR and Ibrutinib) before and after irradiation (3Gy). The results are from the experiments shown in Figure 6.4. The values plotted in **Figure 6.5 A1** do suggest a correlation between cell division rates and the number of cells in G2/M. Results of a similar correlation analysis for samples post-irradiation are shown in **Figure 6.5 A2**. Here again, although less striking, there does seem to a degree of correlation. Overall the cell division rates and cells in G2/M were less in the irradiated samples as previously noted. It is difficult to draw broad conclusions from the UT and FCR cases as there was a wide variation for both parameters and this may in part be due to other variables.

In contrast, Ibrutinib cases consistently showed lower cell division rates and numbers of cells in G2/M.

The distribution of cells in the specific stages of the cell cycle (namely G0, G1, S and G2/M) for each patient cohort (Untreated (n=7), FCR treated (n=4) or Ibrutinib treated (n=7)) are shown in **Figure 6.5 B**.

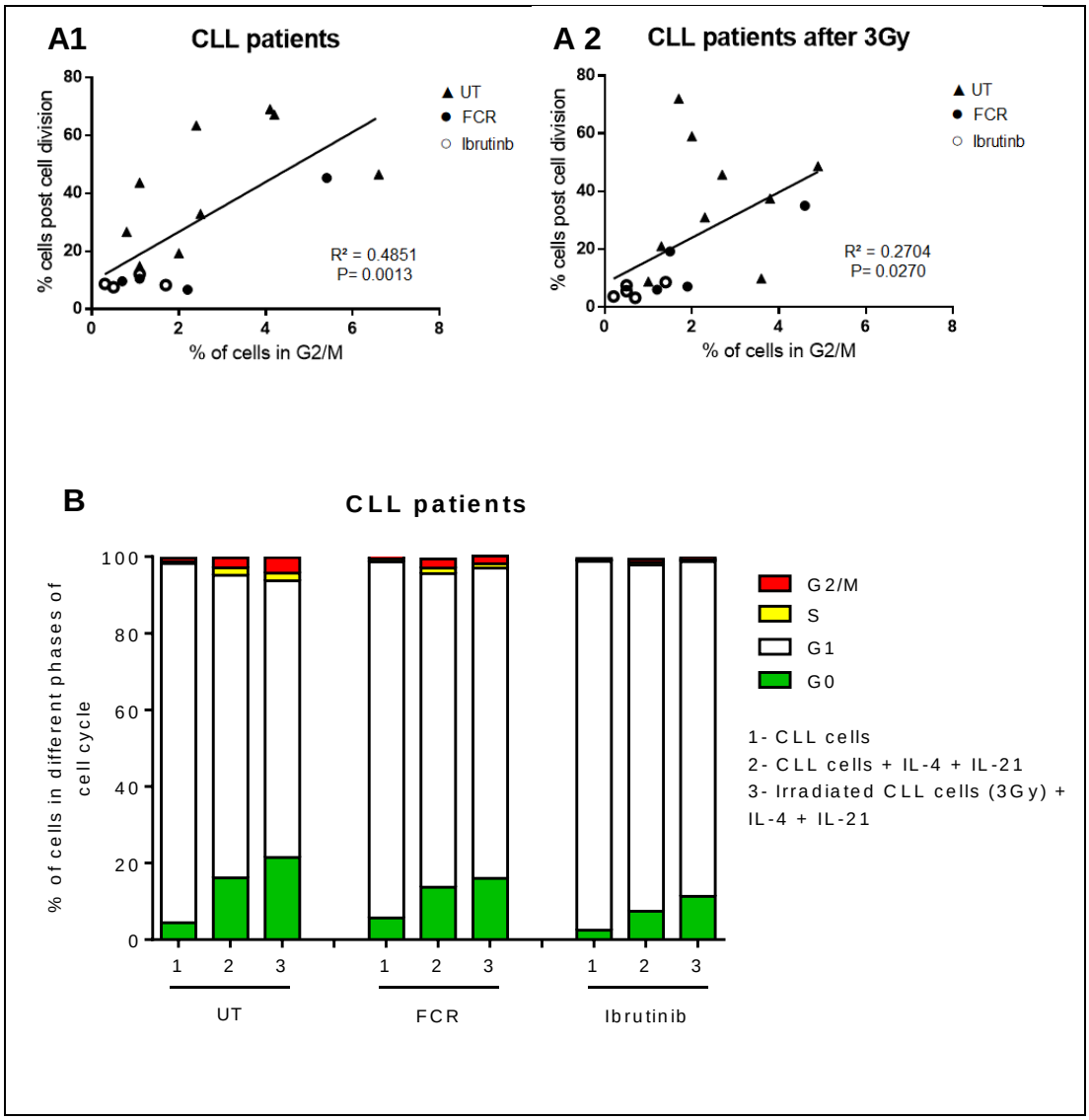

Figure 6. 5: correlation analysis between cell division rates and number of cells in G2/M in untreated and previously treated (FCR or Ibrutinib) CLL cases: CLL patients (UT, n=10; FCR, n=4; Ibrutinib, n=7) were treated as follows: (A1) without irradiation; **(A2)** after irradiation (3Gy). **B)** The distribution of cells in the specific stages of the cell cycle. Regression analysis was used to explore statistically significant differences. The values for this analysis were obtained from the experiment shown in Figure 6.4. (A1: $p< 0.01$**, $R^2= 0.4851$) or with irradiation (A2: $p< 0.05$*, $R^2= 0.2704$).

6.3.5 Impact of cell divisions and G2/M on MN

We next analysed the data if cell division rates or the number of cells in G2/M had more of an effect on MN frequencies. Again, the values examined are from the experiment shown in Figure 6.4. **Figure 6.6 A** shows the relationship of cell division rates vs MN frequencies within the patient cohort. What is immediately apparent is that in UT cases there is wide variation in the number of cells undergoing cell divisions within this group with and without irradiation (**Figures 6.6 A1 and A2**). Except for one case there was less of a variation in the FCR group. In contrast, Ibrutinib treated cases are clearly unable to undergo cell divisions. There is no clear evidence of any correlation between the cell division rates and MN frequencies in this analysis.

In parallel, (**Figure 6.6 B1 and B2**) shows the relation between the MN frequencies and cells in G2/M with and without irradiation in each individual case. The results suggest that irradiation does increase the frequency of MN post irradiation in UT and FCR cases but not in Ibrutinib treated cases. There were no clear patterns of G2/M entry in this cohort of patients with and without irradiation. As mentioned earlier, MN frequency is directly proportional with the increase in the number of cells in G2/M phase.

Whether the variations in MN frequencies, G2/M and cell division rates are predictive of clinical behaviour and therapy response in the long term requires elucidation in longitudinal studies in a larger cohort.

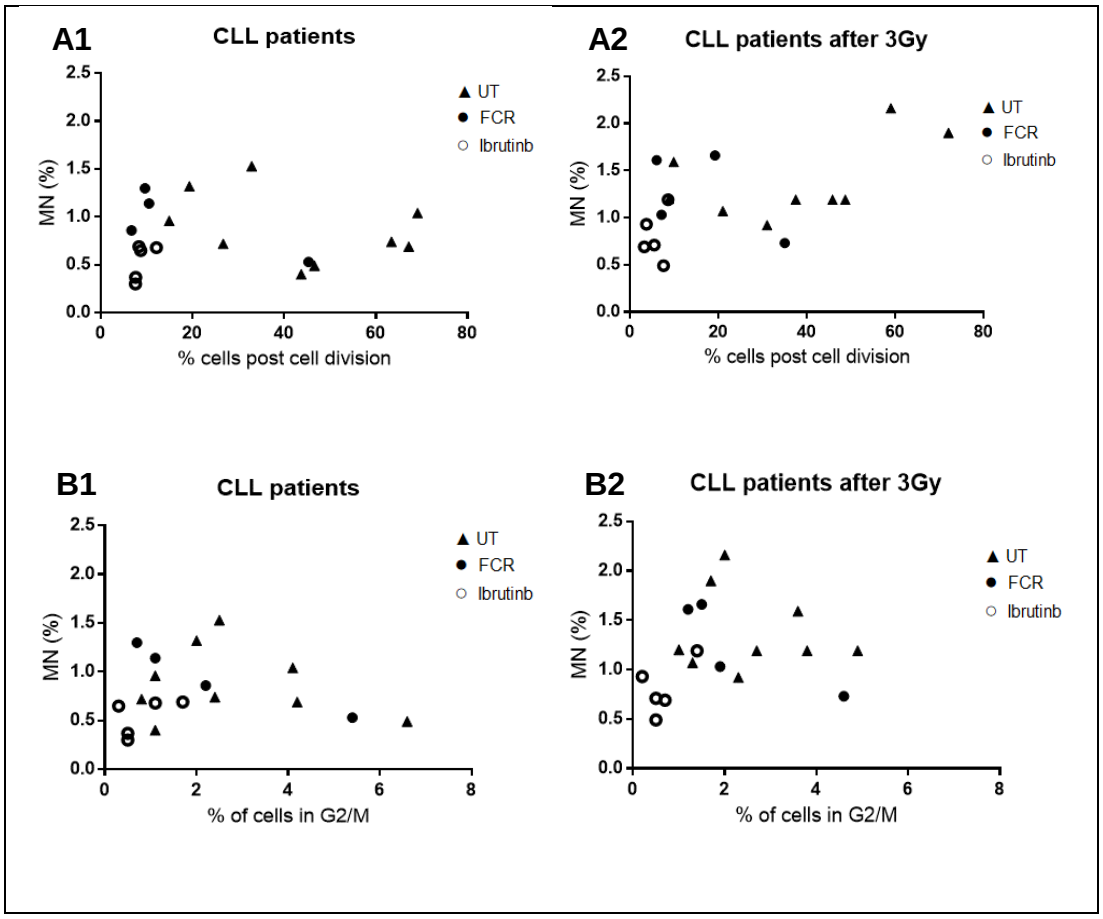

Figure 6. 6: MN enumeration vs cell division rates or G2/M frequencies in untreated and previously treated (FCR or Ibrutinib) CLL cases. A (1 and 2) Relationship between MN count vs cell division rates before and after irradiation; **B (1 and 2)** Relation between MN count vs number of cells in G2/M before and after irradiation.

6.3.6 MN frequencies in relation to prognostic variables

Over the years prognostic variables such as IgVH mutation status, chromosomal abnormalities (11q-, 13q-, 17p-) and p53 mutational status have been shown to impact CLL cell behaviour, therapy response and long term outcomes. As the cohort of cases that were examined in our MN studies had different baseline characteristics we looked to see if there was any relationship between MN frequencies and the prognostic variables.

The results in **Figures 6.7 A1 and A2** show that there is no impact of IgVH mutation status on the frequencies of MN with or without irradiation.

Similarly, **Figures 6.7 B1 and B2** do not show any clear impact of specific karyotypic abnormalities (Normal, 13q-, 11q-, 17p-) although in the one case with 17p- the levels of MN may be slightly higher. **Figures 6.7 C1 and C2** show similar analysis of cases segregated based on p53 mutation status. It is difficult to draw any clear conclusions from this analysis and may need a larger cohort of cases to be studied. The studies in the literature proved that p53 mutation status is associated with increasing the frequency of MN. This observation is not seen in these results, which could be due to low CLL patient samples with mutated p53. In addition, as these cases were a mix of previously treated and untreated cases this may confound the results.

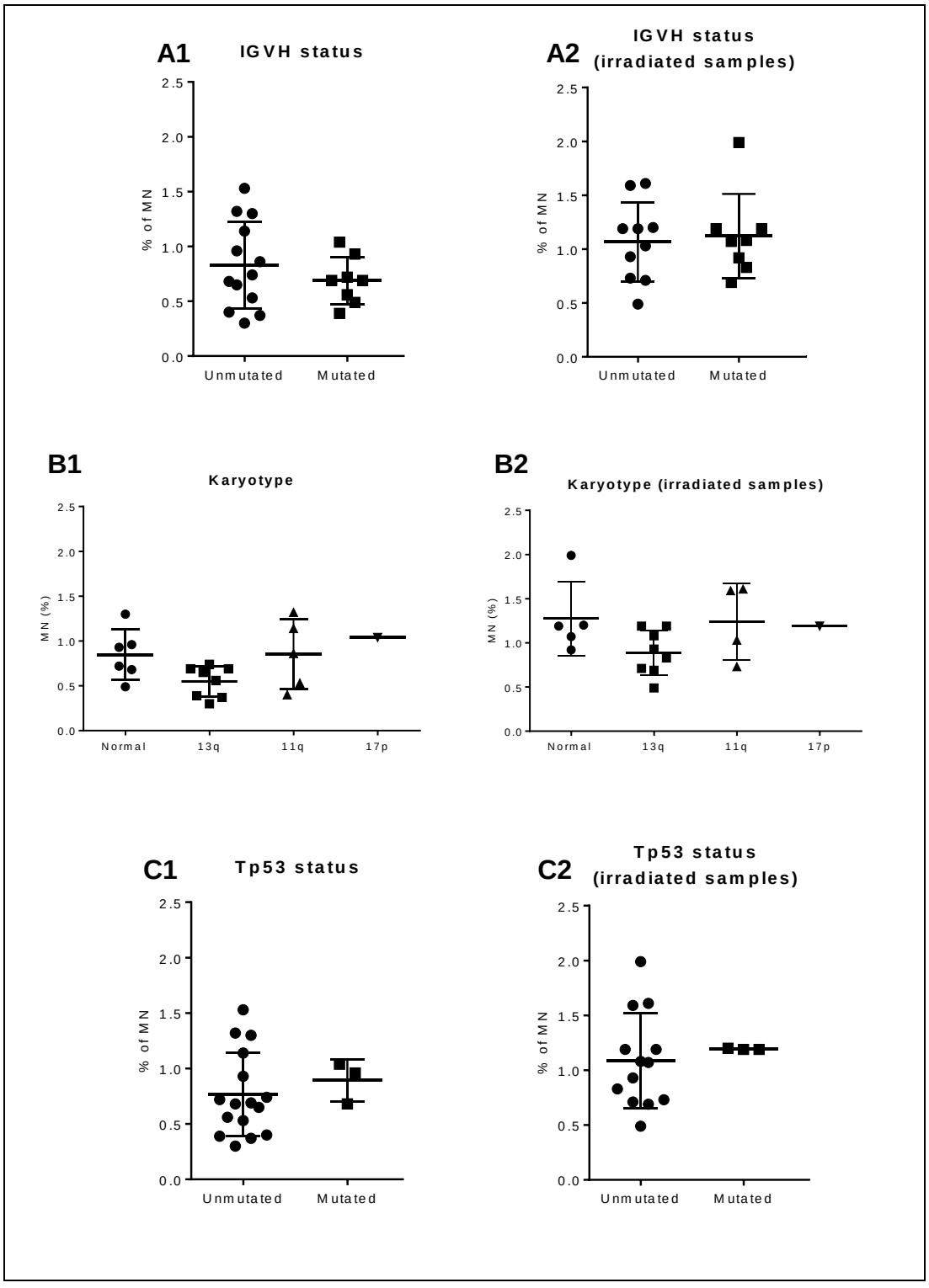

Figure 6. 7: Comparing MN enumeration between different prognostic variables in CLL patients with and without irradiation. A) IGVH status (mutated vs unmutated); **B)** MN count across different karyotypes; **C)** TP53 status (mutated vs unmutated).

6.3.7 MN frequency as a function of the number of adverse prognostic variables

For this analysis we first categorised patient samples based on the number of abnormalities within each case. In summary, we arbitrarily assigned a score of 1 if the sample was UM-IGVH and/or 11q- and/or 17p- or p53 mutated). IGVH mutated or normal/13q- or p53 WT were assigned a score of 0. Based on this categorisation, samples separated into 3 groups with scores of 0, 1 or 2. It is important to note that none of the cases scored 3. Without radiation there is a suggestion cases that score 2 have the highest rates of MN (**Figure 6.8 A**). This apparent difference is not seen after irradiation (**Figure 6.8 B**). Thus, a more genetically abnormal case may indeed have a higher MN frequency at baseline.

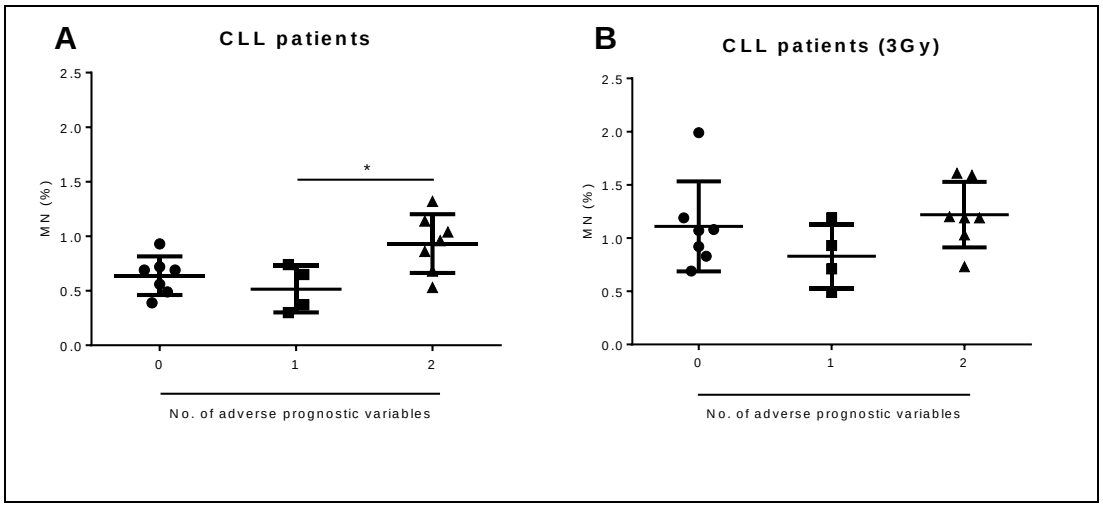

Figure 6. 8: MN frequency in relation to the number of adverse prognostic variables in CLL samples. **A)** MN counts in CLL patients base on the number of abnormalities (0, 1 or 2) as described in section 6.3.7. **B)** The effect of prior irradiation on MN counts within the same categories are shown.

5.4 Discussion

The major aim of this chapter was to investigate the levels of MN in primary patient samples obtained from CLL patients. Here, we have tried to gather a cohort of cases with different, prognostic, and treatment characteristics to see if there were any effects of these variables.

The number of cases that could be analysed was hampered due to the requirement of fresh samples for this study and we could not use frozen samples from our biobank. Our assay is only currently optimised for freshly obtained samples. Another significant challenge in studying CLL samples is that the cells are predominantly dormant and in the G0/G1 phase of the cell cycle. As MN are only formed in the G2/M phase, this needed to be addressed as studying cells straight out from a patient may not be amenable for a true assessment of underlying genomic instability by the MN-FACS assay.

To overcome the latter issue, we first had to establish a CD40 fibroblast-based culture system as this promotes proliferation, survival and cell cycle entry of CLL cells in vitro. To further enhance the capability of this system we included mitogens such IL4 and IL21 in our protocol. As with HeLa cells described in earlier chapters, it was likely that the inclusion of an irradiation step would further uncover a tendency to form MN and hence this was also explored.

In addition to study the frequencies of MN with our co-culture protocol, we have explored the relationship of MN frequencies with cell division rates and G2/M frequencies. This was felt to be essential as unlike the CBMN assay

where the MN are counted in bi-nucleated cells, the MN-FACS assay is currently designed to study all cells and does not incorporate treatment with Cytochalasin B. Despite this limitation, the MN-FACS assay does overcome some of the problems associated with the CBMN assay as previously described in preceding chapters.

The most significant observation from the studies in primary CLL samples, in our opinion, is that samples from patients on Ibrutinib are not able to enter the cell cycle despite co-culture on the CD40 system and even with the addition of mitogens. This has not been previously reported and indeed has not been observed with in vitro studies of Ibrutinib on cell lines or primary cells.

Karyotype mutations are playing an essential role in inducing the formation of MN particularly p53 mutation. A published study showed the effect of the genomic abnormalities (p53 mutation) gene on initiating the DNA replication origins, regulating genome instability at replication forks, and promotes micronuclei formation, thus stimulating the cell proliferation [239].

There is some suggestion from our studies that there is a wide variation of MN frequencies within samples. The finding that when samples have at least 2 adverse prognostic variable the MN frequency is higher would indicate that the assay may provide some information on genomic integrity and its potential effects on prognosis and outcome.

We suggest serial and longitudinal studies of MN frequencies within a single case may indeed allow monitoring of genomic integrity over a period of time

and may be a surrogate marker of acquisition of aggressive phenotype and potential therapy response.

This assay in its current form may be useful in serial observations in untreated and chemotherapy-exposed cases but not in Ibrutinib treated cases. Hence, it does not provide information regarding any potential effects of long-term Ibrutinib use on genome integrity.

It is important to note that the samples obtained from Ibrutinib treated cases were all from patients at the lymphocytic stage. It is likely that the drug was still within the cells when the samples were obtained and hence this may explain the effects noticed on G2/M. Investigate the effect of Ibrutinib on genomic integrity could be possible to assess by the MN-FACS assay but:

1) May require a ‘drug holiday’.
2) May require a robust step in the protocol to induce cell cycle entry/cell division.

Chapter 7: Summary and Conclusions

In this thesis, we describe an optimized FACS based assay that incorporates modifications within the staining protocol and an improved gating strategy for MN identification and enumeration (**Chapter 3**).

We have verified that the MN-FACS performs well in parallel studies comparing it to the CBMN and Comet assays. Here we did find differences that relate to early vs late effects upon genotoxic insults that result in DNA damage. The three assays, and indeed the γH2AX FACS analysis, have differential readouts at early and late time points in studying persistent DNA damage lesions and may be affected by DNA repair (**Chapter 4**).

To address the issue of cumulative genotoxicity of serial chemotherapeutic regimes at different stages of low grade lymphoid malignancies, we studied MN frequencies in CLL and MCL cell lines after sequential exposure to Fludarabine and/or Bendamustine with and without irradiation and have made some significant observations. The effects of cell cycle status and proliferation on the MN-FACS assay were also noted (**Chapter 5**).

Finally, we investigated MN frequencies in freshly obtained CLL patient samples with heterogeneous clinical characteristics including treatment exposure and prognostic variables to test our hypothesis (**Chapter 6**).

Chapter 3: The main focus of the experiments was to address some important issues that were likely to compromise the accuracy of previously described FACS based assays [163]. Towards this end, it was established

that Propidium Iodide (PI) may be better than EMA in only staining apoptotic bodies in dying cells as it does not penetrate the cell membrane of viable cells. In addition, the FACS Canto machine that was used for our experiments is better at detecting PI, which helps in the gating strategy.

We have performed experiments using rainbow beads for objective assessment of MN detection and loss at various steps within the protocol.

We used HeLa cells to perform systematic studies of MN frequencies and temporal dynamics especially in response to radiation induced DNA damage to understand the performance of the MN-FACS assay.

In summary, the conditions, our stepwise protocol and gating strategy are well suited to study MN frequencies and overcome at least some of the disadvantages of the CBMN assay and indeed other assays described earlier in the thesis.

Chapter 4: The main conclusions from this chapter are that the results obtained in our optimised MN-FACS assay correlated very well with MN counts obtained in the CBMN assay. The correlation was enhanced when a correction for the number of binucleated cells was applied to the results of the MN-FACS assay. As previously discussed, the FACS based assay does not currently include 1) a step to induce and block cytokinesis to promote binuclearity or 2) a mechanism for estimating the number of binucleated cells within the sample. Although the MN-FACS assay did not show any immediate correlation with the estimates of DNA damage by the Comet assay, we have made an important observation. The MN-FACS assay is good for assessment of persistent DNA damage, whereas the Comet assay

seems more appropriate to detect immediate DNA damage especially after irradiation. We did find that there was a positive correlation of the extent of early DNA damage (Comet assay) with a persistent loss of DNA integrity (MN-FACS assay). The studies involving correlation with γH2AX suggest that this is again a good indicator of early DNA damage and the conclusions mirror findings of the Comet/MN-FACS correlations.

Chapter 5: Here we attempted to recapitulate sequential genotoxic exposures in cell line models of CLL and MCL. These diseases are low-grade lymphomas/leukaemias when patients are more likely to need multiple lines of therapy. The schedule used involved DNA damaging exposure with very short intervals of drug/treatment holidays and hence may not be truly reflective of in vivo scenarios with prolonged treatment free intervals. Despite this, we do show clear evidence of persistent 'DNA scarring' and genomic instability with sequential treatments. Of significance and relevance, the order and sequence of the chemotherapeutic agents did seem to matter, which has not been previously appreciated. Of potential interest and with likely clinical implications, the sensitivity to irradiation was different with prior fludarabine or bendamustine exposure.

In chapter 5 we have addressed the importance of cell cycle status and proliferative capacity on MN frequencies which is of relevance to interpretation of data that is generated by the MN-FACS assay.

Chapter 6: This chapter describes results that are likely most pertinent to our central hypothesis that sequential genotoxic treatments will lead to increasing genomic instability due the accumulated DNA damage. Here we used our

MN-FACS assay to address the question at hand. The need for fresh CLL cells for the MN-FACS assay did hamper our ability to study a larger cohort of samples within the time frame of the project. Nevertheless, genomic abnormalities such as 11q- or 17p- did show some correlation with MN frequencies. The number of samples with multiple prior chemotherapeutic exposures were small (<10) and hence it was difficult to appreciate any trends or infer definite conclusions. It is possible that the underlying biology of CLL, where most cells tend to be non-proliferative (G0/G1 phase), may affect MN frequencies estimated by the MN-FACS assay. It is likely that due to the low numbers of cells in the G2/M phase, despite stimulation with IL4/IL21 and growth on CD40 expressing fibroblasts, MN-FACS analysis underestimate the true extent of accumulated DNA damage in CLL cells.

A novel observation in the Ibrutinib experienced CLL samples is worthy of emphasis. This mainly resulted from the fact that the samples were collected at the lymphocytosis stage. The results suggest that Ibrutinib does cause cell cycle arrest that is not reversible on in vitro mitogen treatment. This has not been previously appreciated.

Chapter 8: General discussion

Over the years, many researchers have developed techniques to study and investigate DNA damage within cells, tissues and organisms. This is of particular relevance for understanding genotoxic insults that we all face on a day-to-day basis. Most studies use circulating white blood cells such as peripheral blood normal lymphocytes for their studies. While nature has equipped cells with robust mechanisms to correct errors in DNA through repair pathways, insults that are not cytotoxic can be carried over during the cellular lifespan or indeed through subsequent generations with detrimental effects on cellular homeostasis resulting in morbidity and disease states. Hence, studies to understand cumulative DNA damage within various cell types will always be relevant.

Although the CBMN assay has maintained its status as the gold standard to study effects of DNA damaging insults especially in the fields of environmental science, nuclear disasters/leaks, and exposure to known or potential mutagens, the assay is at best semi-automated and subjective. DNA damage could result from exogenous (environmental) or endogenous sources and cause persistent defects. DNA damaging mutagens such as alkylating/oxidizing agents, UV, and ionizing radiation can compromise DNA integrity by creating pyrimidine dimers, inducing thymine glycolysation, 3-methyladenine, 8-oxoguanine, O6-methylguanine, and causing single/double strand breaks [240]. Impairment of DNA repair pathways may also lead to persistence of such lesions with potentially harmful consequences [241, 242].

The CBMN assay predominantly uses peripheral blood lymphocytes for estimation of MN frequencies. There have been multiple studies confirming that this method is useful to assess the long term effects of radiation exposure [243]. CBMN has been used for early detection of several cancers, such as bladder and lung cancers. The technique is convenient to assess chromosome breakages and loss [102, 230].

The assessment of disease/cancer risk following mutagenic exposures can be difficult and requires long-term studies that may be impractical to assign true causality. Multiple assays and methodologies may be necessary for such studies [244]. There is a clear need for more robust and objective automated assays.

Manual scoring of micronuclei in human peripheral lymphocytes or any other cells using CBMN assay is time consuming and it is not practical to assess more than a few hundred cells per experiment. There have been attempts to use imaging software such as CellProfiler and may address some of the deficiencies inherent to the CBMN assay [179].

An automated technique named the FADU assay has been used for detecting DNA strand breaks by SYTOX green staining. The method depends on unwinding of the DNA under particular conditions of pH, temperature and time but may not be particularly useful to assess persistent DNA damage [245]. Spectral karyotyping (SKY) is a useful, accurate and hypersensitive cytogenetic tool recently that can detect complex chromosomal aberrations but may not be useful to detect subtle changes [246].

Most studies on DNA damage focus on potential insults on normal cells. An equally relevant question is the effect of chemotherapeutic interventions on cancer cells that survive the treatment. It is likely that by the nature of the treatments that are designed to disrupt DNA they will lead to accumulation of genetic lesions that provide survival advantage and may accelerate the disease process. Understanding DNA damage in this context may provide insights that address the balance between efficacy and toxicity. Dose-limiting toxicities and the development of drug resistance are important issues that apply to standard chemotherapy as well novel agents [247].

An essential and recurring theme in the treatment of CLL and other low-grade lymphomas/cancers is the need for sequential treatments with alternating episodes of remissions and recurrence. Despite the emergence of small molecule inhibitors such as Ibrutinib that are non-genotoxic, patients frequently need chemotherapeutic agents to achieve remissions. Moreover, the safety of immunotherapeutic agents such as rituximab and newer therapies in the context of DNA integrity remains to be investigated in systematic studies.

In our studies, we have investigated the MN frequency as a surrogate marker of cumulative DNA damage and genomic instability within malignant lymphoid cells in the context of sequential chemotherapeutic and/or irradiation. Before addressing the central hypothesis of the project, we did make some key and significant changes to a FACS based MN assay that can be seen as improvements from previous published reports.

A previous study reported the enumeration of MN by flow cytometry using mouse lymphoma (L5178Y) cells. The cells were stained with EMA/ SYTOX green [178]. This study was followed by another published report on the human lymphoblast cell line TK6 and validated the steps and stains [175]. A subsequent MN-FACS assay based advocated using EMA/ DAPI staining [163].

The main challenge of an MN-FACS assay is the need to distinguish apoptotic debris from true MN. While EMA labelling segregates out most DNA originating from dying cells, it is not effective at labelling those chromatin fragments that are generated before plasma membrane integrity is compromised. In addition, it is not clear if EMA/ SYTOX staining strategy is suitable for primary cells [248]. Our use of PI + DAPI and gating strategy does improve reproducibility, accuracy and speed of the assay.

Additional issues that could not be addressed within the timescale of this project include:

1) The ability to perform the assay on freeze-thawed primary samples.
2) Introducing an additional step that ensures cell cycle entry and
3) Induction of cytokinesis block and binucleation.

The novel outcomes resulting from this thesis are:

1. Established and optimized conditions for MN-FACS assay using PI/ DAPI staining (**Chapter 3**).
2. Proof that the optimized MN-FACS assay is a valid technique to measure MN frequency and is well correlated with CBMN measurements at both 24 and 48 hrs (**Chapter 4**).
3. Cumulative DNA damage seems to be affected by the order of exposure to Fludarabine and Bendamustine (**Chapter 5**).
4. There does seem to be a differential sensitivity to irradiation following fludarabine or bendamustine exposure (**Chapter 5**).
5. Ibrutinib causes cell cycle arrest that cannot be overcome by co-culture with CD40-fibroblasts or mitogens (**Chapter 6**).

Questions that have not been addressed, mainly due to time constraints include:

1. Performance of the MN-FACS assay on a greater variety of cell types and lines.
2. Strategy to induce/estimate the number of bi-nucleated cells in the MN-FACS assay which may improve the assay.
3. Examination of a significant cohort patient samples that reflect sequential chemotherapeutic treatments as such a study may need to be planned over a longer time period and in a larger group of patients. Here serial studies of MN frequencies at each stage may provide unique insights. MN frequency studies within a single case over a long

period of time may be useful to understand compromise of genomic integrity.

Future directions

1- Investigation of the DNA composition of MN in cell lines and primary CLL cells after treatment with genotoxic agents.

In Chapter 5, we found that mutational status and the treatment cycles are responsible for causing variation in the MN enumeration. The origin and the content of MN is still not clear. A published study used Fluorescence in situ hybridization (FISH) showed that the X chromosome is over-represented in MN in both females and males [249].

2- Assessment of gene expression with sequential treatments and correlation with qualitative and quantitative MN parameters.

3- Investigation of the relationship between MN frequencies and expression of DNA repair genes.

Our literature review suggests that expression of some DNA repair genes (XRCC1, ERCC2, and ATM) may be linked with MN formation.

Appendix A

Table 1: Buffers used in this study

Buffer	Components	Purpose
1st lysis buffer	0.584 mg/ml NaCl, 1mg/ml Sodium Citrate, 0.3 µg/ ml IGEPAL-630, 250 µg/ ml RNaseA.	MN-FACS assay
2nd lysis buffer	85.6mg/ ml Sucrose, 15mg/ml Citric Acid, pH (8-10).	MN-FACS assay
Annexin binding buffer	10mM HEPES, 140 mM NACL, and 2.5 mM $CaCl_2$.	Apoptosis assay
Cell dissociation solution	PBS pH 7.2, $CaCl_2$, $MgCl_2$, 1mM EDTA	Analysis of CD154 in transfected fibroblasts
PBS	Powder dissolved in dH2O, pH7.4	Cell culture
Trypsin-EDTA	0.25% trypsin in PBS, Na2-EDTA.	Cell culture (Adherent cells)

Table 2: Drugs used in this study

Drug	Catalogue no.	Manufacturer
Fludarabine	F2773	Sigma
Bendamustine	B5437	Sigma

Table 3: Growth media used in this study

Media	Composition	Cells	Manufacturer
DMEM	10% FBS, 1% L-Glutamine, 1% P/S	HeLa, and CD 154 Fibroblast cells.	Sigma
RPMI	10% FBS, 1% L-Glutamine, 1% P/S	EHEB, HG3, MAVER-1, JeKo-1, and Primary CLL cells.	Sigma
IMDM	10% FBS, 1% L-Glutamine, 1% P/S	MEC1	Sigma

Table 4: Software used for data analysis in this study

Software	Purpose
FRAP-AI (MAG Biosystems Software)	Capture images of comet assay slides in fluorescent microscopy.
ImageJ	Analyse comet tail.
FLOWJO v10	Analysis cell proliferation CFSE.
GraphPad Prism 6	Data analysis
Cellometer Auto T4	Cell count

Table 5: General Reagents, stains and antibodies used

Supplier	Reagents
Life technologies	rhIL-4, rhIL-21 Recombinant human protein, Fetal bovine serum, and RNase.
Cell signalling	p-Histone H2AX Rabbit antibody
Invitrogen	Alexa Fluor donkey anti-rabbit antibody, and Rabbit IgG isotype control.
BD Biosciences	FITC Annexin V
Sigma	DAPI and PI stain
Fisher scientific	Methanol, and DMSO

Appendix B

Table 1: The MN enumeration after 7 days with and without irradiation (3Gy)

Patient sample no.	MN count on day 7		
	Fibroblast	**Fibroblast + IL-4 + IL-21**	**Fibroblast + IL-4 + IL-21 + 3Gy**
3620	0.52	0.93	1.99
3621	0.27	0.39	0.83
3623	0.40	0.56	1.08
3624	0.31	0.86	1.03
3627	0.26	0.30	0.71
3631	0.19	0.57	0.69
3637	0.33	0.40	2.16 (MMC)*
3639	0.19	0.65	0.93
3640	0.72	1.81	1.90 (MMC)*
3642	0.75	1.30	1.66 (MMC)*
3644	0.20	0.37	0.49
3645	0.30	0.96	1.20
3647	0.60	0.72	1.07
3650	0.49	0.61	0.92
3652	0.29	0.53	0.73
3655	0.27	1.14	1.61
3656	0.20	1.32	1.59
3658	0.35	0.74	1.19
3660	0.35	0.68	1.17
3661	0.36	1.04	1.22
3663	0.33	0.72	1.20

* Treated with Mitomycin C (MMC) instead of irradiation (3Gy)

Table 2: Clinical data of CLL cases used within this thesis

Patient samples no.	Date of diagnosis	TP 53 mutation	IGVH mutation	Karyotype	Treatment
3561	2010	-	-	11q-	FCR
3564	1981				Interferon/ Ofatumumab-Chlorambucil/ Ibrutinib
3586	2016	-	+	13q-	Ibrutininb/ rituximab
3620	2009	-	+	Normal	UT
3621	2016	-	+	13q-	1 cycle of Ibrutinib
3623	2017	-	+	13q-	Ibrutinib + rituximab
3624	2012	-	-	11q-/ 13q-	FCR
3627	2008	-	-	13q-	Ibrutinib
3631	2014	-	+	13q-	Ibrutinib
3637	2014	-	-	11q -/ 13q-	UT (stage A)
3639	2013	-	-	13q-	1 cycle Ibrutinib
3640	2013	-	-	13q-	UT (stage A)
3642	2014	-	-	Normal	FCR 3 cycle
3644	2013	-	-	13q-	1 cycle Ibrutinib
3645	2013	+	-	Normal	UT (Pre Ibrutinib)
3647	2006	-	+	Normal	UT (Pre FCR)
3650	2010	-	+	Normal	UT
3652	2012	-	-	11q-/ 13q-	FCR
3655	2014	-	-	11q-/ Trisomy 12	FCR 2 Cycles
3656	2019	-	-	11q-	UT (stage A)

3658	2009	-	-	13q-	UT (Stage A)
3660	2018	+	-	Normal	Post Ibrutinib
3661	2013	+	+	13q-/ 17p-	UT
3663	2012	-	+	13q-	UT

Appendix C

Flow cytometry results:

Figure 1: MN-FACS assay gating strategy

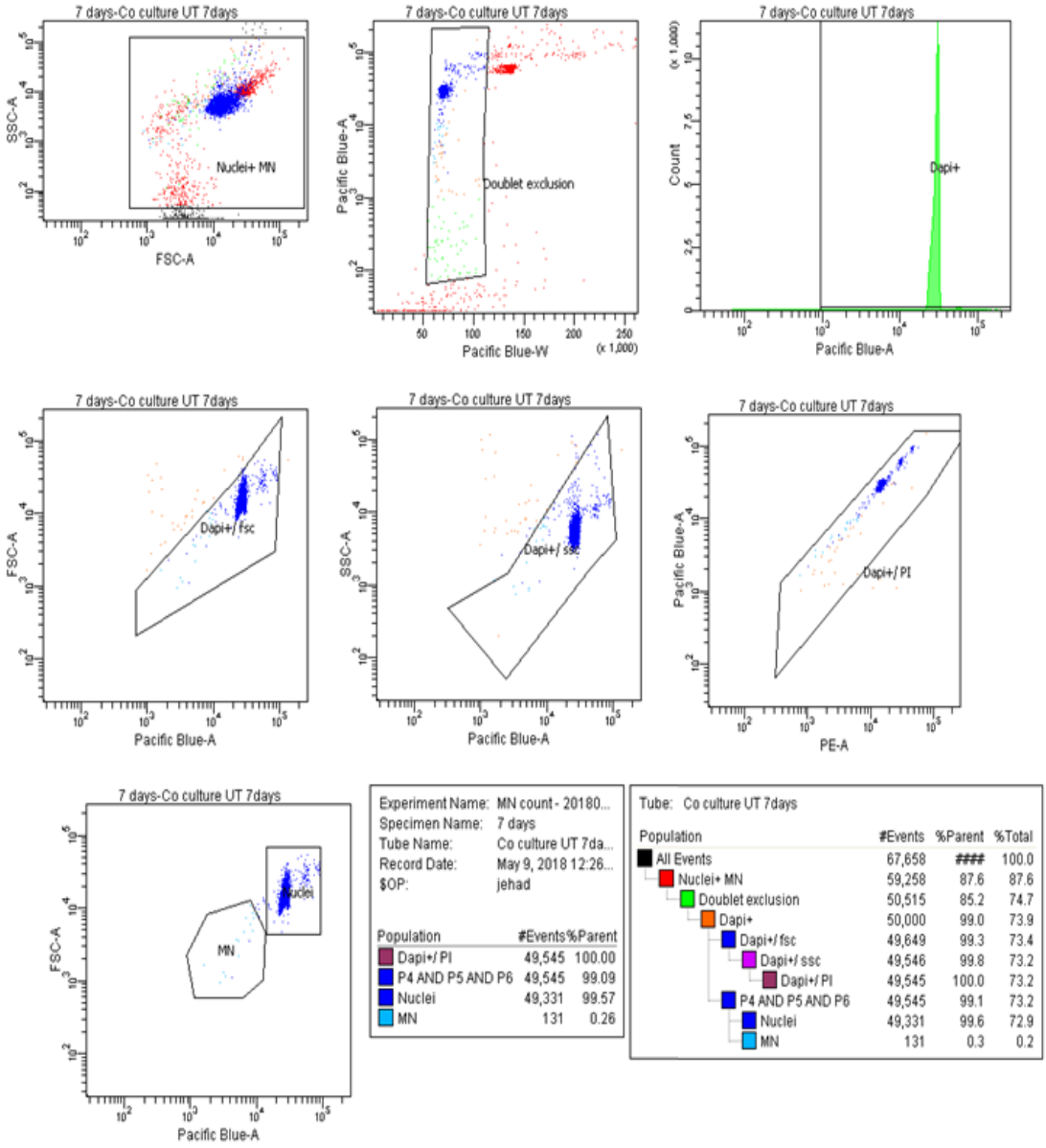

Figure 2: Cell cycle analysis: **A)** UT JeKo-1 cells, and **B)** Treated JeKo-1 cells with chemotherapy + Irradiation

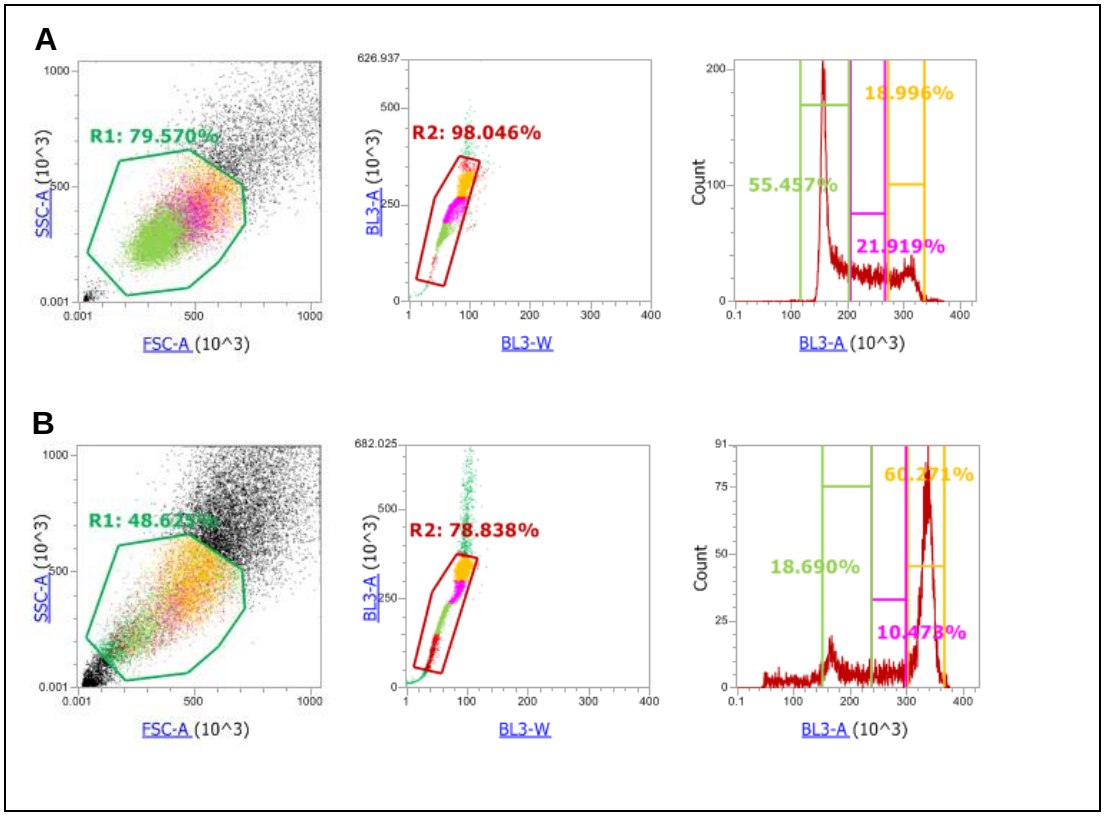

Figure 3: Cell apoptosis assay: **A)** UT JeKo-1 cells, and **B)** JeKo-1 cells after irradiation

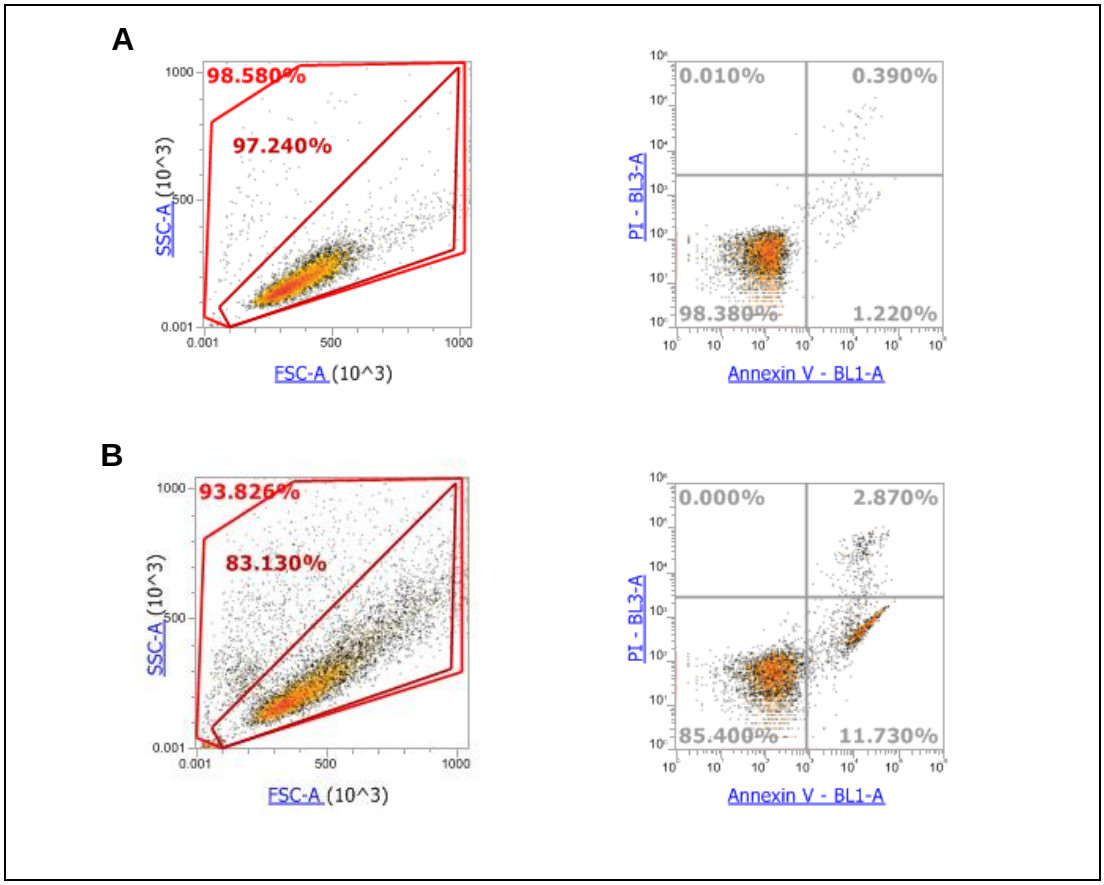

Figure 4: CFSE staining on co-culture system: **A)** UT JeKo-1 cells, **B)** JeKo-1 cells after treated with mitogens IL-4, IL-21, and **C)** JeKo-1 cells treated with mitogens IL-4, IL-21 after irradiation

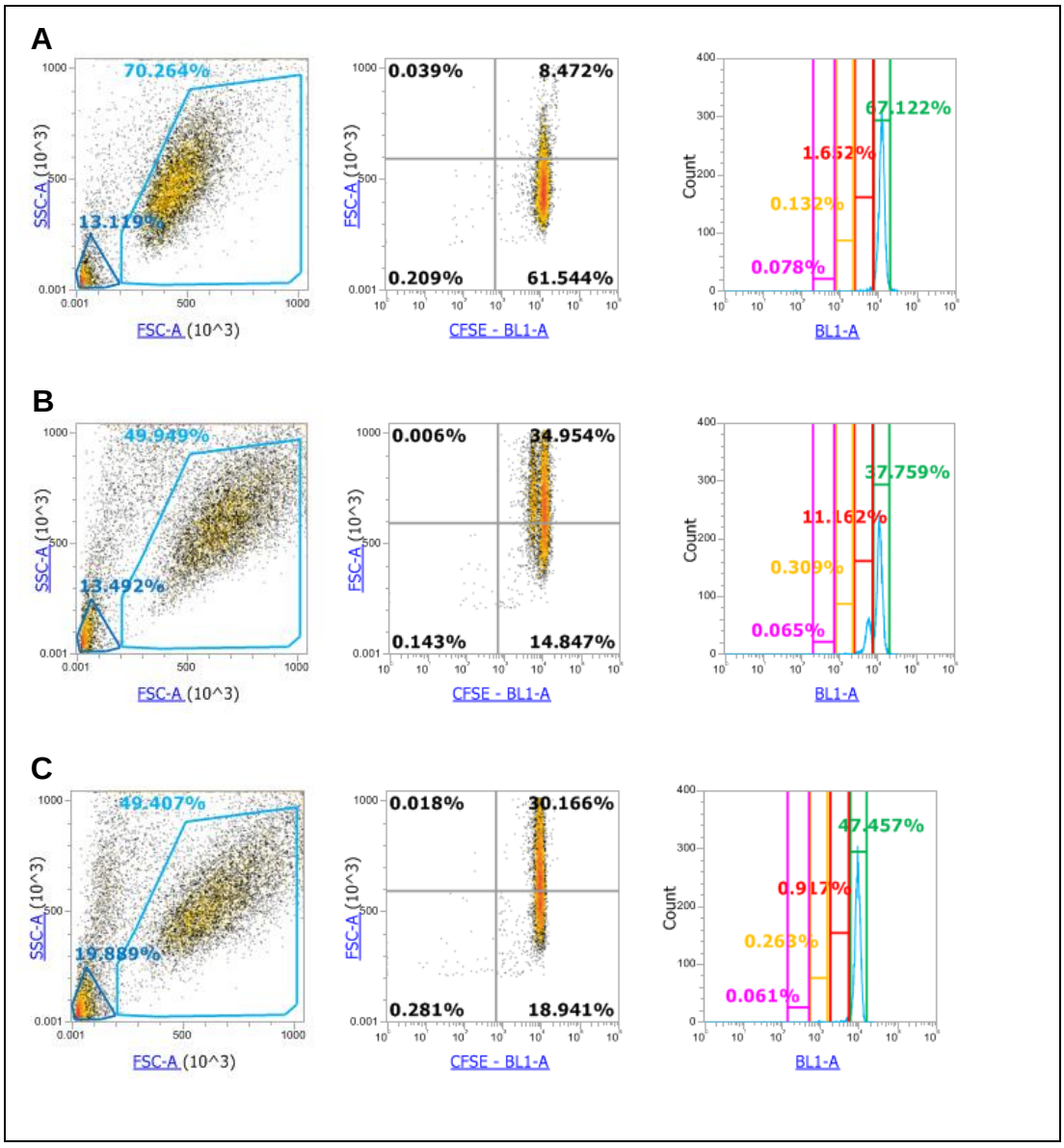

Bibliography

1. Srinivas, U.S., et al., *ROS and the DNA damage response in cancer.* Redox Biology, 2018: p. 101084.
2. Terradas, M., et al., *Genetic activities in micronuclei: Is the DNA entrapped in micronuclei lost for the cell?* Mutation Research/Reviews in Mutation Research, 2010. **705**(1): p. 60-67.
3. Köhler, K., et al., *Regulation of the Initiation of DNA Replication upon DNA Damage in Eukaryotes*. The Initiation of DNA Replication in Eukaryotes, ed. D.L. Kaplan. 2016, Cham: Springer International Publishing. 443-460.
4. Cannan, W.J. and D.S. Pederson, *Mechanisms and Consequences of Double-Strand DNA Break Formation in Chromatin.* Journal of cellular physiology, 2016. **231**(1): p. 3-14.
5. Jackson, S.P. and J. Bartek, *The DNA-damage response in human biology and disease.* Nature, 2009. **461**(7267): p. 1071-1078.
6. Pucci, B., M. Kasten, and A. Giordano, *Cell cycle and apoptosis.* Neoplasia (New York, N.Y.), 2000. **2**(4): p. 291-299.
7. Basu, A.K., *DNA Damage, Mutagenesis and Cancer.* International Journal of Molecular Sciences, 2018. **19**(4): p. 970.
8. GM, C., *The Cell: A Molecular Approach. 2nd edition*. 2000: Sunderland (MA): Sinauer Associates.
9. Arjunan, K.P., V.K. Sharma, and S. Ptasinska, *Effects of atmospheric pressure plasmas on isolated and cellular DNA-a review.* International journal of molecular sciences, 2015. **16**(2): p. 2971-3016.
10. Fenech, M., *Chromosomal biomarkers of genomic instability relevant to cancer.* Drug Discov Today, 2002. **7**(22): p. 1128-37.
11. Bartek, J., *DNA damage response, genetic instability and cancer: from mechanistic insights to personalized treatment.* Molecular oncology, 2011. **5**(4): p. 303-307.
12. Fuchs, Y. and H. Steller, *Programmed cell death in animal development and disease.* Cell, 2011. **147**(4): p. 742-758.
13. Tang, H.L., et al., *Cell survival, DNA damage, and oncogenic transformation after a transient and reversible apoptotic response.* Molecular biology of the cell, 2012. **23**(12): p. 2240-2252.
14. Vignard, J., G. Mirey, and B. Salles, *Ionizing-radiation induced DNA double-strand breaks: A direct and indirect lighting up.* Radiotherapy and Oncology, 2013. **108**(3): p. 362-369.
15. *3 - Principles of Ionizing Radiation*, in *Industrial Hygiene Engineering (Second Edition)*, J.T. Talty, Editor. 1998, William Andrew Publishing: Park Ridge, NJ. p. 621-647.
16. Lomax, M.E., L.K. Folkes, and P. O'Neill, *Biological Consequences of Radiation-induced DNA Damage: Relevance to Radiotherapy.* Clinical Oncology, 2013. **25**(10): p. 578-585.
17. Baskar, R., et al., *Biological response of cancer cells to radiation treatment.* Frontiers in molecular biosciences, 2014. **1**: p. 24-24.

18. Harrison, J.C. and J.E. Haber, *Surviving the breakup: the DNA damage checkpoint.* Annu Rev Genet, 2006. **40**: p. 209-35.
19. McGowan, C.H. and P. Russell, *The DNA damage response: sensing and signaling.* Current Opinion in Cell Biology, 2004. **16**(6): p. 629-633.
20. Bartek, J., J. Lukas, and J. Bartkova, *DNA Damage Response as an Anti-Cancer Barrier: Damage Threshold and the Concept of 'Conditional Haploinsufficiency'.* Cell Cycle, 2007. **6**(19): p. 2344-2347.
21. Maréchal, A. and L. Zou, *DNA Damage Sensing by the ATM and ATR Kinases.* Cold Spring Harbor Perspectives in Biology, 2013. **5**(9): p. a012716.
22. Giglia-Mari, G., A. Zotter, and W. Vermeulen, *DNA damage response.* Cold Spring Harbor perspectives in biology. **3**(1): p. a000745-a000745.
23. Gorgoulis, V.G., et al., *Activation of the DNA damage checkpoint and genomic instability in human precancerous lesions.* Nature, 2005. **434**: p. 907.
24. Hanahan, D. and Robert A. Weinberg, *Hallmarks of Cancer: The Next Generation.* Cell, 2011. **144**(5): p. 646-674.
25. Bristow, R.G. and R.P. Hill, *Hypoxia, DNA repair and genetic instability.* Nature Reviews Cancer, 2008. **8**: p. 180.
26. Halazonetis, T.D., V.G. Gorgoulis, and J. Bartek, *An Oncogene-Induced DNA Damage Model for Cancer Development.* Science, 2008. **319**(5868): p. 1352-1355.
27. Giglia-Mari, G., A. Zotter, and W. Vermeulen, *DNA Damage Response.* Cold Spring Harbor Perspectives in Biology, 2011. **3**(1): p. a000745.
28. Maréchal, A. and L. Zou, *DNA damage sensing by the ATM and ATR kinases.* Cold Spring Harbor perspectives in biology. **5**(9): p. a012716.
29. Ciccia, A. and S.J. Elledge, *The DNA Damage Response: Making it safe to play with knives.* Molecular cell, 2010. **40**(2): p. 179-204.
30. McKinnon, P.J., *DNA repair deficiency and neurological disease.* Nature reviews. Neuroscience, 2009. **10**(2): p. 100-112.
31. Barnum, K.J. and M.J. O'Connell, *Cell cycle regulation by checkpoints.* Methods in molecular biology (Clifton, N.J.), 2014. **1170**: p. 29-40.
32. Alberts B, J.A., Lewis J, et al., *Molecular Biology of the Cell. 4th edition*. 2002, New York: Garland Science.
33. Branzei, D. and M. Foiani, *Regulation of DNA repair throughout the cell cycle.* Nature Reviews Molecular Cell Biology, 2008. **9**: p. 297.
34. Ashworth, A., *A Synthetic Lethal Therapeutic Approach: Poly(ADP) Ribose Polymerase Inhibitors for the Treatment of Cancers Deficient in DNA Double-Strand Break Repair.* Journal of Clinical Oncology, 2008. **26**(22): p. 3785-3790.
35. Bouwman, P. and J. Jonkers, *The effects of deregulated DNA damage signalling on cancer chemotherapy response and resistance.* Nature Reviews Cancer, 2012. **12**: p. 587.
36. Dalla-Favera, R., *Lymphoid malignancies: many tumor types, many altered genes, many therapeutic challenges.* The Journal of clinical investigation, 2012. **122**(10): p. 3396-3397.
37. Hiraoka, N., Y. Ino, and R. Yamazaki-Itoh, *Tertiary Lymphoid Organs in Cancer Tissues.* Frontiers in immunology, 2016. **7**: p. 244-244.

38. Swerdlow, S.H., et al., *The 2016 revision of the World Health Organization classification of lymphoid neoplasms.* Blood, 2016. **127**(20): p. 2375-2390.
39. Terwilliger, T. and M. Abdul-Hay, *Acute lymphoblastic leukemia: a comprehensive review and 2017 update.* Blood cancer journal, 2017. **7**(6): p. e577-e577.
40. Van Vlierberghe, P. and A. Ferrando, *The molecular basis of T cell acute lymphoblastic leukemia.* The Journal of clinical investigation, 2012. **122**(10): p. 3398-3406.
41. Mullighan, C.G., *Molecular genetics of B-precursor acute lymphoblastic leukemia.* The Journal of clinical investigation, 2012. **122**(10): p. 3407-3415.
42. Küppers, R., A. Engert, and M.-L. Hansmann, *Hodgkin lymphoma.* The Journal of clinical investigation, 2012. **122**(10): p. 3439-3447.
43. Liu, W.R. and M.A. Shipp, *Signaling pathways and immune evasion mechanisms in classical Hodgkin lymphoma.* Hematology. American Society of Hematology. Education Program, 2017. **2017**(1): p. 310-316.
44. Jares, P., D. Colomer, and E. Campo, *Molecular pathogenesis of mantle cell lymphoma.* The Journal of clinical investigation, 2012. **122**(10): p. 3416-3423.
45. Luminari, S., et al., *Follicular lymphoma - treatment and prognostic factors.* Revista brasileira de hematologia e hemoterapia, 2012. **34**(1): p. 54-59.
46. Cheah, C.Y., J.F. Seymour, and M.L. Wang, *Mantle Cell Lymphoma.* Journal of Clinical Oncology, 2016. **34**(11): p. 1256-1269.
47. Li, S., K.H. Young, and L.J. Medeiros, *Diffuse large B-cell lymphoma.* Pathology, 2018. **50**(1): p. 74-87.
48. Molyneux, E.M., et al., *Burkitt's lymphoma.* Lancet, 2012. **379**(9822): p. 1234-44.
49. Board, P.A.T.E., *Plasma Cell Neoplasms (Including Multiple Myeloma) Treatment (PDQ®): Health Professional Version.* 2002: Bethesda (MD): National Cancer Institute (US).
50. Al-Farsi, K., *Multiple myeloma: an update.* Oman medical journal, 2013. **28**(1): p. 3-11.
51. Rodriguez, D., et al., *Molecular pathogenesis of CLL and its evolution.* Int J Hematol, 2015. **101**(3): p. 219-28.
52. Kipps, T.J., et al., *Chronic lymphocytic leukaemia.* Nature Reviews Disease Primers, 2017. **3**: p. 16096.
53. Zhang, S. and T.J. Kipps, *The pathogenesis of chronic lymphocytic leukemia.* Annu Rev Pathol, 2014. **9**: p. 103-18.
54. Stephan, S., L. Peter, and D. Hartmut, *Genetic Features of B-Cell Chronic Lymphocytic Leukemia.* Reviews in Clinical and Experimental Hematology, 2000. **4**(1): p. 48-72.
55. Kipps, T.J., et al., *Chronic lymphocytic leukaemia.* Nature reviews. Disease primers, 2017. **3**: p. 16096-16096.
56. Mehta, K., et al., *Multi-targeted approach to cancer treatment: an international translational cancer research symposium.* Anticancer Res, 2014. **34**(11): p. 6791-5.
57. Hallek, M., *Chronic lymphocytic leukemia: 2017 update on diagnosis, risk stratification, and treatment.* Am J Hematol, 2017. **92**(9): p. 946-965.

58. Boyd, S.D., et al., *Selective immunophenotyping for diagnosis of B-cell neoplasms: immunohistochemistry and flow cytometry strategies and results.* Applied immunohistochemistry & molecular morphology : AIMM, 2013. **21**(2): p. 116-131.
59. Hallek, M., et al., *Guidelines for the diagnosis and treatment of chronic lymphocytic leukemia: a report from the International Workshop on Chronic Lymphocytic Leukemia updating the National Cancer Institute-Working Group 1996 guidelines.* Blood, 2008. **111**(12): p. 5446-56.
60. Damle, R.N., et al., *Ig V gene mutation status and CD38 expression as novel prognostic indicators in chronic lymphocytic leukemia.* Blood, 1999. **94**(6): p. 1840-7.
61. Hamblin, T.J., et al., *Unmutated Ig V(H) genes are associated with a more aggressive form of chronic lymphocytic leukemia.* Blood, 1999. **94**(6): p. 1848-54.
62. Orchard, J.A., et al., *ZAP-70 expression and prognosis in chronic lymphocytic leukaemia.* Lancet, 2004. **363**(9403): p. 105-11.
63. Jares, P., D. Colomer, and E. Campo, *Genetic and molecular pathogenesis of mantle cell lymphoma: perspectives for new targeted therapeutics.* Nature Reviews Cancer, 2007. **7**: p. 750.
64. Pérez-Galán, P., M. Dreyling, and A. Wiestner, *Mantle cell lymphoma: biology, pathogenesis, and the molecular basis of treatment in the genomic era.* Blood, 2011. **117**(1): p. 26-38.
65. Herrmann, A., et al., *Improvement of overall survival in advanced stage mantle cell lymphoma.* J Clin Oncol, 2009. **27**(4): p. 511-518.
66. Shanbhag, S. and R.F. Ambinder, *Hodgkin lymphoma: A review and update on recent progress.* CA: A Cancer Journal for Clinicians, 2018. **68**(2): p. 116-132.
67. Lee, C.-T., et al., *Drug delivery systems and combination therapy by using vinca alkaloids.* Current topics in medicinal chemistry, 2015. **15**(15): p. 1491-1500.
68. Cook, A.M., et al., *Dexamethasone co-medication in cancer patients undergoing chemotherapy causes substantial immunomodulatory effects with implications for chemo-immunotherapy strategies.* Oncoimmunology, 2015. **5**(3): p. e1066062-e1066062.
69. Hallek, M., T.D. Shanafelt, and B. Eichhorst, *Chronic lymphocytic leukaemia.* Lancet, 2018. **391**(10129): p. 1524-1537.
70. J.T. Dipiro, R.L.T., G.C. Yee, G.R. Matzke, B.G. Wells, L.M. Posey, *Pharmacology: A Pathophysiologic Approach*. 10th edition ed. 2018.
71. Casan, J.M.L., et al., *Anti-CD20 monoclonal antibodies: reviewing a revolution.* Human vaccines & immunotherapeutics, 2018. **14**(12): p. 1-22.
72. Husby, S. and K. Grønbæk, *Mature lymphoid malignancies: origin, stem cells, and chronicity.* Blood Advances, 2017. **1**(25): p. 2444-2455.
73. Leibel, S.A. and T.L. Phillips, *Textbook of radiation oncology*. 1998: London: WB Saunders, 1998.
74. *Chemotherapeutic options in chronic lymphocytic leukemia: a meta-analysis of the randomized trials. CLL Trialists' Collaborative Group.* J Natl Cancer Inst, 1999. **91**(10): p. 861-8.

75. Ghia, P. and M. Hallek, *Management of chronic lymphocytic leukemia.* Haematologica, 2014. **99**(6): p. 965-972.
76. Frustaci, A.M., et al., *Ofatumumab plus chlorambucil as a first-line therapy in less fit patients with chronic lymphocytic leukemia: analysis of COMPLEMENT1 and other monoclonal antibodies association data.* Therapeutic Advances in Hematology, 2016. **7**(4): p. 222-230.
77. Ricci, F., et al., *Fludarabine in the treatment of chronic lymphocytic leukemia: a review.* Therapeutics and Clinical Risk Management, 2009. **5**: p. 187-207.
78. Plunkett, W., et al., *Comparison of the toxicity and metabolism of 9-beta-D-arabinofuranosyl-2-fluoroadenine and 9-beta-D-arabinofuranosyladenine in human lymphoblastoid cells.* Cancer Res, 1980. **40**(7): p. 2349-55.
79. Hallek, M., et al., *Addition of rituximab to fludarabine and cyclophosphamide in patients with chronic lymphocytic leukaemia: a randomised, open-label, phase 3 trial.* Lancet, 2010. **376**(9747): p. 1164-74.
80. Knauf, W.U., et al., *Phase III randomized study of bendamustine compared with chlorambucil in previously untreated patients with chronic lymphocytic leukemia.* J Clin Oncol, 2009. **27**(26): p. 4378-84.
81. Brown, J.R., M.J. Hallek, and J.M. Pagel, *Chemoimmunotherapy Versus Targeted Treatment in Chronic Lymphocytic Leukemia: When, How Long, How Much, and in Which Combination?* Am Soc Clin Oncol Educ Book, 2016. **35**: p. e387-98.
82. Tam, C.S., et al., *Long-term results of the fludarabine, cyclophosphamide, and rituximab regimen as initial therapy of chronic lymphocytic leukemia.* Blood, 2008. **112**(4): p. 975-80.
83. Fischer, K., et al., *Bendamustine combined with rituximab in patients with relapsed and/or refractory chronic lymphocytic leukemia: a multicenter phase II trial of the German Chronic Lymphocytic Leukemia Study Group.* J Clin Oncol, 2011. **29**(26): p. 3559-66.
84. Eichhorst, B., et al., *First-line chemoimmunotherapy with bendamustine and rituximab versus fludarabine, cyclophosphamide, and rituximab in patients with advanced chronic lymphocytic leukaemia (CLL10): an international, open-label, randomised, phase 3, non-inferiority trial.* Lancet Oncol, 2016. **17**(7): p. 928-942.
85. Shan, D., J.A. Ledbetter, and O.W. Press, *Signaling events involved in anti-CD20-induced apoptosis of malignant human B cells.* Cancer Immunol Immunother, 2000. **48**(12): p. 673-83.
86. Sandhu, S. and S.P. Mulligan, *Ofatumumab and its role as immunotherapy in chronic lymphocytic leukemia.* Haematologica, 2015. **100**(4): p. 411-414.
87. Said, R. and A.M. Tsimberidou, *Obinutuzumab for the treatment of chronic lymphocytic leukemia and other B-cell lymphoproliferative disorders.* Expert opinion on biological therapy, 2017. **17**(11): p. 1463-1470.
88. Wiestner, A., *Emerging role of kinase-targeted strategies in chronic lymphocytic leukemia.* Hematology Am Soc Hematol Educ Program, 2012. **2012**: p. 88-96.
89. Herman, S.E.M., et al., *Bruton tyrosine kinase represents a promising therapeutic target for treatment of chronic lymphocytic leukemia and is effectively targeted by PCI-32765.* Blood, 2011. **117**(23): p. 6287-6296.

90. Lampson, B.L., et al., *Idelalisib given front-line for treatment of chronic lymphocytic leukemia causes frequent immune-mediated hepatotoxicity.* Blood, 2016. **128**(2): p. 195-203.
91. Vangapandu, H.V., N. Jain, and V. Gandhi, *Duvelisib: a phosphoinositide-3 kinase δ/γ inhibitor for chronic lymphocytic leukemia.* Expert opinion on investigational drugs, 2017. **26**(5): p. 625-632.
92. Roberts, A.W., et al., *Targeting BCL2 with Venetoclax in Relapsed Chronic Lymphocytic Leukemia.* New England Journal of Medicine, 2016. **374**(4): p. 311-322.
93. Davids, M.S., et al., *Comprehensive Safety Analysis of Venetoclax Monotherapy for Patients with Relapsed/Refractory Chronic Lymphocytic Leukemia.* Clinical Cancer Research, 2018. **24**(18): p. 4371-4379.
94. Frenzel, L.P., et al., *Mechanisms of Venetoclax Resistance in Chronic Lymphocytic Leukemia.* Blood, 2017. **130**(Suppl 1): p. 263-263.
95. Dreyling, M., et al., *Treatment for patients with relapsed/refractory mantle cell lymphoma: European-based recommendations.* Leukemia & Lymphoma, 2018. **59**(8): p. 1814-1828.
96. Vacchelli, E., et al., *Trial watch: Chemotherapy with immunogenic cell death inducers.* Oncoimmunology, 2012. **1**(2): p. 179-188.
97. Meng, Y., et al., *Radiation-inducible immunotherapy for cancer: senescent tumor cells as a cancer vaccine.* Molecular therapy : the journal of the American Society of Gene Therapy, 2012. **20**(5): p. 1046-1055.
98. Mayer, E.L., *Early and late long-term effects of adjuvant chemotherapy.* Am Soc Clin Oncol Educ Book, 2013: p. 9-14.
99. Landau, D.A., et al., *The evolutionary landscape of chronic lymphocytic leukemia treated with ibrutinib targeted therapy.* Nature Communications, 2017. **8**(1): p. 2185.
100. Barcellos-Hoff, M.H., C. Park, and E.G. Wright, *Radiation and the microenvironment – tumorigenesis and therapy.* Nature Reviews Cancer, 2005. **5**(11): p. 867-875.
101. Krem, M.M., et al., *Mechanisms and clinical applications of chromosomal instability in lymphoid malignancy.* British Journal of Haematology, 2015. **171**(1): p. 13-28.
102. El-Zein, R.A., et al., *Cytokinesis-Blocked Micronucleus Assay as a Novel Biomarker for Lung Cancer Risk.* Cancer Research, 2006. **66**(12): p. 6449-6456.
103. Kirsch-Volders, M., et al., *The in vitro MN assay in 2011: origin and fate, biological significance, protocols, high throughput methodologies and toxicological relevance.* Archives of Toxicology, 2011. **85**(8): p. 873-899.
104. Makowski, M. and K.J. Archer, *Generalized monotone incremental forward stagewise method for modeling count data: application predicting micronuclei frequency.* Cancer Inform, 2015. **14**(Suppl 2): p. 97-105.
105. Fenech, M., et al., *Molecular mechanisms by which in vivo exposure to exogenous chemical genotoxic agents can lead to micronucleus formation in lymphocytes in vivo and ex vivo in humans.* Mutation Research/Reviews in Mutation Research, 2016. **770**: p. 12-25.

106. Kirsch-Volders, M., et al., *Indirect mechanisms of genotoxicity.* Toxicol Lett, 2003. **140-141**: p. 63-74.
107. Iarmarcovai, G., et al., *Genetic polymorphisms and micronucleus formation: A review of the literature.* Mutation Research/Reviews in Mutation Research, 2008. **658**(3): p. 215-233.
108. Alkan, O., et al., *Modeling chemotherapy-induced stress to identify rational combination therapies in the DNA damage response pathway.* Science Signaling, 2018. **11**(540).
109. Driessens, G., et al., *Micronuclei to detect in vivo chemotherapy damage in a p53 mutated solid tumour.* British journal of cancer, 2003. **89**(4): p. 727-729.
110. Paz, M., et al., *Persistent Increased Frequency of Genomic Instability in Women Diagnosed with Breast Cancer: Before, during, and after Treatments.* Oxidative Medicine and Cellular Longevity, 2018. **2018**: p. 10.
111. Gascoigne, K.E. and I.M. Cheeseman, *Induced dicentric chromosome formation promotes genomic rearrangements and tumorigenesis.* Chromosome research : an international journal on the molecular, supramolecular and evolutionary aspects of chromosome biology, 2013. **21**(4): p. 407-418.
112. Mateuca, R., et al., *Chromosomal changes: induction, detection methods and applicability in human biomonitoring.* Biochimie, 2006. **88**(11): p. 1515-31.
113. Bhuyan, B.K., et al., *Comparative Genotoxicity of Adriamycin and Menogarol, Two Anthracycline Antitumor Agents.* Cancer Research, 1983. **43**(11): p. 5293-5297.
114. Vallarino-Kelly, T. and P. Morales-Ramírez, *Kinetics of micronucleus induction and cytotoxic activity of colchicine in murine erythroblast in vivo.* Mutation Research/Genetic Toxicology and Environmental Mutagenesis, 2001. **495**(1): p. 51-59.
115. Utani, K.-i., et al., *Emergence of micronuclei and their effects on the fate of cells under replication stress.* PloS one, 2010. **5**(4): p. e10089-e10089.
116. Erenpreisa, J. and M.S. Cragg, *Mitotic death: a mechanism of survival? A review.* Cancer cell international, 2001. **1**(1): p. 1-1.
117. Mateuca, R., et al., *Chromosomal changes: induction, detection methods and applicability in human biomonitoring.* Biochimie, 2006. **88**(11): p. 1515-1531.
118. Luzhna, L., P. Kathiria, and O. Kovalchuk, *Micronuclei in genotoxicity assessment: from genetics to epigenetics and beyond.* Frontiers in genetics, 2013. **4**: p. 131-131.
119. Potapova, T. and G.J. Gorbsky, *The Consequences of Chromosome Segregation Errors in Mitosis and Meiosis.* Biology, 2017. **6**(1): p. 12.
120. Ramírez, T., et al., *Prevention of aneuploidy by S-adenosyl-methionine in human cells treated with sodium arsenite.* Mutation Research/Fundamental and Molecular Mechanisms of Mutagenesis, 2007. **617**(1): p. 16-22.
121. Guttenbach, M. and M. Schmid, *Exclusion of Specific Human Chromosomes into Micronuclei by 5-Azacytidine Treatment of Lymphocyte Cultures.* Experimental Cell Research, 1994. **211**(1): p. 127-132.
122. Fuso, A., *The 'golden age' of DNA methylation in neurodegenerative diseases.* Clin Chem Lab Med, 2013. **51**(3): p. 523-34.

123. Lu, L., et al., *Choline and/or folic acid deficiency is associated with genomic damage and cell death in human lymphocytes in vitro.* Nutr Cancer, 2012. **64**(3): p. 481-7.
124. Lazalde-Ramos, B.P., et al., *DNA and Oxidative Damages Decrease After Ingestion of Folic Acid in Patients with Type 2 Diabetes.* Archives of Medical Research, 2012. **43**(6): p. 476-481.
125. Gashi, G., et al., *The association between micronucleus, nucleoplasmic bridges, and nuclear buds frequency and the degree of uterine cervical lesions.* Biomarkers, 2018. **23**(4): p. 364-372.
126. Bitgen, N., et al., *Increased micronucleus, nucleoplasmic bridge, nuclear bud frequency and oxidative DNA damage associated with prolactin levels and pituitary adenoma diameters in patients with prolactinoma.* Biotechnic & Histochemistry, 2016. **91**(2): p. 128-136.
127. Rodriguez-Brenes, I.A. and D. Wodarz, *Preventing clonal evolutionary processes in cancer: Insights from mathematical models.* Proceedings of the National Academy of Sciences, 2015. **112**(29): p. 8843-8850.
128. Ibragimova, M.K., M.M. Tsyganov, and N.V. Litviakov, *Natural and chemotherapy-induced clonal evolution of tumors.* Biochemistry (Moscow), 2017. **82**(4): p. 413-425.
129. Caldas, C., *Cancer sequencing unravels clonal evolution.* Nature Biotechnology, 2012. **30**: p. 408.
130. Greaves, M. and C.C. Maley, *Clonal evolution in cancer.* Nature, 2012. **481**(7381): p. 306-313.
131. McGranahan, N. and C. Swanton, *Clonal Heterogeneity and Tumor Evolution: Past, Present, and the Future.* Cell, 2017. **168**(4): p. 613-628.
132. Grimaldi, K.A., et al., *PCR-based methods for detecting DNA damage and its repair at the sub-gene and single nucleotide levels in cells.* Molecular Biotechnology, 2002. **20**(2): p. 181-196.
133. Paull, T.T., et al., *A critical role for histone H2AX in recruitment of repair factors to nuclear foci after DNA damage.* Current Biology, 2000. **10**(15): p. 886-895.
134. Talty, J.T., *Principles of Ionizing Radiation, in Industrial Hygiene Engineering*. Second Edition ed. 1998: William Andrew Publishing: Park Ridge.
135. Podhorecka, M., A. Skladanowski, and P. Bozko, *H2AX Phosphorylation: Its Role in DNA Damage Response and Cancer Therapy.* Journal of nucleic acids, 2010. **2010**: p. 920161.
136. Collins, A.R. and A. Azqueta, *DNA repair as a biomarker in human biomonitoring studies; further applications of the comet assay.* Mutation Research/Fundamental and Molecular Mechanisms of Mutagenesis, 2012. **736**(1): p. 122-129.
137. Fernández, J.L., et al., *DBD-FISH on Neutral Comets: Simultaneous Analysis of DNA Single- and Double-Strand Breaks in Individual Cells.* Experimental Cell Research, 2001. **270**(1): p. 102-109.
138. Henry, C.M., E. Hollville, and S.J. Martin, *Measuring apoptosis by microscopy and flow cytometry.* Methods, 2013. **61**(2): p. 90-97.

139. Kriste, A.G., B.S. Martincigh, and L.F. Salter, *A sensitive immunoassay technique for thymine dimer quantitation in UV-irradiated DNA.* Journal of Photochemistry and Photobiology A: Chemistry, 1996. **93**(2): p. 185-192.
140. Cinquanta, L., D.E. Fontana, and N. Bizzaro, *Chemiluminescent immunoassay technology: what does it change in autoantibody detection?* Auto- immunity highlights, 2017. **8**(1): p. 9-9.
141. El-Yazbi, A.F. and G.R. Loppnow, *Detecting UV-induced nucleic-acid damage.* TrAC Trends in Analytical Chemistry, 2014. **61**: p. 83-91.
142. Rindgen, D., R.J. Turesky, and P. Vouros, *Determination of in vitro formed DNA adducts of 2-amino-1-methyl-6-phenylimidazo[4,5-b]pyridine using capillary liquid chromatography/electrospray ionization/tandem mass spectrometry.* Chem Res Toxicol, 1995. **8**(8): p. 1005-13.
143. Dawson, D.W. and H.P. Bury, *The significance of Howell-Jolly bodies and giant metamyelocytes in marrow smears.* Journal of clinical pathology, 1961. **14**(4): p. 374-380.
144. Luzhna, L., P. Kathiria, and O. Kovalchuk, *Micronuclei in genotoxicity assessment: from genetics to epigenetics and beyond.* Frontiers in Genetics, 2013. **4**(131).
145. Offer, T., et al., *A simple assay for frequency of chromosome breaks and loss (micronuclei) by flow cytometry of human reticulocytes.* The FASEB Journal, 2005. **19**(3): p. 485-487.
146. Schreiber, G., et al., *An automated flow cytometric micronucleus assay for human lymphocytes.* International journal of radiation biology, 1992. **62**(6): p. 695-709.
147. Verhaegen, F., et al., *Scoring of radiation-induced microuclei in cytokinesis-blocked human lymphocytes by automated image analysis.* Cytometry: The Journal of the International Society for Analytical Cytology, 1994. **17**(2): p. 119-127.
148. Varga, D., et al., *An automated scoring procedure for the micronucleus test by image analysis.* Mutagenesis, 2004. **19**(5): p. 391-397.
149. Sabharwal, R., et al., *Emergence of micronuclei as a genomic biomarker.* Indian journal of medical and paediatric oncology : official journal of Indian Society of Medical & Paediatric Oncology, 2015. **36**(4): p. 212-218.
150. Jdey, W., et al., *Micronuclei Frequency in Tumors Is a Predictive Biomarker for Genetic Instability and Sensitivity to the DNA Repair Inhibitor AsiDNA.* Cancer Research, 2017. **77**(16): p. 4207-4216.
151. Disis, M.L., et al., *Maximizing the retention of antigen specific lymphocyte function after cryopreservation.* Journal of Immunological Methods, 2006. **308**(1): p. 13-18.
152. Zamo, A., et al., *Establishment of the MAVER-1 cell line, a model for leukemic and aggressive mantle cell lymphoma.* Haematologica, 2006. **91**(1): p. 40-47.
153. Jeon, H.J., et al., *Establishment and characterization of a mantle cell lymphoma cell line.* British Journal of Haematology, 1998. **102**(5): p. 1323-1326.
154. Macville, M., et al., *Comprehensive and Definitive Molecular Cytogenetic Characterization of HeLa Cells by Spectral Karyotyping.* Cancer Research, 1999. **59**(1): p. 141-150.

155. Saltman, D., et al., *Establishment of a karyotypically normal B-chronic lymphocytic leukemia cell line; evidence of leukemic origin by immunoglobulin gene rearrangement.* Leuk Res, 1990. **14**(4): p. 381-7.
156. Stacchini, A., et al., *MEC1 and MEC2: two new cell lines derived from B-chronic lymphocytic leukaemia in prolymphocytoid transformation.* Leukemia Research, 1999. **23**(2): p. 127-136.
157. Rosén, A., et al., *Lymphoblastoid cell line with B1 cell characteristics established from a chronic lymphocytic leukemia clone by in vitro EBV infection.* Oncoimmunology, 2012. **1**(1): p. 18-27.
158. Pegg, D.E., *Principles of Cryopreservation*, in *Cryopreservation and Freeze-Drying Protocols*, J.G. Day and G.N. Stacey, Editors. 2007, Humana Press: Totowa, NJ. p. 39-57.
159. Funato, N., et al., *Common regulation of growth arrest and differentiation of osteoblasts by helix-loop-helix factors.* Molecular and cellular biology, 2001. **21**(21): p. 7416-7428.
160. Fenech, M., *Cytokinesis-block micronucleus cytome assay.* Nature Protocols, 2007. **2**: p. 1084.
161. Nickson, C.M. and J.L. Parsons, *Monitoring regulation of DNA repair activities of cultured cells in-gel using the comet assay.* Frontiers in Genetics, 2014. **5**(232).
162. Taylor, W.R., *FACS-Based Detection of Phosphorylated Histone H3 for the Quantitation of Mitotic Cells*, in *Checkpoint Controls and Cancer: Volume 2: Activation and Regulation Protocols*, A.H. Schönthal, Editor. 2004, Humana Press: Totowa, NJ. p. 293-299.
163. Lukamowicz, M., et al., *In vitro primary human lymphocyte flow cytometry based micronucleus assay: simultaneous assessment of cell proliferation, apoptosis and MN frequency.* Mutagenesis, 2011. **26**(6): p. 763-770.
164. Cummings, B.S. and R.G. Schnellmann, *Measurement of cell death in mammalian cells.* Current protocols in pharmacology, 2004. **Chapter 12**: p. 10.1002/0471141755.ph1208s25-12.8.
165. Pozarowski, P. and Z. Darzynkiewicz, *Analysis of Cell Cycle by Flow Cytometry*, in *Checkpoint Controls and Cancer: Volume 2: Activation and Regulation Protocols*, A.H. Schönthal, Editor. 2004, Humana Press: Totowa, NJ. p. 301-311.
166. Riedhammer, C., D. Halbritter, and R. Weissert, *Peripheral Blood Mononuclear Cells: Isolation, Freezing, Thawing, and Culture*, in *Multiple Sclerosis: Methods and Protocols*, R. Weissert, Editor. 2016, Springer New York: New York, NY. p. 53-61.
167. Schleiss, C., et al., *BCR-associated factors driving chronic lymphocytic leukemia cells proliferation ex vivo.* Scientific Reports, 2019. **9**(1): p. 701.
168. Wiesmüller, L., J.M. Ford, and R.H. Schiestl, *DNA Damage, Repair, and Diseases.* Journal of biomedicine & biotechnology, 2002. **2**(2): p. 45-45.
169. Hakem, R., *DNA-damage repair; the good, the bad, and the ugly.* The EMBO journal, 2008. **27**(4): p. 589-605.
170. Takagi, M., *DNA damage response and hematological malignancy.* International Journal of Hematology, 2017. **106**(3): p. 345-356.

171. Karran, P., *Mechanisms of tolerance to DNA damaging therapeutic drugs.* Carcinogenesis, 2001. **22**(12): p. 1931-1937.
172. Wilson, D.M., 3rd, V.A. Bohr, and P.J. McKinnon, *DNA damage, DNA repair, ageing and age-related disease.* Mechanisms of ageing and development, 2008. **129**(7-8): p. 349-352.
173. Schmid, T.E., O. Zlobinskaya, and G. Multhoff, *Differences in Phosphorylated Histone H2AX Foci Formation and Removal of Cells Exposed to Low and High Linear Energy Transfer Radiation.* Current Genomics, 2012. **13**(6): p. 418-425.
174. Figueroa-González, G. and C. Pérez-Plasencia, *Strategies for the evaluation of DNA damage and repair mechanisms in cancer.* Oncology letters, 2017. **13**(6): p. 3982-3988.
175. Bryce, S.M., et al., *In vitro micronucleus assay scored by flow cytometry provides a comprehensive evaluation of cytogenetic damage and cytotoxicity.* Mutation research, 2007. **630**(1-2): p. 78-91.
176. Fenech, M., et al., *HUMN project: detailed description of the scoring criteria for the cytokinesis-block micronucleus assay using isolated human lymphocyte cultures.* Mutation Research/Genetic Toxicology and Environmental Mutagenesis, 2003. **534**(1): p. 65-75.
177. Gyori, B.M., et al., *OpenComet: An automated tool for comet assay image analysis.* Redox Biology, 2014. **2**: p. 457-465.
178. Avlasevich, S.L., et al., *In vitro micronucleus scoring by flow cytometry: Differential staining of micronuclei versus apoptotic and necrotic chromatin enhances assay reliability.* Environmental and Molecular Mutagenesis, 2006. **47**(1): p. 56-66.
179. Ramadhani, D.W.I. and S. Purnami, *Automated Detection of Binucleated Cell and Micronuclei using CellProfiler 2.0 Software.* HAYATI Journal of Biosciences, 2013. **20**(4): p. 151-156.
180. Bryce, S.M., et al., *High content flow cytometric micronucleus scoring method is applicable to attachment cell lines.* Environmental and molecular mutagenesis, 2010. **51**(3): p. 260-266.
181. Nüsse, M. and J. Kramer, *Flow cytometric analysis of micronuclei found in cells after irradiation.* Cytometry, 1984. **5**(1): p. 20-25.
182. L., A.S., et al., *In vitro micronucleus scoring by flow cytometry: Differential staining of micronuclei versus apoptotic and necrotic chromatin enhances assay reliability.* Environmental and Molecular Mutagenesis, 2006. **47**(1): p. 56-66.
183. Avlasevich, S., et al., *Flow cytometric analysis of micronuclei in mammalian cell cultures: past, present and future.* Mutagenesis, 2011. **26**(1): p. 147-152.
184. Seinige, D., et al., *Comparative analysis and limitations of ethidium monoazide and propidium monoazide treatments for the differentiation of viable and nonviable campylobacter cells.* Applied and environmental microbiology, 2014. **80**(7): p. 2186-2192.
185. Lorge, E., et al., *SFTG international collaborative study on in vitro micronucleus test: I. General conditions and overall conclusions of the study.* Mutation Research/Genetic Toxicology and Environmental Mutagenesis, 2006. **607**(1): p. 13-36.

186. Hashimoto, K., et al., *An in vitro micronucleus assay with size-classified micronucleus counting to discriminate aneugens from clastogens.* Toxicology in Vitro, 2010. **24**(1): p. 208-216.
187. Landry, J.J.M., et al., *The genomic and transcriptomic landscape of a HeLa cell line.* G3 (Bethesda, Md.), 2013. **3**(8): p. 1213-1224.
188. Xu, W., *Functional Nucleic Acids Detection in Food Safety: Theories and Applications*. 2016: Springer.
189. Karg, T.J. and K.G. Golic, *Photoconversion of DAPI and Hoechst dyes to green and red-emitting forms after exposure to UV excitation.* Chromosoma, 2018. **127**(2): p. 235-245.
190. Antberg, L., et al., *Pathway-centric analysis of the DNA damage response to chemotherapeutic agents in two breast cell lines.* EuPA Open Proteomics, 2015. **8**: p. 128-136.
191. Pagès, V. and R.P.P. Fuchs, *How DNA lesions are turned into mutations within cells?* Oncogene, 2002. **21**: p. 8957.
192. Fenech, M., *The in vitro micronucleus technique.* Mutation Research/Fundamental and Molecular Mechanisms of Mutagenesis, 2000. **455**(1): p. 81-95.
193. Fenech, M., et al., *Molecular mechanisms of micronucleus, nucleoplasmic bridge and nuclear bud formation in mammalian and human cells.* Mutagenesis, 2011. **26**(1): p. 125-132.
194. Thomas, P. and M. Fenech, *Cytokinesis-Block Micronucleus Cytome Assay in Lymphocytes*, in *DNA Damage Detection In Situ, Ex Vivo, and In Vivo: Methods and Protocols*, V.V. Didenko, Editor. 2011, Humana Press: Totowa, NJ. p. 217-234.
195. Thomas, P. and M. Fenech, *Cytokinesis-block micronucleus cytome assay in lymphocytes.* Methods Mol Biol, 2011. **682**: p. 217-34.
196. Rodrigues, M.A., et al., *The potential for complete automated scoring of the cytokinesis block micronucleus cytome assay using imaging flow cytometry.* Mutation Research/Genetic Toxicology and Environmental Mutagenesis, 2018.
197. Singh, N.P., et al., *A simple technique for quantitation of low levels of DNA damage in individual cells.* Exp Cell Res, 1988. **175**(1): p. 184-91.
198. Hartley, J.M., V.J. Spanswick, and J.A. Hartley, *Measurement of DNA Damage in Individual Cells Using the Single Cell Gel Electrophoresis (Comet) Assay*, in *Cancer Cell Culture: Methods and Protocols*, I.A. Cree, Editor. 2011, Humana Press: Totowa, NJ. p. 309-320.
199. Forchhammer, L., et al., *Variation in the measurement of DNA damage by comet assay measured by the ECVAG inter-laboratory validation trial.* Mutagenesis, 2010. **25**(2): p. 113-23.
200. Olive, P.L. and J.P. Banath, *The comet assay: a method to measure DNA damage in individual cells.* Nat Protoc, 2006. **1**(1): p. 23-9.
201. Kuo, L.J. and L.X. Yang, *Gamma-H2AX - a novel biomarker for DNA double-strand breaks.* In Vivo, 2008. **22**(3): p. 305-9.
202. Dickey, J.S., et al., *Intercellular communication of cellular stress monitored by γ-H2AX induction.* Carcinogenesis, 2009. **30**(10): p. 1686-1695.

203. Azqueta, A., et al., *Towards a more reliable comet assay: Optimising agarose concentration, unwinding time and electrophoresis conditions.* Mutation Research/Genetic Toxicology and Environmental Mutagenesis, 2011. **724**(1): p. 41-45.
204. Kadioglu, E., et al., *Determination of DNA damage by alkaline halo and comet assay in patients under sevoflurane anesthesia.* Toxicology and Industrial Health, 2009. **25**(3): p. 205-212.
205. Lee, Y.-J., et al., *An in vivo analysis of MMC-induced DNA damage and its repair.* Carcinogenesis, 2006. **27**(3): p. 446-453.
206. Bryce, S.M., et al., *Interlaboratory evaluation of a flow cytometric, high content in vitro micronucleus assay.* Mutation research, 2008. **650**(2): p. 181-195.
207. Reese, J.S., L. Liu, and S.L. Gerson, *Repopulating defect of mismatch repair–deficient hematopoietic stem cells.* Blood, 2003. **102**(5): p. 1626-1633.
208. Fraczkowska, K., et al., *Alterations of biomechanics in cancer and normal cells induced by doxorubicin.* Biomedicine & Pharmacotherapy, 2018. **97**: p. 1195-1203.
209. White, F.H., Y. Jin, and L. Yang, *An evaluation of the role of nuclear cytoplasmic ratios and nuclear volume densities as diagnostic indicators in metaplastic, dysplastic and neoplastic lesions of the human cheek.* Histol Histopathol, 1997. **12**(1): p. 69-77.
210. Guillem, V. and M. Tormo, *Influence of DNA damage and repair upon the risk of treatment related leukemia.* Leukemia & Lymphoma, 2008. **49**(2): p. 204-217.
211. Sill, H., et al., *Therapy-related myeloid neoplasms: pathobiology and clinical characteristics.* British journal of pharmacology, 2011. **162**(4): p. 792-805.
212. Morse, H.R., et al., *Chemotherapy-induced genotoxic damage to bone marrow cells: long-term implications.* Mutagenesis, 2018. **33**(3): p. 241-251.
213. Andor, N., C.C. Maley, and H.P. Ji, *Genomic Instability in Cancer: Teetering on the Limit of Tolerance.* Cancer Research, 2017. **77**(9): p. 2179-2185.
214. Kumar, D., et al., *Genetic Instability in Lymphocytes is Associated With Blood Plasma Antioxidant Levels in Health Care Workers Occupationally Exposed to Ionizing Radiation.* International Journal of Toxicology, 2016. **35**(3): p. 327-335.
215. Abegglen, L.M., et al., *Potential Mechanisms for Cancer Resistance in Elephants and Comparative Cellular Response to DNA Damage in Humans.* JAMA, 2015. **314**(17): p. 1850-1860.
216. Gerlinger, M. and C. Swanton, *How Darwinian models inform therapeutic failure initiated by clonal heterogeneity in cancer medicine.* British journal of cancer, 2010. **103**(8): p. 1139-1143.
217. Höglander, E.K., et al., *Time series analysis of neoadjuvant chemotherapy and bevacizumab-treated breast carcinomas reveals a systemic shift in genomic aberrations.* Genome medicine, 2018. **10**(1): p. 92-92.
218. Look, A.T., et al., *Cellular DNA Content as a Predictor of Response to Chemotherapy in Infants with Unresectable Neuroblastoma.* New England Journal of Medicine, 1984. **311**(4): p. 231-235.

219. Venkatesan, S., et al., *Treatment-Induced Mutagenesis and Selective Pressures Sculpt Cancer Evolution.* Cold Spring Harbor perspectives in medicine, 2017. **7**(8): p. a026617.
220. Slavotinek, A., et al., *The frequency of micronuclei in bone-marrow erythroblasts during the treatment of childhood acute lymphoblastic leukaemia.* Mutation Research Letters, 1993. **303**(1): p. 11-18.
221. Padjas, A., et al., *Cytogenetic damage in lymphocytes of patients undergoing therapy for small cell lung cancer and ovarian carcinoma.* Toxicology and Applied Pharmacology, 2005. **209**(2): p. 183-191.
222. Piroth, M.D., et al., *Sequencing chemotherapy and radiotherapy in locoregional advanced breast cancer patients after mastectomy – a retrospective analysis.* BMC Cancer, 2008. **8**(1): p. 114.
223. Jdey, W., et al., *Micronuclei frequency in tumors is a predictive biomarker for genetic instability and sensitivity to the DNA repair inhibitor AsiDNA.* Cancer Research, 2017.
224. Varga, D., et al., *On the difference of micronucleus frequencies in peripheral blood lymphocytes between breast cancer patients and controls.* Mutagenesis, 2006. **21**(5): p. 313-320.
225. Quintero Ojeda, J.E., et al., *Increased Micronuclei Frequency in Oral and Lingual Epithelium of Treated Diabetes Mellitus Patients.* Biomed Res Int, 2018. **2018**: p. 4898153.
226. Thierens, H., et al., *Micronucleus Induction in Peripheral Blood Lymphocytes of Patients under Radiotherapy Treatment for Cervical Cancer or Hodgkin's Disease.* International Journal of Radiation Biology, 1995. **67**(5): p. 529-539.
227. Lewis, C.W. and R.M. Golsteyn, *Cancer cells that survive checkpoint adaptation contain micronuclei that harbor damaged DNA.* Cell Cycle, 2016. **15**(22): p. 3131-3145.
228. Rode, A., et al., *Chromothripsis in cancer cells: An update.* Int J Cancer, 2016. **138**(10): p. 2322-33.
229. Kokenek Unal, T.D. and I. Coban, *Increased micronucleus count predicts malignant behavior in pleural effusion fluid.* Turk J Med Sci, 2018. **48**(2): p. 354-360.
230. Pardini, B., et al., *Increased micronucleus frequency in peripheral blood lymphocytes predicts the risk of bladder cancer.* British Journal Of Cancer, 2016. **116**: p. 202.
231. Maffei, F., et al., *Micronucleus frequency in human peripheral blood lymphocytes as a biomarker for the early detection of colorectal cancer risk.* Mutagenesis, 2014. **29**(3): p. 221-225.
232. Driessens, G., et al., *Micronuclei to detect in vivo chemotherapy damage in a p53 mutated solid tumour.* Br J Cancer, 2003. **89**(4): p. 727-9.
233. Jadhav, K., N. Gupta, and B. Ahmed Mujib, *Micronuclei: An essential biomarker in oral exfoliated cells for grading of oral squamous cell carcinoma.* Journal of Cytology, 2011. **28**(1): p. 7-12.
234. Nikolouzakis, T.K., et al., *Effect of systemic treatment on the micronuclei frequency in the peripheral blood of patients with metastatic colorectal cancer.* Oncology letters, 2019. **17**(3): p. 2703-2712.

235. Kipps, T.J., et al., *Chronic lymphocytic leukaemia.* Nature reviews. Disease primers, 2017. **3**: p. 16096-16096.
236. Parikh, S.A., *Chronic lymphocytic leukemia treatment algorithm 2018.* Blood cancer journal, 2018. **8**(10): p. 93-93.
237. Chapman, E.A., et al., *Delineating the distinct role of AKT in mediating cell survival and proliferation induced by CD154 and IL-4/IL-21 in chronic lymphocytic leukemia.* Oncotarget, 2017. **8**(61): p. 102948-102964.
238. Saito, T., et al., *Effective collaboration between IL-4 and IL-21 on B cell activation.* Immunobiology, 2008. **213**(7): p. 545-555.
239. Singh, S., et al., *Mutant p53 establishes targetable tumor dependency by promoting unscheduled replication.* The Journal of Clinical Investigation, 2017. **127**(5): p. 1839-1855.
240. Friedberg, E. and G. Walker, *Siede W.* DNA Repair and Mutagenesis. Washington, DC: ASM Press, 1995.
241. Fry, R.C., T.J. Begley, and L.D. Samson, *GENOME-WIDE RESPONSES TO DNA-DAMAGING AGENTS.* Annual Review of Microbiology, 2005. **59**(1): p. 357-377.
242. Cunningham, R.P., *DNA repair: caretakers of the genome?* Current Biology, 1997. **7**(9): p. R576-R579.
243. Fenech, M., *The cytokinesis-block micronucleus technique: A detailed description of the method and its application to genotoxicity studies in human populations.* Mutation Research/Fundamental and Molecular Mechanisms of Mutagenesis, 1993. **285**(1): p. 35-44.
244. Etzel, C.J., R. El-Zein, and A. Vral, *Cytokinesis-blocked micronucleus assay and cancer risk assessment.* Mutagenesis, 2011. **26**(1): p. 101-106.
245. Junk, M., et al., *Mathematical modelling of the automated FADU assay for the quantification of DNA strand breaks and their repair in human peripheral mononuclear blood cells.* BMC Biophysics, 2014. **7**(1): p. 9.
246. Guo, B., et al., *Spectral karyotyping: an unique technique for the detection of complex genomic rearrangements in leukemia.* Translational pediatrics, 2014. **3**(2): p. 135-139.
247. Cheung-Ong, K., G. Giaever, and C. Nislow, *DNA-Damaging Agents in Cancer Chemotherapy: Serendipity and Chemical Biology.* Chemistry & Biology, 2013. **20**(5): p. 648-659.
248. Bryce, S., et al., *Flow cytometric analysis of micronuclei in mammalian cell cultures: past, present and future.* Mutagenesis, 2011. **26**(1): p. 147-152.
249. Norppa, H. and G.C. Falck, *What do human micronuclei contain?* Mutagenesis, 2003. **18**(3): p. 221-33.